63-4-2

RTD-TDR-63-14

CATALOGED BY DDC
AS AD No. 408744

408744

DEVELOPMENT OF MECHANICAL FITTINGS
• PHASE I •

TECHNICAL DOCUMENTARY REPORT NO. RTD-TDR-63-14
February 1963

Air Force Flight Test Center
Rocket Propulsion Laboratories
Edwards Air Force Base, California

Project No. 6753, Task No. 675304

(Prepared under Contract No. AF 04(611)-8176 by
E. C. Rodabaugh, J. W. Adam, B. Goobich, and
T. M. Trainer, Battelle Memorial Institute, Columbus,
Ohio)

FOREWORD

This report summarizes the research activities performed under USAF Contract No. 04(611)-8176, from April 1, 1962, to November 30, 1962. The research was performed by Battelle Memorial Institute under the auspices of the Rocket Propulsion Laboratories, Air Force Systems Command, Edwards Air Force Base, with Lt. P. Olekszyk serving as contract monitor. The principal investigators were J. W. Adam, J. C. Gerdeen, and B. Goobich, Research Engineers; E. C. Rodabaugh, Senior Research Engineer; W. A. Spraker, Staff Mechanical Engineer; and T. M. Trainer, Group Director.

DISTRIBUTION LIST

Mr. Ralph Middleton
Lockheed Aircraft Corp.
2555 N. Hollywood Way
Burbank, California

Mr. J. B. Smith
Systems and Controls
Aerojet General
Sacramento, California

Mr. Marvin G. Luebben
Dept. 64-62
Lockheed Missiles and Space Co.
Sunnyvale, California

Mr. Adrien Aitkin
Stanford Research Institute
Menlo Park, California

Mr. John C. Bloom, Test Group Engineer
Hydromechanical Design Section
Douglas Aircraft Co., Inc.
Long Beach, California

Mr. L. Andrews, Supervisor
Space Propulsion Group
Douglas Aircraft Co., Inc.
Santa Monica, California

Mr. W. E. Currie
The Parker Appliance Co.
17325 Euclid Avenue
Cleveland 12, Ohio

Mr. Bruce Pauly
The Weatherhead Company
Cleveland, Ohio

Mr. E. Floreen, Sr., Project Engineer
Marman Division
Aeroquip Corp.
11214 Exposition Boulevard
Los Angeles 64, California

Mr. Jasper McKee, Chief
Mechanical Testing
Flexonics Co.
Bartlett, Illinois

Mr. Glen Howell
Space Technology Laboratory
Radiation and Compton Boulevard
Los Angeles, California

Mr. Sherwin Lewis, Propulsion Engineer
Aerospace Corp.
Los Angeles, California

Mr. Richard Weiner
Development Engineer
Jet Propulsion Laboratory
4800 Oak Grove Drive
Pasadena, California

Mr. C. M. Richards, Design Engineer
Astronautics Division
General Dynamics Corp.
San Diego, California

Mr. John F. Mayer
Department 596, Group 121
Rocketdyne Division
North American Aviation
6633 Canoga Park
Canoga Park, California

Mr. Frank Brock
Resistoflex Corp.
Roseland, New Jersey

Mr. Paul Bauer, Project Engineer
Mechanics Research Division
Armour Research Foundation
10 West 35th Street
Chicago 16, Illinois

Mr. M. H. Weisman, Research Specialist
Metallic Materials Laboratory
Los Angeles Division
North American Aviation, Inc.
International Airport
Los Angeles 9, California

ABSTRACT

The purpose of this program is to develop a family of improved lightweight mechanical fittings for service with rockets' fluid systems under stringent environmental and operating conditions. Phase I was to define and investigate the parameters significantly affecting the fitting classes and to initiate preliminary fitting designs. The work consisted of (1) a review of the design and use of present fittings for missiles, (2) a review of candidate materials for the required operating conditions, (3) the establishment of recommended classifications for improved fittings, and (4) the development of preliminary design concepts for the proposed classifications. Three major conclusions were drawn from Phase I: (1) the reconnectable union should be either threaded or flanged, (2) the connection between the tube and the fitting should be a permanent joint made independent of the seal mechanism or the reconnectable union, and (3) three sealing methods show promise of being developed for the improved fittings.

The following recommendations were made for future work: (1) the brazed or welded joining method developed by North American Aviation should be adapted for joining tubing to fittings and components, (2) high-energy-rate tube-to-fitting joining methods should be investigated as an eventual improvement of the welded or brazed methods, (3) the best of the three promising seals should be selected and developed, and (4) the preliminary fitting-to-fitting designs initiated during Phase I should be detailed and evaluated. Recommendations (3) and (4) are recommended for inclusion in Phase II.

PUBLICATION REVIEW

This technical documentary report has been reviewed and is approved.

<u>TABLE OF CONTENTS</u>

TABLE OF CONTENTS
(Continued)

TABLE OF CONTENTS
(Continued)

TABLE OF CONTENTS
(Continued)

LIST OF FIGURES

LIST OF FIGURES
(Continued)

LIST OF FIGURES
(Continued)

LIST OF FIGURES
(Continued)

LIST OF TABLES

DEVELOPMENT OF MECHANICAL FITTINGS

INTRODUCTION

The purposes of this program are (1) to design, develop, and fabricate a family of lightweight mechanical fittings for service with rockets' fluid systems under stringent environmental and operational conditions and (2) to provide and prepare specifications and drawings and test requirements for the fittings in such a manner that military specifications and standards may be published.

The fittings currently in general use in the fluid systems of rocket-propulsion vehicles were developed primarily for use in the aircraft industry. Because of the severe missile environments and the use of new and exotic fluids, which have posed problems of vibration, temperature, and chemical activity never before encountered, standard aircraft tube fittings in common use by Governmental agencies have been subject to failure. This program is an attempt to develop new and fresh fitting-design concepts to optimize weight, misalignment capability, and leakage characteristics consistent with high operational reliability. No one connector design can satisfy the requirements of the complete range of temperatures, pressures, and fluids encountered in advanced missile systems. Therefore a basic requirement of this program is to identify and develop families and classes of fittings. It is also required that the designs to be considered should be new and unique where applicable and not restricted to modifications of present aircraft designs. This goal is to be attained through:

(1) Use of new and unique concepts of mechanical fitting design

(2) New methods of joining tubing and fittings

(3) Optimum combinations of materials

(4) Effective use of manufacturing techniques.

SCOPE AND OBJECTIVES OF PHASE I

Phase I was to consist of an investigation of parameters such that classes and types of fittings could be chosen and preliminary designs could be initiated. The investigation was to begin with a literature survey of present technology and a materials review for determination of the most suitable materials.

Investigations were to be made of (a) satisfactory methods of joining tubing and fittings, (b) forces required to tighten and seal, (c) effects of thread form on torque relaxation, (d) effect of thread lubricant on sealing, thread galling, and torque relaxation, (e) the use of computer techniques to evaluate design criteria, and (f) methods to alleviate or eliminate the chances of human error in the assembly of fittings.

The preliminary design of proposed connectors was to begin concurrently or on conclusion of these investigations. A stress analysis was to be made of each type of fitting. Optimum operational service ranges were to be determined showing crossover points between threaded and flanged fittings. Maximum strength under operational conditions vs. minimum weight was to serve as a major criterion.

REPORT ORGANIZATION

The preparation of this report on Phase I constituted a considerable problem because of the large quantity of information that was assembled and created and because of the interrelation of many of the design areas. The format finally selected is an arrangement of subjects such that the reader can best understand the proposed concepts and the reasons for these concepts.

The first part, "Determination of Fitting Classes", outlines the requirements which determined the selection of candidate fitting materials, details the reasons for selecting the three recommended materials, and describes how the characteristics of the three selected fitting materials combined with certain operational and handling requirements define the recommended fitting classes. The fitting classifications affect many of the subsequent design decisions.

The next three parts discuss in detail the major results of Phase I – that is, the design thinking on improved mechanical fittings. Early in Phase I it was concluded that a reconnectable mechanical fitting could be made to seal helium satisfactorily only if the seal were not a part of the tubing, as is the case with the present flared and flareless fittings. The reasons for this conclusion are given elsewhere in the report. As a result of this decision, the fitting design was divided into three elements. While these elements were not entirely independent of each other, their aspects were sufficiently unique that during much of Phase I they were considered to be separate design problems. The three elements, as shown in Figure 1, are:

- The fitting-to-fitting connection, a reconnectable union in the fitting which provides the necessary structural integrity
- The tube-to-fitting connection, a permanent transition connection between the fitting and the piping.
- The seal, a metallic disposable seal independent of the structural connections except for the seal seating surface.

The design thinking is presented in this report in terms of these individual elements for two reasons: (1) they provide excellent means of discussing the many design aspects of the fitting in a systematic manner and (2) the conclusions and recommendations concerning each element are different and more easily formulated when considered independently.

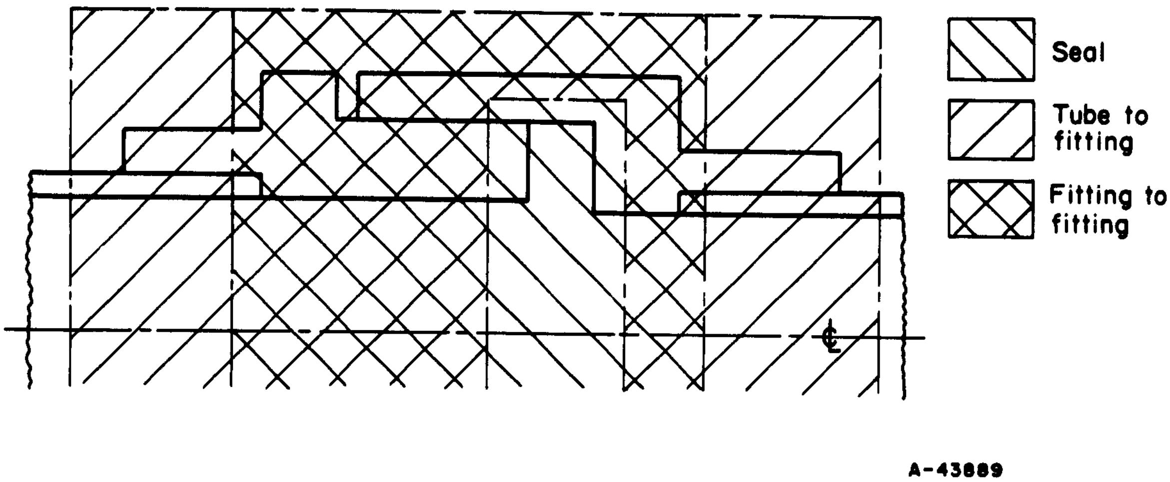

FIGURE 1. DESIGN ELEMENTS OF A TOTAL FITTING

The fitting-to-fitting design is discussed first of the three because it provides the opportunity also to discuss many of the design problems which affect two or all three elements. The tube-to-fitting design is discussed next because many of the loads described for the fitting-to-fitting connection apply also to the tube-to-fitting problem. Finally, the seal-design discussion is given. While the section on the seal design is the most important design section, from the standpoint that the seal is the element furthest from solution, it is presented last because the sealing problems can best be appreciated and the recommended seal designs best understood after the other aspects of the fitting have been discussed.

The final part of the body of the report is the "Summary of Recommendations". Although many specific conclusions and recommendations are presented in most of the major sections, the more important ones are summarized at the end of the report for convenience.

Five appendixes contain important and pertinent information of two types: (1) information which is back-up material for discussions in the report body, and (2) selected detailed information pertaining to Phase-I activities.

DETERMINATION OF FITTING CLASSES

General Service Requirements

Materials Selection

Assembly Torque

Recommended Fitting Classes

References

DETERMINATION OF FITTING CLASSES

To achieve minimum weight in a missile piping system, each fitting and component should be designed on the basis of the exact operating requirements for that particular component. Even if these requirements were known at every point in the system, such a procedure would be impractical because of the excessive expenditure of time and money. Fortunately, if the smaller fittings are designed within certain ranges of selected parameters, the production and logistics problems are reduced considerably, and the weight penalty is small. The most significant parameters considered in determining the recommended fitting classes were (1) general service requirements, (2) materials selection, and (3) assembly torque.

General Service Requirements

The general service requirements applicable to missiles' and rockets' fluid systems are shown in Table 1. It was agreed between Rocket Propulsion Laboratories and Battelle that the problems of developing a satisfactory fitting for up to 1500 F were sufficiently difficult that the upper design temperature at least for Phase I would be limited to 1500 F.

TABLE 1. GENERAL SERVICE REQUIREMENTS

Service	Pressure Range, psi	Temperature Range, F	Dimensional Range, inches
Propellant	0 to 1500	-425 to 200	1 to 16
Pneumatic	0 to 2000	-425 to 200	1/8 to 1
	0 to 10,000	-425 to 600	
	0 to 4000	-425 to 1500	
Hot Gas	0 to 1500	1000 to 3000	1 to 3

As presented in the table, the breakdown by fluids established natural "families" of fittings. However, within each family further classification was necessary. This was especially true for propellant and hot-gas systems where operating pressures may be much less than the maximum values stipulated.

Materials Selection

The selection of the fitting materials was determined largely by the mechanical properties of the materials and by the compatibility of the materials with the fluid media. In a few cases other considerations, such as machinability, governed. Since it would be impractical to review all of the candidate materials in detail, the characteristics of the classes of materials that were considered are discussed in general terms. The selected materials are subsequently described in some detail.

Materials Considered

General groupings of candidate materials and the major characteristics of the groups are discussed below.

Low-Density Materials. The low-density materials include the aluminum, magnesium, and titanium alloys. Even though the aluminum and magnesium alloys have a very low density, the low strengths and their tendency to lose strength drastically as temperature is increased above about 300 F, make them undesirable. Compatibility with missile propellants is also a severe limitation.

Titanium, which has good mechanical properties up to about 600 F, is generally not acceptable for service with oxidizers.

300 Series Stainless Steels. The 300 series stainless steels are easy to machine and fabricate, and are almost universally compatible with the fluids considered. However, because of their relatively low yield strength-to-density ratio it is not possible to design a lightweight fitting which can satisfy the operational limits specified in Table 1. Strength can be increased to some degree by cold working, but this increase is marginal when the final strength is compared with that of the age-hardenable stainless steels and other alloys discussed below. At temperature conditions exceeding 1000 F, the 300 series alloys are too sensitive to creep to be practical for this application.

400 Series Stainless Steels. The 400 series stainless steels have a good combination of physical properties over the temperature range of interest. They are easily fabricated, and are available in production quantities. However, the heat treatment required includes an oil or water quench, or at least a rapid cool, from temperatures of 1760 to 1850 F. This procedure causes distortions in the fitting that could be detrimental to the sealing surface.

High-Strength Tool Steels. The high-strength tool steels of the H-11 type, such as Potomac M, are difficult to weld and have poor corrosion resistance. Hence, they are not considered candidate materials.

Maraging Steels. The 18Ni-Co-Mo maraging steels possess extremely high strengths. However, these steels are still under development. Most work to date has emphasized ambient applications, and no compatability data are available. Also, because they are new, their availability is limited. For these reasons, they have not been considered further.

Nickel- and Cobalt-Base Metals. This category includes materials such as Haynes 25, Inconel "X", and René 41, all of which are considered possible choices. Of this group, René 41 has the best combination of properties over the temperature range of interest.

Age-Hardenable Stainless Steels. The precipitation-hardenable stainless steels include 17-7PH, PH 15-7 Mo, AM-350, 17-4PH, AM-355, and A-286. Of these, 17-7PH, PH 15-7 Mo, and AM-350 are not available as bar stock or plate and hence cannot be considered. 17-4PH, AM-355, and A-286 are available as plate and bar stock.

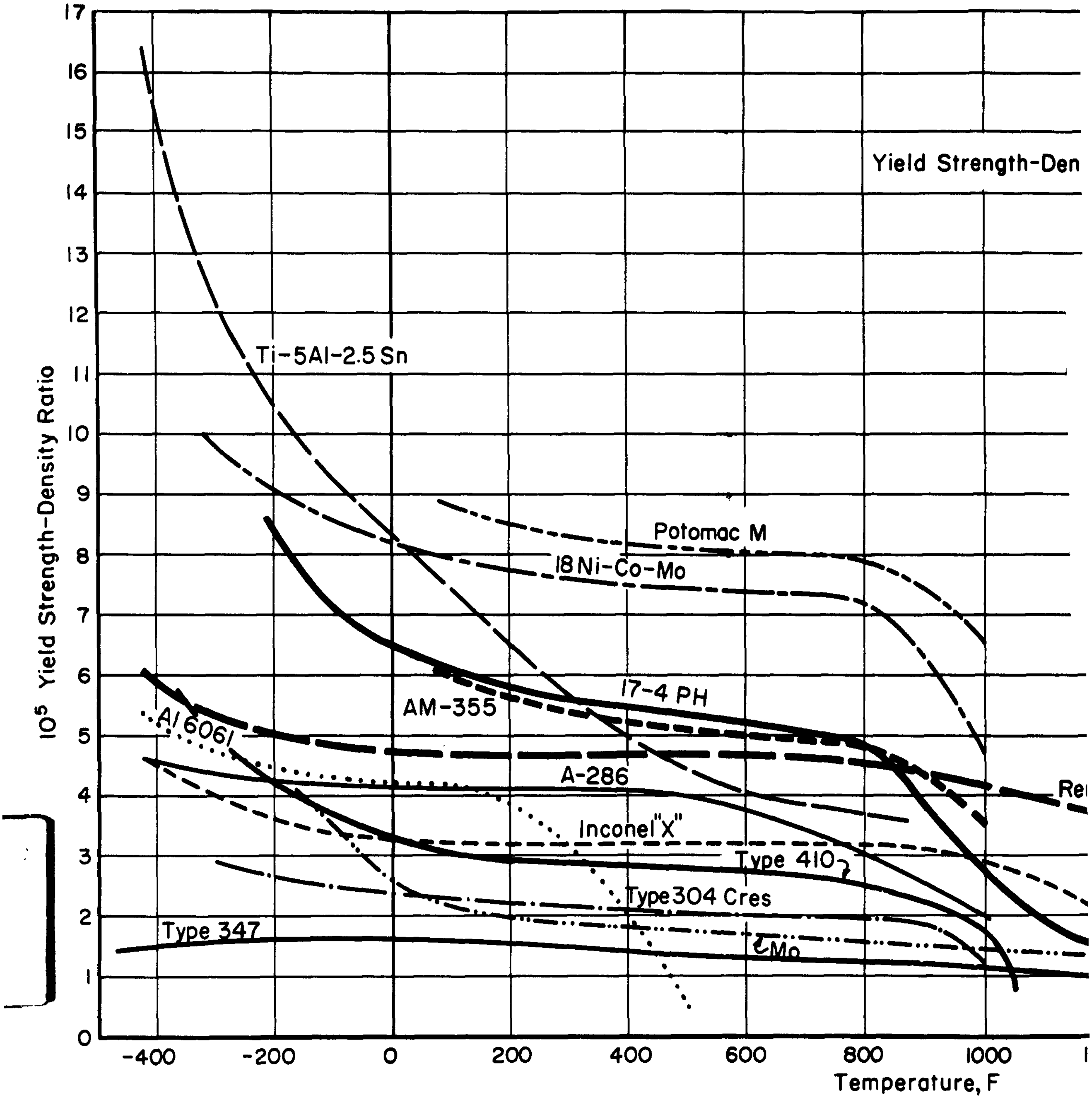

FIGURE 2. YIELD STRENGTH-DENSITY RATIO OVER SERVICE TEMPERATURE RANGE

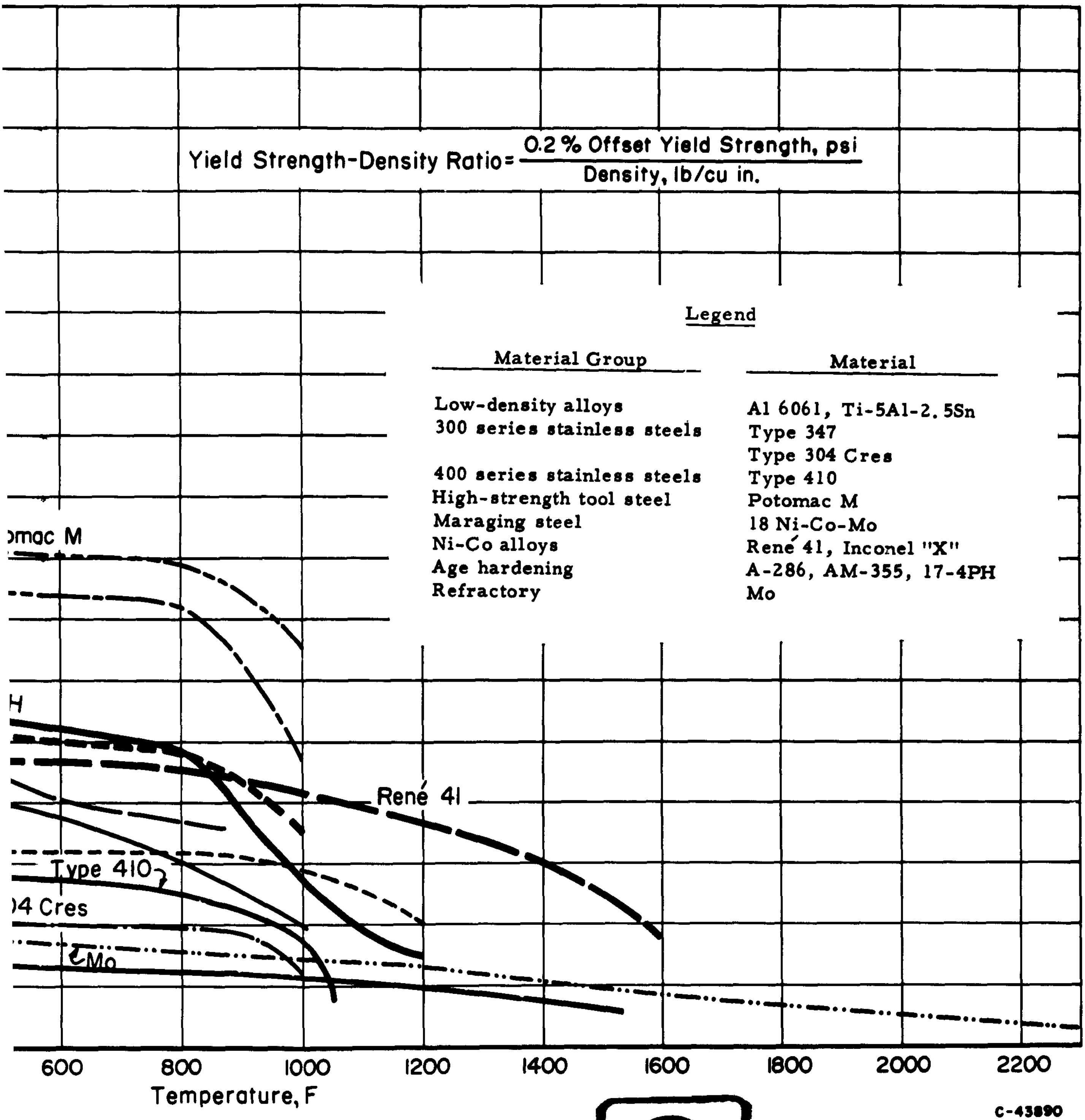

2

EMPERATURE

One important characteristic for design purposes is a low thermal expansion. Because of the martensitic structure of 17-4PH and AM-355 in the hardened condition, their coefficient of thermal expansion is approximately 60 per cent of the coefficient of the austenitic types such as A-286, 17-10P, and HNM.

The high strength/density ratio available over the temperature span of interest and the extensive experience developed by the aircraft and missile industries in the use of 17-4PH and AM-355 also help to make these alloys good choices.

Refractory Metals. Refractory metals such as tungsten, molybdenum, and tantalum are brittle, heavy, and hard to fabricate. Even so, the refractory metals are the best metals available for use at 1800 to 3000 F. However, they must be coated for oxidation and embrittlement protection. Except for applications at extremely high temperatures, they do not appear as promising as the other materials listed above.

Materials Selected

The three materials chosen as being most applicable are René 41, AM-355, and 17-4PH. Although there are a few fluids with which these materials are not compatible, they are considered to have the best combination of properties over the temperature range considered. They are produced by several companies; availability is not a problem. Considerable interest in these materials by the aircraft and missile industries in the last few years has resulted in much experience and data that can be used for design purposes.

These materials are harder to weld and fabricate than the 300 series stainless steels, but several companies are presently developing acceptable welding procedures.

Mechanical Properties

Materials used in mechanical fittings should have (1) a high yield strength-to-density ratio as a function of temperature, (2) creep resistance at elevated temperatures, and (3) low notch-sensitivity at cryogenic temperatures. In general, the yield strength, tensile strength, and elastic modulus of a given alloy decrease as temperature increases. As the temperature decreases, these properties increase, but the ductility and fracture toughness tend to decrease.

Yield Strength-to-Density Ratio. When weight is important, the yield strength-to-density ratio versus temperature curve is a major design criterion. Figure 2 shows these curves for the materials selected. Also, curves for some of the other materials considered are included for comparison.

The effect of the strength-to-density ratios on fitting weight can be illustrated by a simple example in which bending loads are not considered. If it is assumed that a missile contains 300 fittings having an average weight of 1 pound each when made from A-286, the total weight per missile would be 300 pounds. As shown in Figure 2, the yield-strength-to-density ratio at 200 F for Inconel "X", A-286, René 41, and 17-4PH is 3.2, 4.1, 4.7, and 5.8 x 10^5 respectively. Fabricating the 300 fittings from Inconel "X" would increase the total weight to 383 pounds. When fabricated from René 41 and 17-4PH the total weight would decrease to 262 and 212 pounds respectively. The total fitting weight therefore could be reduced by more than 29 per cent if 17-4PH were used instead of A-286. At high temperatures, above 800 F, the comparison of yield strength-to-density ratio is also important even though the strength of materials decreases markedly as temperature increases, because the change is different for each metal.

Creep. Although the creep rate of metals is generally disregarded at temperatures less than 800 F, it increases rapidly as temperatures exceed 800 F. For most materials there is some temperature at which the creep resistance or stress-to-rupture strength becomes less than the tensile yield strength, and hence the creep resistance rather than the yield strength must be used as the design basis.

Because the factors governing tubing design in a fluid system also are major factors governing the design of a fitting for that system, the time and temperature dependency of the fitting weight can be illustrated by considering the time and temperature dependency of the tubing. The curve in Figure 3, tube weight versus temperature, is based on a 2-inch length of 2-inch outside-diameter tube of René 41 for a pressure of 1500 psi and a life of 1000 hours. The creep strength for René 41 becomes the controlling strength factor at about 1100 F, as evidenced by the change in slope. The curve in Figure 4 represents tube weight versus time for a 2-inch length of 2-inch outside diameter tubing of René 41 for a pressure of 1500 psi and a temperature of 1500 F. From these curves it is apparent that either a decrease in temperature or a decrease in service-life requirement would result in a significant weight saving. Thus, it is important that the expected service temperature and desired life be known to achieve an optimum design.

Creep and stress-to-rupture data at elevated temperatures are commonly available for all of the materials listed in the preceding section. The two best materials are René 41 and Inconel "X". AM-355 and 17-4PH are likely to become embrittled when kept at temperatures above 700 F and hence should be restricted to 600 F service for missile fittings.

Notch Sensitivity. At cryogenic temperatures, one of the most important considerations is the material's fracture toughness or its ability to fail in a ductile manner when notches are present. This property, which can be measured by impact tests or by center-notch tensile tests, decreases rapidly with decreasing temperatures.

Because of the high stress levels dictated when designing for minimum weight, and because of the importance of fracture toughness, the effects of intrinsic defects (flaws, inclusions) and manufacturing defects (surface scratches, designed notches, welds) must be considered at cryogenic temperatures, even though such imperfections do not cause problems at "normal" temperatures. An Air Force technical manual[1]* states that "metals with a minimum impact resistance of 15 ft-lb Charpy keyhole notch, or 18 ft-lb Izod V-notch are generally suitable for cryogenic service". However, there are many versions of impact tests; specifications have not been established to govern the evaluation at cryogenic temperatures, and minimum acceptable values have not been established for each of the various tests.

*References are listed on page 22.

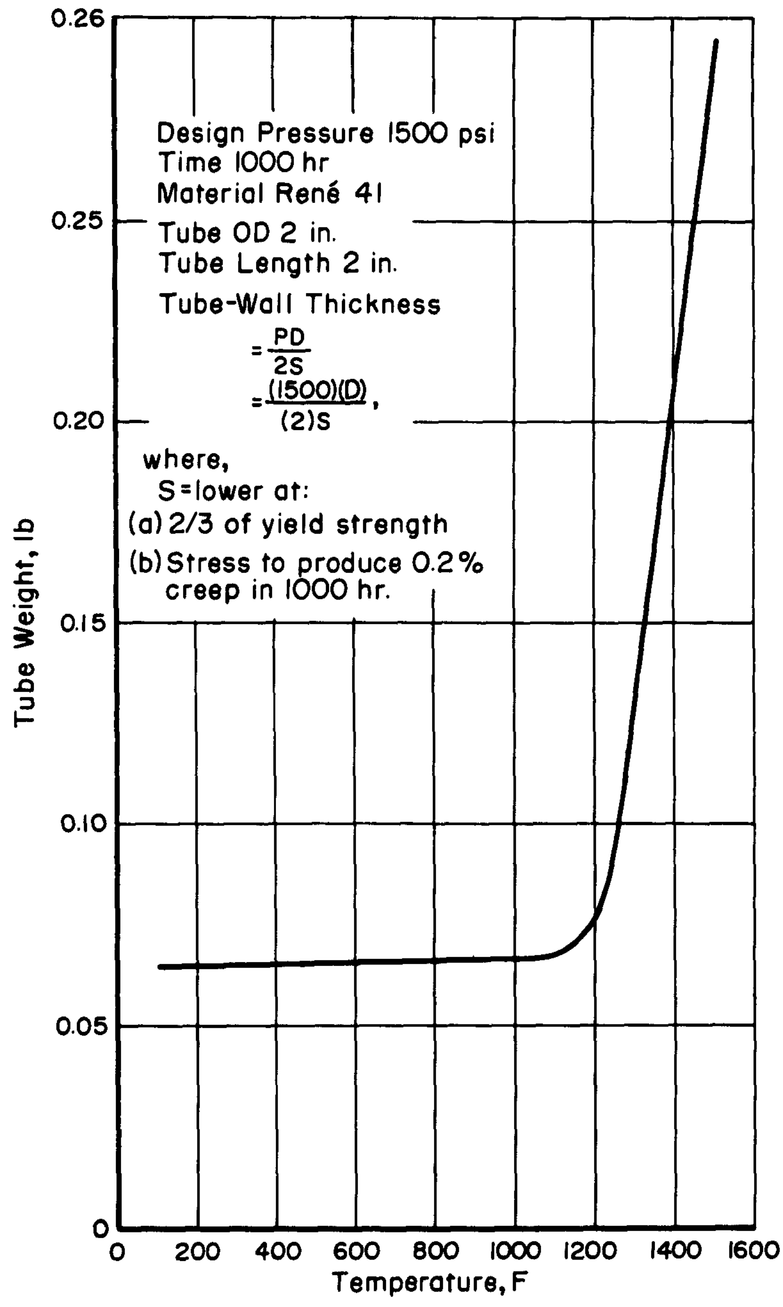

FIGURE 3. TUBE WEIGHT VS. TEMPERATURE

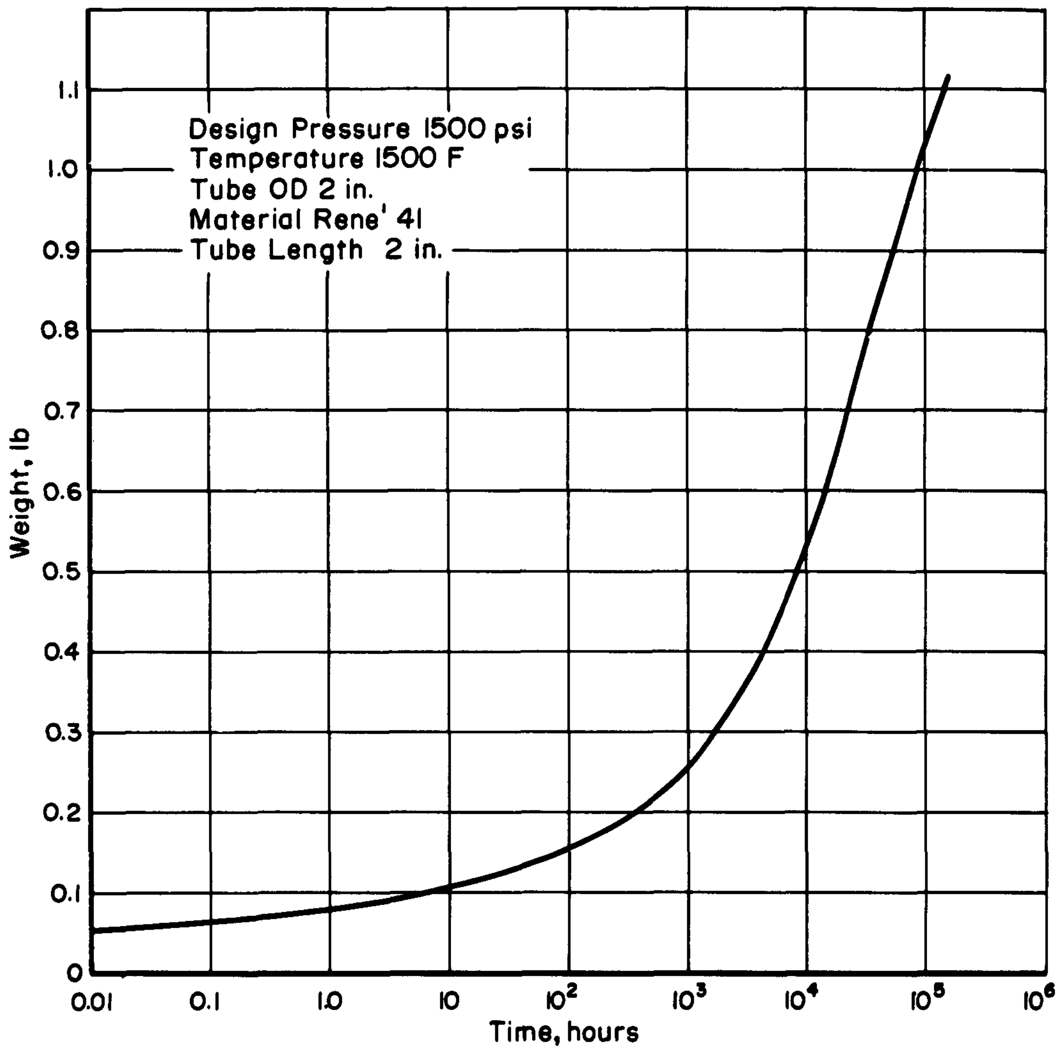

FIGURE 4. TUBE WEIGHT VS. TIME

The notched/unnotched tensile ratio-vs.-temperature curves given in Figure 5 show a sharp decrease in the notched/unnotched ratio below -100 F for AM-355 as compared to an almost constant value for René 41. The tendency for the notched-unnotched tensile ratio to drop rapidly as temperatures are decreased is typical for martensitic materials. It appears on the basis of available data that this is true of 17-4PH as well. On the basis of this curve, and because there is a lack of definitive data specifying minimum acceptable values, the lower service temperature for AM-355 and for the comparable material 17-4PH has been set at -100 F.

Fluid Compatibility

The fluids considered in this program and their useful temperature ranges are shown in Figure 6. As shown by Figure 6, the fluids could be divided into two groups on the basis of minimum service temperature. It was noted that the lower temperature extreme for Group A was approximately equal to the lower design-temperature (-100 F) limit for AM-355 and 17-4PH.

A summary of the compatibility data found for the compatibility of AM-355, 17-4PH, and René 41 with the fluids is given in Table 2. Compatibility data for these three materials with propellants are generally scarce and are nonexistent for some combinations. Also, many of the available data are contradictory. Therefore, estimates of the compatibility with some fluids have been extrapolated on the basis of data for other materials with similar chemical compositions. The following conclusions can be made on the basis of the data in Table 2:

(1) AM-355 is acceptable for general service with the majority of fluids.

(2) 17-4PH is acceptable for general service with the majority of fluids. It is unsatisfactory for use with hydrazine and MMH at all temperatures.

(3) René 41 is acceptable for general service with the exception that no data were found for hydrazine, 50 UDMH/50 hydrazine mixtures, and MMH. It is unsatisfactory for use with hydrogen peroxide.

Other data collected during the program indicate that the 18-8 type stainless steels are possible materials of construction for use with UDMH, UDMH/hydrazine mixtures, MMH, and hydrogen peroxide, as are many of the aluminum alloys.

Conclusions

Three materials were selected for minimum-weight fittings. René 41 can be used for the entire temperature range, -423 to +1500 F, whereas AM-355 and 17-4PH are restricted to the limits of -100 and 600 F. Within the narrower range, use of AM-355 or 17-4PH would result in a lighter fitting than would use of René 41. Also, both AM-355 and 17-4PH are more readily available and cost less than René 41. Although Type 347 stainless steel is widely used in this limited temperature range, a comparison of the yield strength-to-density ratio of Type 347 with that of AM-355 or 17-4PH (Figure 2) shows that a weight penalty might result if it were used. It is recognized that Type 347 is more readily available, is more easily machined, and has excellent compatibility. However minimum weight is considered to be a more critical selection criterion when designing for missile applications. Therefore, when considering the choice of materials three temperature service ranges are identifiable and three materials appear to be the best choice for these temperature ranges:

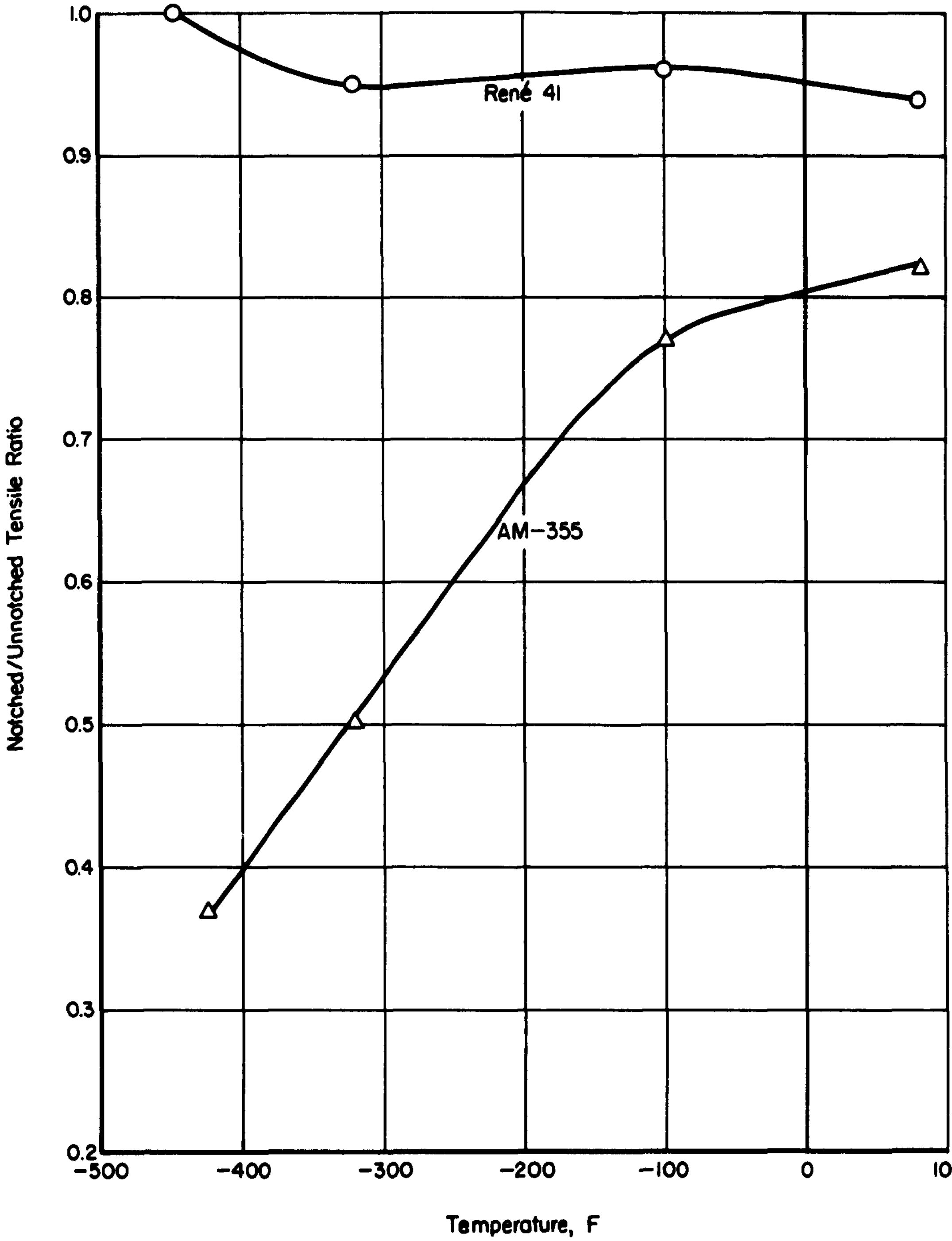

FIGURE 5. NOTCHED (K_t=6.3)/UNNOTCHED TENSILE RATIO VS. TEMPERATURE (TRANSVERSE)

Source: References (2) and (3).

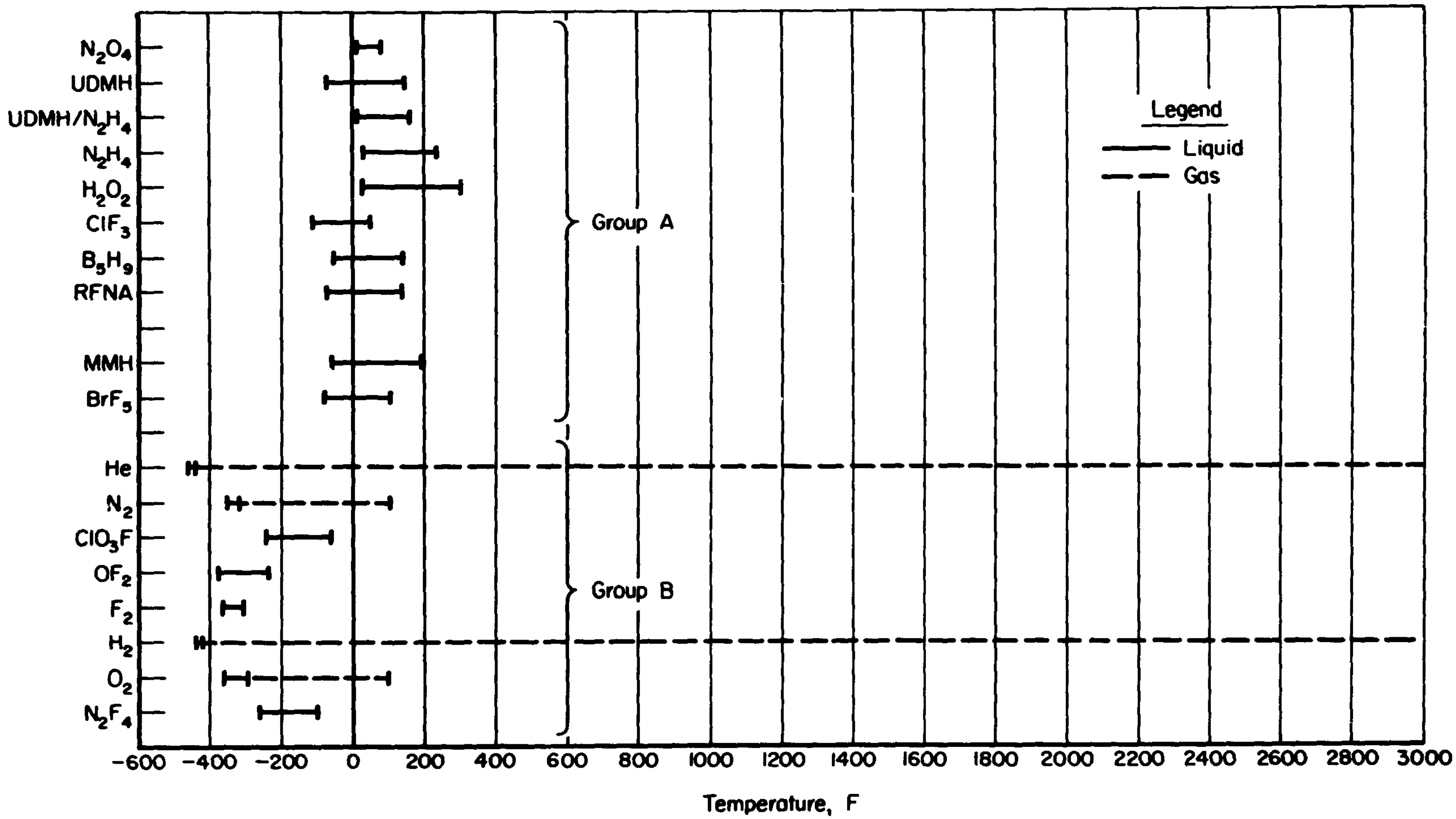

FIGURE 6. USEFUL TEMPERATURE RANGES OF FLUIDS

TABLE 2. SUMMARY OF FLUID-COMPATIBILITY DATA

Propellants	AM-355	17-4PH	René 41
		Group A	
N_2O_4	General service at 100 F[4] General service at 65 F[5] General service[6]	General service at 100 F[4] General service at 65 F[5] General service[6]	General service based on Inconel, nickel, and stainless steels if the N_2O_4 is dry[5]
UDMH	General service at ambient temperature[7]; limited service below 160 F[6]	General service at ambient temperature[7]; limited service[6]	Limited service at ambient temperature[7]; general service up to 85 F[8]
N_2H_4	Limited service below 160 F[6]	Unsatisfactory[6]	No data
50 UDMH/50 N_2H_4	Not usable at >160 F[7] General service at 160 F[4] General service at 160 F[5] Limited service below 160 F[6]	Limited service at 160 F[7] General service below 160 F[4] General service below 160 F[5] Limited service[6]	No data
H_2O_2	Limited service[7] Limited service 151 F[9]	Limited service 151 F[9]	Unsatisfactory based on other nickel- and Mo-containing alloys[8]
ClF_3	General service at ambient temperature based on AM-350 and mild steel	General service at ambient temperature based on AM-350 and mild steel	General service[6] General service at 80 F[10]
RFNA	Unsatisfactory above 130 F, based on 17-7PH[10]	Unsatisfactory above 130 F, based on 17-7PH[10]	Probably unsatisfactory at all temperatures[10]
WFNA	No data	No data	Unsatisfactory at all temperatures[10]

TABLE 2. (Continued)

Propellants	AM-355	17-4PH	René 41
MMH	Metals containing 0.5% Mo, Cu, limited service below 160 F[6]	Alloys cannot be used[7] Unsatisfactory[6]	No data
BrF_5	Probably the same as ClF_3	Probably the same as ClF_3	General service[6] General service[10]
RP_1	General service	General service	General service
		Group B	
O_2	General service down to -100 F based on mechanical properties	General service down to -100 F based on mechanical properties	General service in liquid oxygen[7]
NF_3	General service, liquid, based on stainless steel[7]	General service, liquid, based on stainless steel[7]	General service, liquid and vapor, based on compatibility with nickel and carbon steel[7]
PB	No metals are known to be incompatible at room temperatures and pressures[7]		
He	General service to 1500 F	General service to 1500 F	General service to 1500 F
N_2	General service to about 1300 F, at which temperature nitriding may be severe, depending upon exposure time[11]	General service to about 1300 F at which temperature nitriding may be severe, depending on exposure time[11]	General service to 1500 F[12]
$ClOF_3$	General service to 160 F, based on stainless steel and mild steel[10]	General service to 160 F, based on stainless steel and mild steel[10]	General service to 160 F, based on nickel and nickel alloys[10]

TABLE 2. (Continued)

Propellants	AM-355	17-4PH	René 41
OF_2	General service at ambient temperature based on stainless steel and mild steel; probably general service at higher temperatures(13)	General service at ambient temperature based on stainless steel and mild steel; probably general service at higher temperatures(13)	General service at ambient temperature based on stainless steel and nickel; probably general service at higher temperatures(13)
F_2	General service to 400 F based on 300 and 400 series stainless steels(10)	General service to 400 F based on 300 and 400 series stainless steels(10)	General service to 600 F based on 300 series stainless steel and nickel
H_2	Not usable in liquid H_2(7) General service above -100 F (based on mechanical properties)	Not usable in liquid H_2(7) General service above -100 F, based on mechanical properties	General service, liquid H_2

(1) -100 to 600 F: Recommended materials: AM-355 and 17-4PH

(2) -425 to 600 F: Recommended material: René 41

(3) -425 to 1500 F: Recommended material: René 41

Above 1500 F it will probably be necessary to use a refractory material, although René 41 can be used for short-life fittings up to 1800 F.

Assembly Torque

A torque of 2000 in-lb has been chosen as a reasonable limit for individual threaded assemblies whether they are threaded connectors or nut-and-bolt assemblies. Torque is determined by the amount of preload needed to assure the sealing and structural integrity of the fitting during the expected service life. Preliminary analysis summarized in a later discussion, indicates that all propellant and hot-gas fittings should be flanged connections. Threaded connections can be used up to 1-in. size for pneumatic service up to 2000 psi and 600 F. For service at 10,000 psi - 600 F, or 4000 psi - 1500 F, the apparent limit for threaded connections is the 3/4-in. size.

Recommended Fitting Classes

Based on the above considerations, five fitting classes are recommended, as shown in Table 3.

TABLE 3. RECOMMENDED FITTING CLASSES

Class	Temperature, F	Maximum Design Pressure, psi	Size, in.	Service	Type of Connection	Material
Ia	-100 to 600	2000	1/8 to 1	Pneumatic	Threaded	AM-355 or 17-4PH
b[b]	-100 to 200	1500	1 to 16	Propellants A[a]	Flanged	
IIa	-425 to 600	2000	1/8 to 1	Pneumatic	Threaded	René 41
b[b]	-425 to 200	1500	1 to 16	Propellants A and B	Flanged	René 41
IIIa	-425 to 600	10,000	1/8 to 3/4	Pneumatic	Threaded	René 41
b	-425 to 600	10,000	3/4 to 1	Pneumatic	Flanged	René 41
IVa[c]	-425 to 1500	4000	1/8 to 3/4	Pneumatic	Threaded	René 41
b	-425 to 1500	4000	3/4 to 1	Pneumatic	Flanged	René 41
V	1000 to 3000	1500	1 to 3	Hot gas	Flanged	Refractory

(a) The propellants are distinguished by two groups, as given in Figure 6.
(b) For large sizes where true maximum operating pressure is less than 1500 psi, a design on the basis of actual service pressure would result in a significant weight savings. Designs presented in this report are rated at maximum pressures.
(c) Fittings operating at higher temperatures (above 800 F) must be further qualified according to service life.

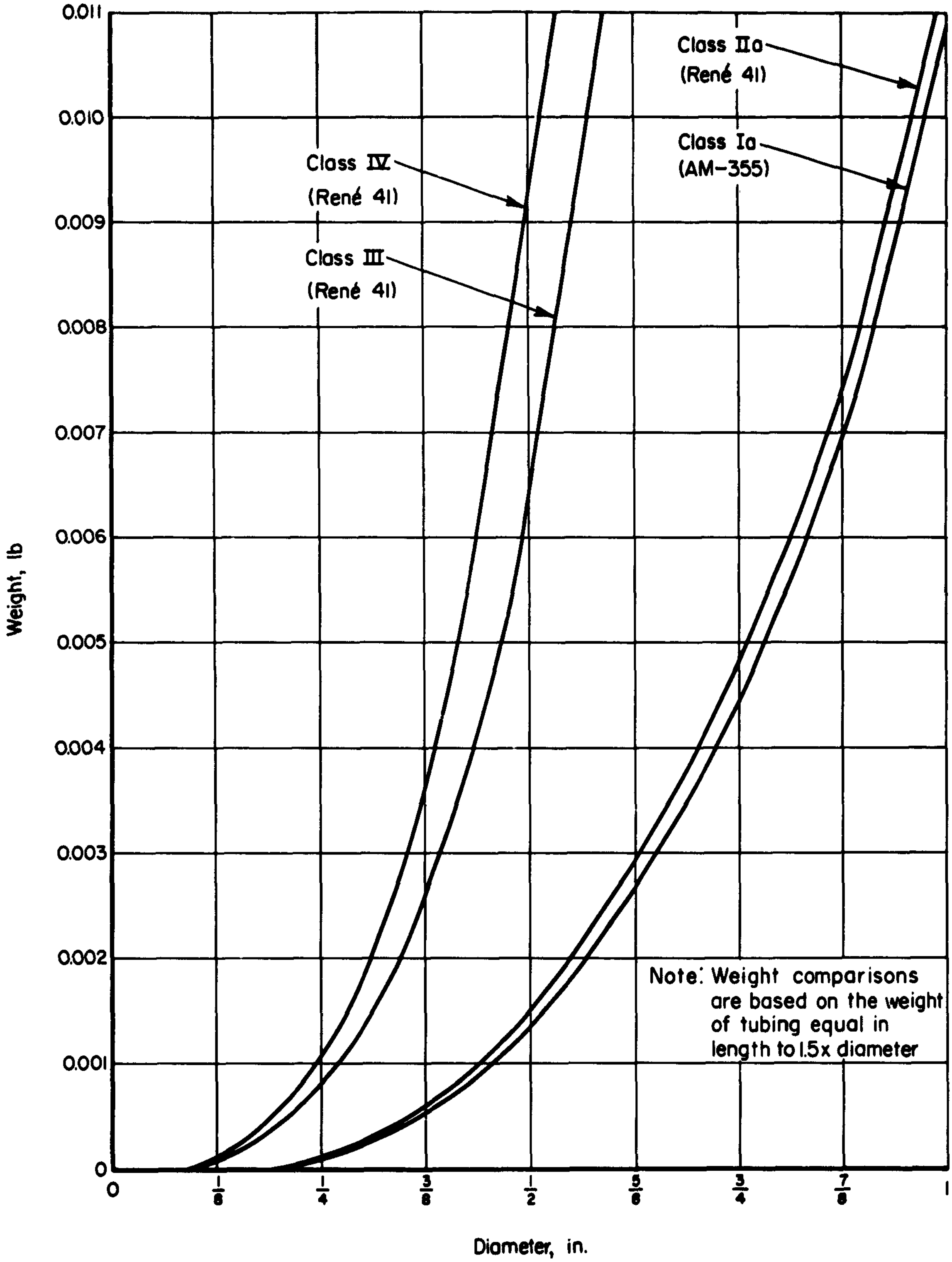

FIGURE 7. WEIGHT COMPARISON OF THREADED FITTING CLASSES

Class I is distinguished from Class II by the lower temperature limit, which allows for use of AM-355 or 17-4PH alloys. The high-pressure and high-temperature fittings are separated into Classes III and IV, on the basis of maximum service temperature. The Class IV fittings must be designed for a specified service life because of creep. Weight comparisons based on equivalent tube lengths (Figure 7) show that a 1/2-in. Class IV fitting may be 46.5 per cent heavier than a 1/2-in. Class III fitting. A 1-in. Class IIa fitting may be 4.7 per cent heavier than a 1-in. Class Ia fitting. However, the total weight increase per fitting may amount to less than 0.01 pound. Therefore, a class simplification is possible if these additional weights are not considered to be a severe penalty.

Classes III and IV are subdivided because of the 2000 in-lb torque limitation. It does not appear possible to overcome this limiting factor since the torque requirement for the 3/4 to 1-in. range is beyond a reasonable expectation of a man's capability with reasonable wrench lengths.

Although Classes Ib and IIb are designated, it is not recommended that discrete classes be established for large fittings. Instead a rigorous design procedure based on specific types of flanges should be developed as the controlling design specification. The flanges to be considered as the basis for this design procedure should be of the types illustrated in Figure 8. It may appear that this will complicate the logistics problem, but it should be noted that only a few large pipe fittings are used on each missile and that they vary significantly with missile type. Once a fitting is designed for a particular missile system, that fitting will probably be assigned a specific part number and can be ordered and stocked in appropriate quantities by that part number.

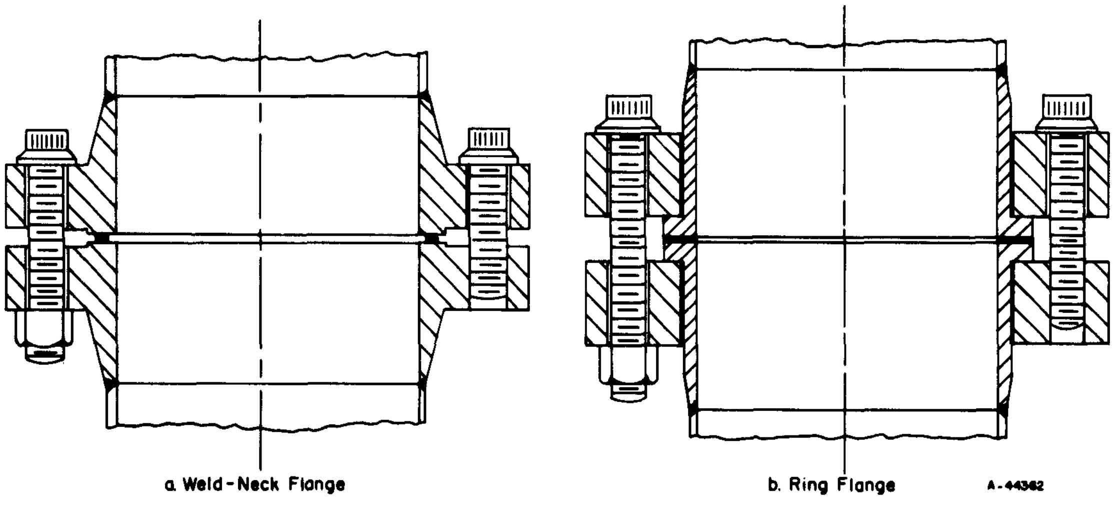

FIGURE 8. TYPES OF FLANGES CONSIDERED FOR RECOMMENDED FLANGE DESIGN PROCEDURE

References

(1) "Integrated Pressure Systems and Components (Portable and Installed)", Air Force Technical Manual T.O. 00-25-223 (February 1, 1962).

(2) Churchill, J. L., and Watson, J. F., "Properties of R-41 Sheet, A Vacuum-Melted, Nickel Based Alloy", Rept MGR-164, Convair Astronautics Division of General Dynamics Corporation (June 19, 1960).

(3) Christian, J. L., "Physical and Mechanical Properties of Pressure Vessel Materials for Application in a Cryogenic Environment", ASD-TDR-62-258 (March 1962).

(4) Liberto, Ralph R., "Storable Propellant Data for the Titan II Program", Bell Aerospace Systems Company, Contract No. AF 04(694)-72 (March 1962).

(5) Liberto, Ralph R., "Storable Propellant Data for the Titan II Program", Bell Aerospace Systems Company, Report No. AFBMD-TR-61-55, Contract No. AF 04(647)-846 (July, 1961).

(6) Headquarters Office Instruction Data Sheets, HOI 74-30-1 through HOI 74-30-13, 6593 Test Group Development, Edwards Air Force Base, California.

(7) Liquid Propellants Manual, Liquid Propellants Information Agency, Contract NORD 7386.

(8) "Compatibility of Materials With Demazine", Food Machinery and Chemical Corp., Inorganic Research and Development Department.

(9) Bloom, Ralph, Weeks, Loren E., and Raleigh, Charles W., "Materials for Construction of Equipment in Use with Hydrogen Peroxide", Becco Chemical Division, Food Machinery and Chemical Corp. (1959).

(10) Boyd, W. K., and White, E. L., "Compatibility of Rocket Propellants With Materials of Construction", Defense Metals Information Center, Memorandum No. 65 (September 15, 1960).

(11) Private communication from Herbert J. Wagner and Carl Lund, Battelle Memorial Institute.

(12) Baughman, R. A., "Gas Atmosphere Effects on 32367 Metals", General Electric Company Interim Progress Report No. 3R59AGT 137, Contract AF 33(616)-5667 (February 15, 1959).

(13) "Oxygen Difluoride (OF_2)", Product Data Sheet, Product Development Department, General Chemical Division, Allied Chemical Corporation (November, 1962).

FITTING-TO-FITTING CONNECTION

Design Parameters

Designs Considered

Design Procedure for Threaded Fittings

Design Procedure for Bolted Fittings

Application of Computer to Optimization of Design

References

FITTING-TO-FITTING CONNECTION

During the course of Phase I, many methods of assembling a mechanical connection in a pressurized piping system were studied. Evaluation of these concepts, however, made it apparent that none could compete in simplicity, ruggedness, and reliability with the conventional attachments consisting of either threaded nuts mated with threaded stub ends, in small sizes, or bolted-flanged connections in larger sizes. A comparatively large amount of experience with such structures is available, as are the results of substantial analytical and experimental research on threads, bolts, nuts, and flanges. These data are extremely helpful in establishing reliable designs in a relatively short time. In addition, designs based on these configurations can benefit from improvements which may be made in the future on such critical, basic mechanical elements.

While the fitting-to-fitting connection designs are conventional in the sense that threaded or bolted-flanged connections are basic configurations, the proposed designs contain a number of unique features in which light weight, ruggedness, and reliability are achieved by use of high-strength materials and suitable design procedures. To aid in the establishment of fitting classes, preliminary designs of five representative fittings have been prepared. Three of these correspond to the recommended classes (see Table 4), whereas the other two are presented for illustrative purposes only. These five designs are:

(1) 1-in. threaded fitting, maximum pressure 2000 psi, temperature range -100 to 600 F (Class Ia)

(2) 1/8-in. threaded fitting, maximum pressure 10,000 psi, temperature range -425 to 600 F (Class IIIa)

(3) 1-in. flanged fitting, maximum pressure 2000 psi, temperature range -100 to 600 F (for comparison with Class Ia)

(4) 1-in. flanged fitting, maximum pressure 10,000 psi, temperature range -100 to 600 F and 4,000 psi at 1500 F

(5) 3-in. flanged fitting, maximum pressure 1500 psi, temperature range -100 to 200 F (Class Ib).

In the following discussion the significant design parameters involved in designing a mechanical connection are first presented in general terms. Graphs and equations are given to indicate the approximate magnitude and significance of the effect of each parameter on the final design. Subsequently, the basic features of each selected design are described. Load and temperature factors, previously discussed in general terms, are applied to the specific fitting designs to illustrate the design procedure. The discussion is presented in four sections:

- Design Parameters
- Designs Considered
- Design Procedure for Threaded Fittings
- Design Procedure for Bolted Fittings
- Application of Computer to Optimization of Design

Design Parameters

The general discussion of design parameters presented below enumerates and explains the effects on the structural components of the fitting-to-fitting connection of such factors as structural loads, seal seating loads, preload, temperature, and fatigue. Also, the interactions between the seal, the tube-to-fitting joint, and the fitting-to-fitting structure are briefly discussed.

Structural Loads

The structure of a mechanical connection must be designed to withstand several types of load, which may be imposed individually or in combinations. These loads are shown in Figure 9.

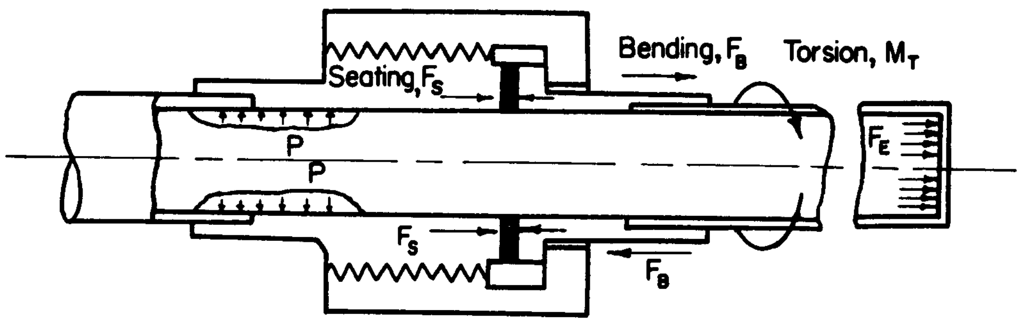

FIGURE 9. TYPICAL LOADS IMPOSED ON FITTINGS

Hoop Stresses From Internal Pressure. In the design of a tube for internal pressure, the hoop stresses are largest and control the design. In design of a fitting, however, the structure necessary to transfer axial loads requires an increase in wall thickness, so hoop stress from internal pressure becomes a secondary consideration.

Pressure End Load. The pressure end load acting on the structure is equal to

$$F_E = \frac{\pi}{4} G^2 P, \tag{1}$$

where

F_E = pressure end load, lb

G = effective seal diameter, in.

P = internal pressure, psi

Figure 10 shows values of the end load, F_E, for the maximum internal pressures of Fitting Classes I through V based on the approximation that G is equal to 1.1 the

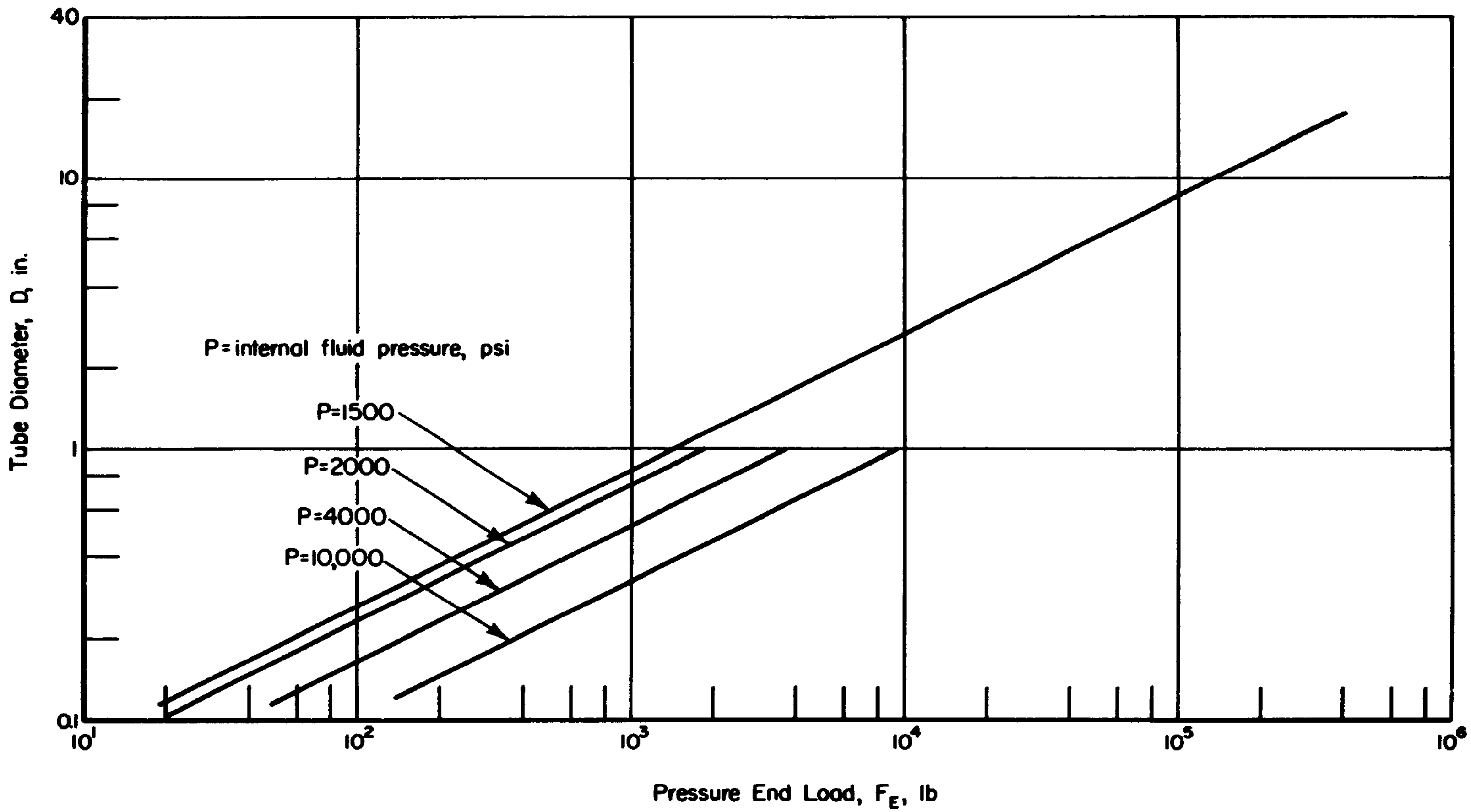

FIGURE 10. PRESSURE END LOAD ACTING ON FITTINGS AS A FUNCTION OF TUBE DIAMETER AND DESIGN PRESSURE

tubing diameter. For the larger sizes, this load becomes very high: 360,000 lb for a 16-in. fitting withstanding 1500-psi internal fluid pressure.

In some systems, the pressure end load may be absorbed primarily by anchors or clamps rather than transmitted through the fitting. In such systems, it may be possible to use lighter fittings. However, for general use fittings must be designed to withstand the total pressure end-load.

Bending Moments. A bending moment, M, producing bending loads, F_B, may be present because of tubing misalignment, thermal expansion or contraction of the tubing system, vibrations, displacements of anchors, or acceleration forces. Bending moments imposed on a fitting in a tubing system cannot be determined in advance, since these moments depend upon the specific tubing system, its operating conditions and the location of the fitting in the system. However, some limits, even if arbitrary, must be established to make design possible. For the fitting designs presented in this report the design limits are based on (1) the strength of the tube in the system and (2) the strength of equipment (compressors, pumps, pressure vessels, etc.) to which the tubing system is attached.

The maximum bending moment that can be applied to a fitting through the attached tubing is given by the equation

$$M = SZ, \tag{2}$$

where

S = limiting stress of tube material, psi

Z = section modulus of tube cross section, in.^{3}

Since both S and Z in Equation (2) depend on the material used for the tubing and its wall thickness, the bending moment, M, can be established only after the tube is selected. In the following, a procedure for establishing the design moment is shown for an assumed tube material and related wall thickness. Analogous bending moments for other tubing can readily be established by the same procedure.

It is assumed for illustrations of the procedure that the tube will be made of AM-350 stainless steel. This material is being used to some extent in missiles and, because of its high yield strength, a lightweight tube would be possible. The pertinent properties of AM-350 are:

Yield Strength at 70 F(14)*, psi	150,000
Fatigue Strength at 70 F(15), psi	
10^5 cycles	95,000
10^6 cycles	85,000
10^7 cycles	84,000

On the basis of the yield strength, S in Equation (2) could be as high as 150,000 psi. However, considering the requirement that the fitting, and therefore the tubing must be designed to withstand 200,000 cycles of reversed bending,** it is apparent that the fatigue strength rather than the yield strength will control.

*Numbers in parenthesis denote references listed on page 77.

**Paragraph III 2 g (page 5) Exhibit A "Technical Requirements, Development of Mechanical Fittings", Contract AF No. 04(611)-8176, March 13, 1962.

The fatigue strength of AM-350 for 200,000 cycles is about 90,000 psi. This, of course, is based on a smooth-specimen fatigue tests. In tubing systems there will be points of stress intensification at clamps and at curved tube sections. The stress-intensification factors may be of the order of two or larger. Accordingly, a fatigue stress limit of 50,000 psi has been used in computing the bending moment limit from Equation (2).

To compute the design bending moment by Equation (2), it is also necessary to determine the tube wall thickness, since the section modulus of the tube depends upon its thickness. Tube thickness can be computed with the following equation (based on hoop stresses):

$$t = \frac{PD}{2S_h} = \frac{PD}{200,000} \geq .005, \tag{3}$$

where

t = tube-wall thickness, in.

P = internal pressure, psi

D = tube diameter, in.

S_h = design stress, taken as two-thirds of the yield strength of AM-350 at 70 F

The thickness computed from Equation (3) can be very small, e.g., .001 in. for 1/8-in. tubing at 1500 psi. It is improbable that such very thin-walled tubing will be used. Accordingly, a minimum thickness of 0.005 in. has been used as the lower limit for tube thickness, t, in cases when Equation (3) gives values smaller than this limit.

For thin-walled tubing, the section modulus can be closely approximated by

$$Z = \frac{\pi D^2 t}{4} . \tag{4}$$

By substituting the value $S = 50,000$ and the expressions $t = \frac{PD}{200,000}$ and $Z = \frac{\pi D^2 t}{4}$ in Equation (2), the bending moment can be determined as

$$M = 0.197\ PD^3 \quad t > .005 . \tag{5}$$

When $t = 0.005$, the bending moment is

$$M = 197D^2. \tag{6}$$

In smaller fittings for lower pressures the design will be controlled by the seal-seating load (discussed in the next section); hence, there will be a substantially larger bending-moment allowance than indicated directly by Equations (5) and (6). The approximate bending-moment allowance for small fittings is shown on Figure 11, along with bending-moment requirements implied by MIL-F-18280A, Par. 4.3.3.3.3 for comparison.

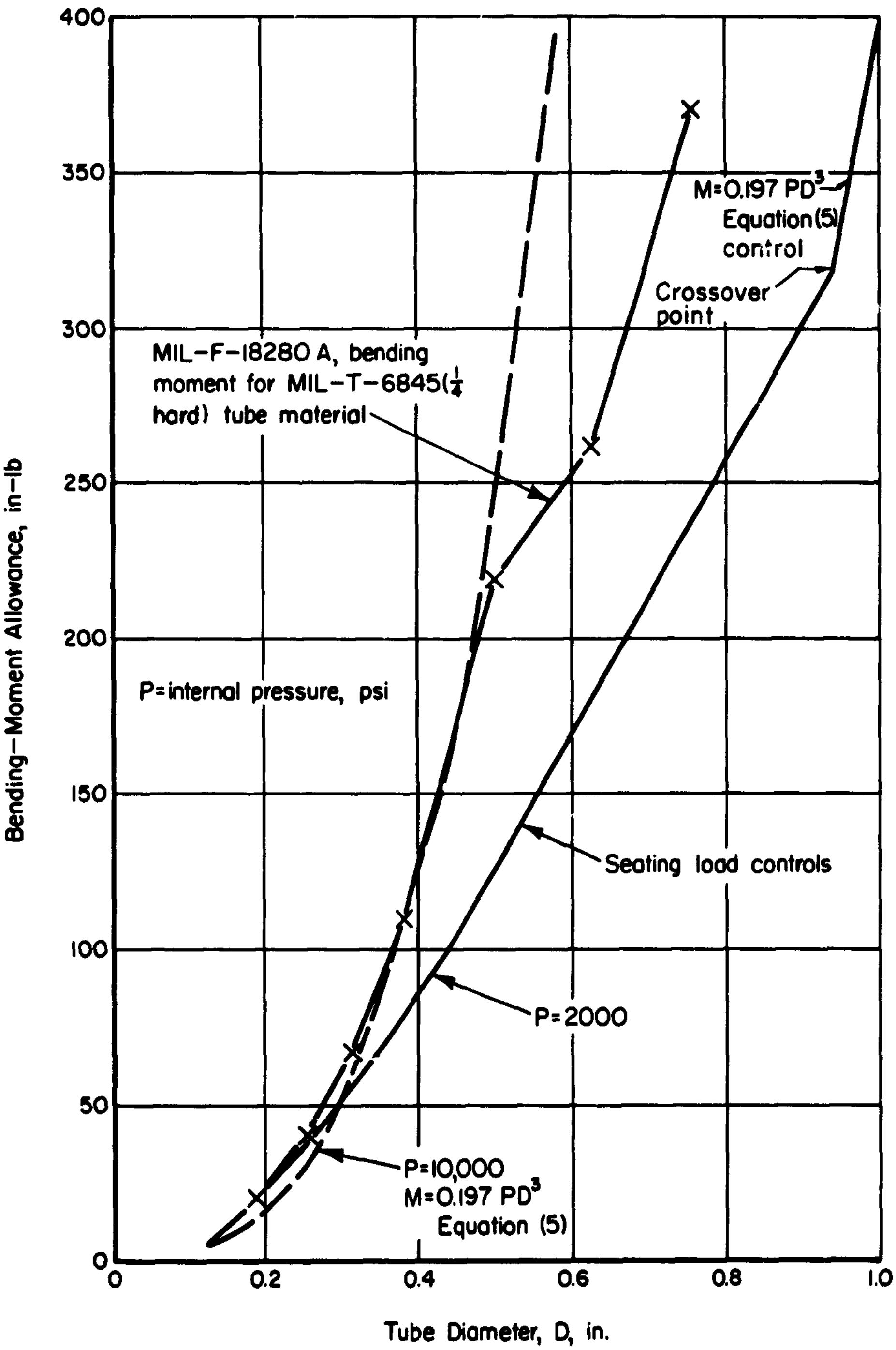

FIGURE 11. COMPARISON OF BENDING-MOMENT ALLOWANCE FOR SMALL FITTINGS

While Equations (5) and (6) provide a reasonable design basis for small fittings, the bending moments calculated may be unnecessarily high for large fittings. The limitations on bending moments which can be applied to equipment to which the tubing is attached are not known; however, some indication of the limits may be obtained from the bending moments permitted on the piping connections to steam turbines[17], as shown on Figure 12. It is apparent that, even for equipment as heavily constructed as power-plant steam turbines, the bending-moment allowance is substantially less than that given by Equation (5).

Another general indication of typical bending moments on flanged joints given by Rossheim and Markl[18] is

$$M = 60\,(D + 3)^3 \text{ in-lb.} \tag{7}$$

Equation (7) was originally developed as part of a review of a large number of stress calculations on piping systems. It may be considered as a typical bending moment that may occur in piping systems in power plants, chemical process plants, and oil refineries. Equation (7) is also plotted on Figure 12.

Design bending moments obtained from the larger of the moments from Equations (5) and (6), but not exceeding the moment obtained from Equation (7), are shown on Figure 13. These are the moments proposed for use in designing the fitting-to-fitting structure.

<u>External Axial and Torsional Loads</u>. External axial and torsional loads arise from the same causes as do bending loads. External axial loads are usually minor and can be discounted. Torsional loads are basically limited to three-dimensional tubing systems and may be a problem if sufficiently large to cause rotation of one part of the joint with respect to the other. Rotation could cause leakage, in either threaded or bolted fittings, because the seal is disturbed. It could also cause back-off and preload relaxation in a threaded joint. A torsional resistance of the fitting equal to that which can be safely imposed on the fitting by the attached tube is suggested as a design basis.

Seal-Seating Load

Quite independent of the structural load, the fitting structure must also be designed to withstand those loads required to produce intimate mating between the fitting's seal-contact faces and the seal. The factors involved are discussed on pages 97 through 99. For the purpose of fitting-to-fitting design, it has been assumed that an initial seating load of 1000 lb per linear in. of gasket length is required. The seal-seating load, F_G, is given by the equation

$$F_G = 1000\,\pi G \text{ (lb)}, \tag{8}$$

where G = effective seal diameter. For preliminary evaluation, G may be taken as 1.1 D, where D is the tube size, giving

$$F_G = 3460\,D \text{ (lb)}. \tag{9}$$

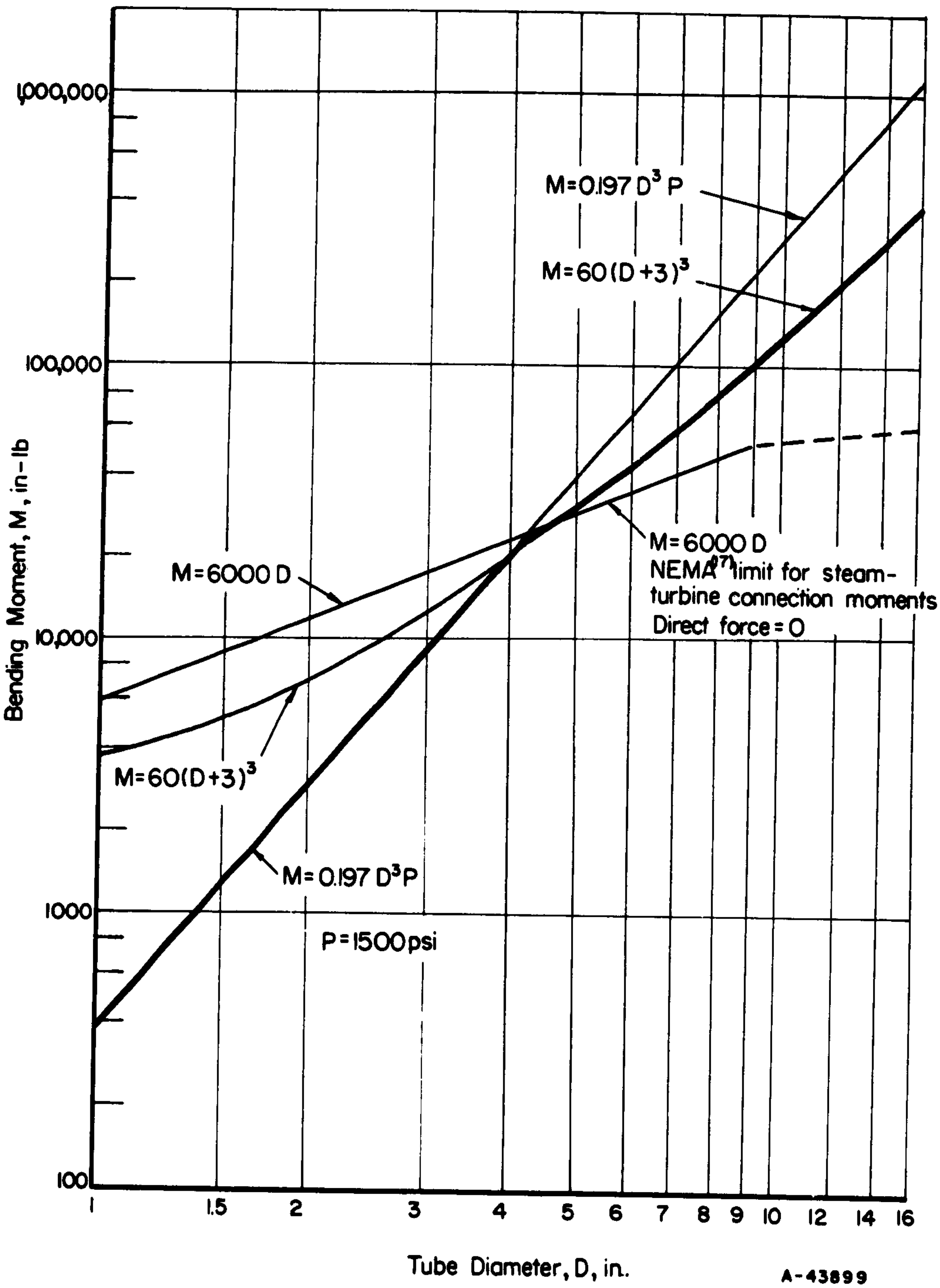

FIGURE 12. BENDING-MOMENT-LIMITED COMPARISON FOR LARGE FITTINGS, DESIGN PRESSURE AT 1500 PSI

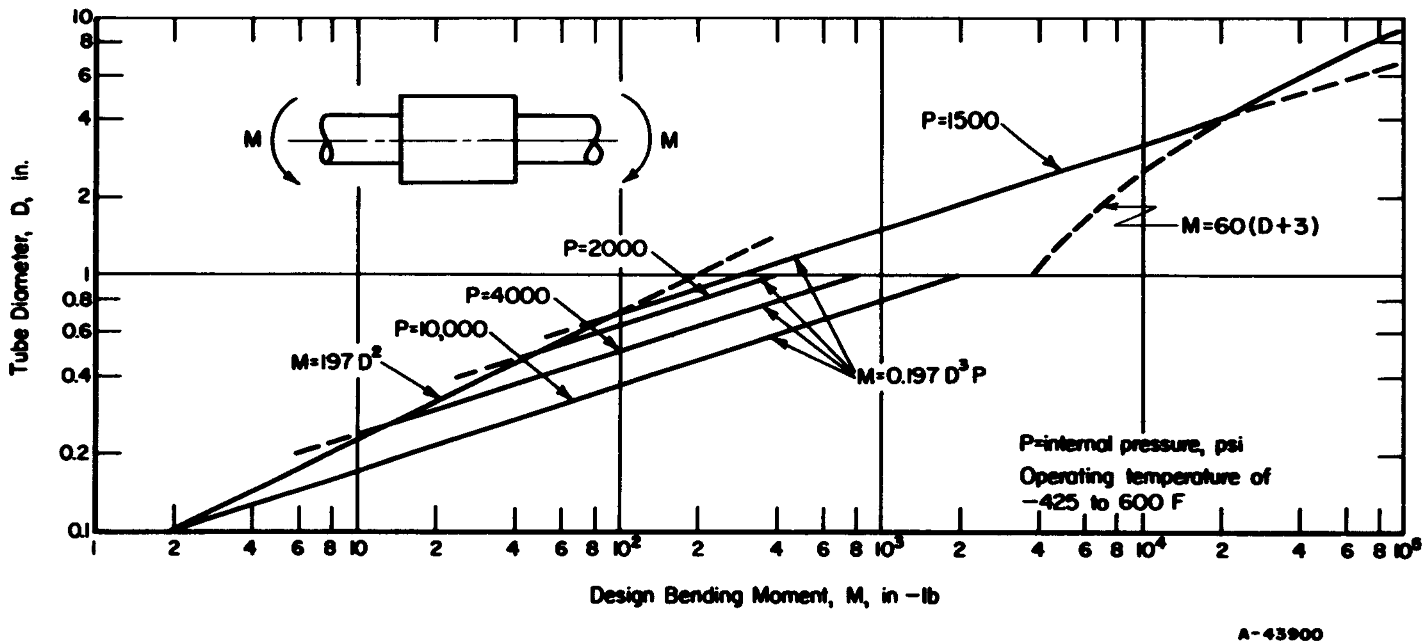

FIGURE 13. PROPOSED DESIGN BENDING MOMENTS FOR FITTINGS

Design Loads

The structural load applied by internal pressure is an axially symmetric load with respect to the fitting structure, since the fitting structure, in the design concepts proposed, is itself symmetric about the longitudinal axis of the tube. Although an analysis of axially symmetric structures similar to the configurations used in the fittings is quite complex, theoretical methods are available which make possible a fairly precise engineering design of axially symmetric loads such as that produced by internal pressure.

The structural load applied by bending, however, is not symmetrical. In the following, a pressure, P_B, equivalent to the bending moment, will be derived. The equivalent pressure, P_B, can then be handled in the same way as the actual pressure, P, i.e., by using theoretical methods for axially symmetric loads.

When a bending load is imposed on the fitting through the piping, a maximum tensile stress will exist at one point on the circumference. A diametrically opposed maximum compressive stress will arise simultaneously. However compressive failure is not likely to occur since the cumulative sum of the tensile stresses due to bending and the pressure end load is greater. In any case, the minimum strength of the fitting is equal to or greater than the maximum strength of the tubing under conditions where compressive failure might occur. The maximum tensile stress will be given by the equation

$$S_B = \frac{M}{Z}\ , \tag{10}$$

where

S_B = maximum bending stress in tube, psi

M = design bending load, in-lb (From Figure 12)

Z = section modulus of tube, in^3.

While this tensile stress exists at only one point on the circumference, it can be conservatively assumed that the fitting may be designed as if S_B, the maximum bending stress, existed uniformly all around the tube circumference. With this assumption, it is possible to express the bending load as an equivalent internal pressure, P_B, which is given by the equation

$$P_B = \frac{4S_B t}{D}\ , \tag{11}$$

where

P_B = equivalent internal pressure, psi, from design moment, M.

S_B = maximum bending stress in tube, psi

t = tube-wall thickness, in.

D = outside diameter of tube, in.

If it is assumed that a tubing material such as AM-350 precipitation-hardening stainless steel with a design stress of S_h = 100,000 psi is used, the required tube-wall thickness can be determined by Equation (3). The equivalent axial load, F_B, in terms of P_B is

$$F_B = P_B \frac{\pi}{4} G^2\ . \tag{12}$$

Figure 14 shows F_B as a function of size and pressure.

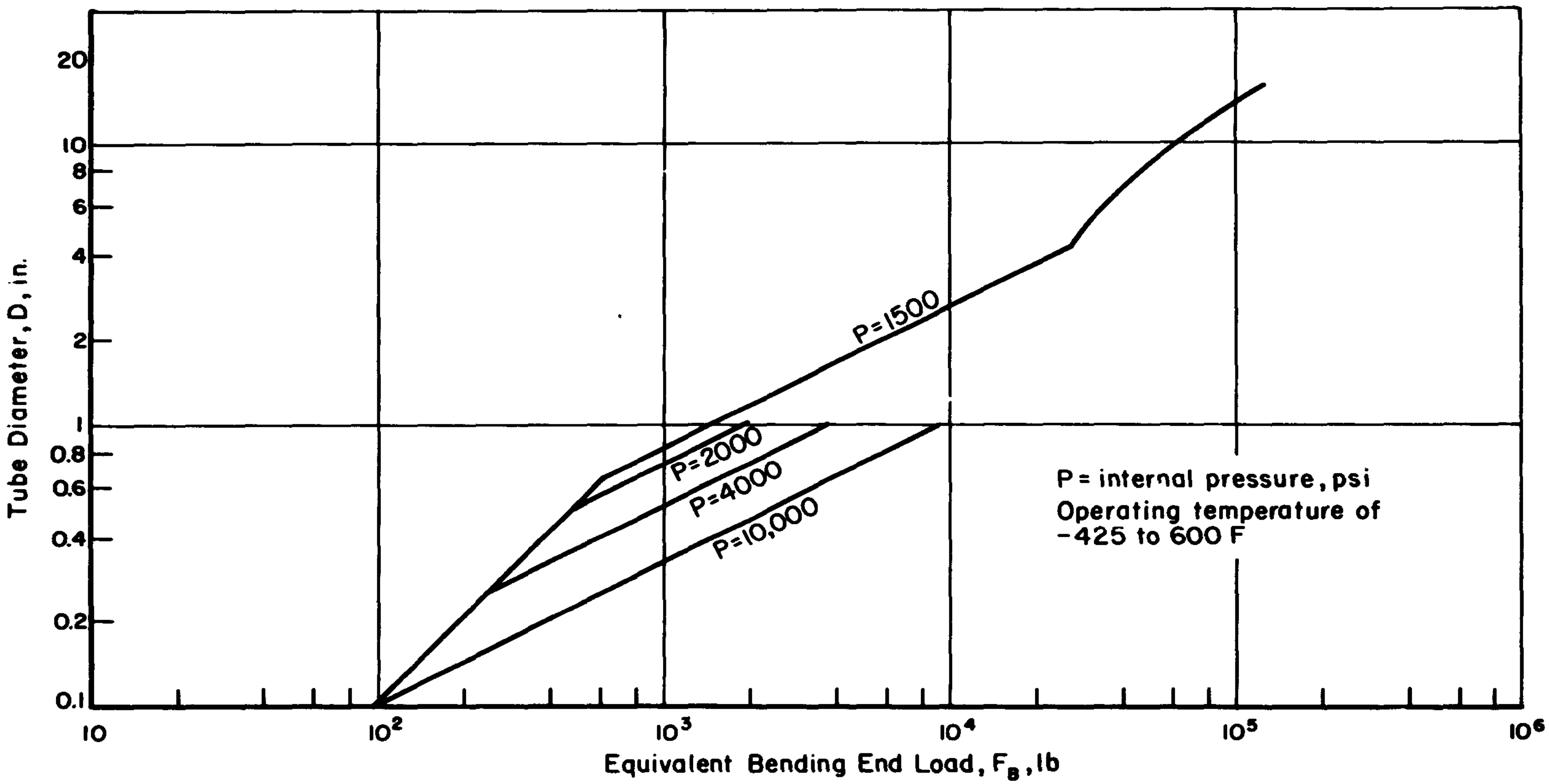

FIGURE 14. EQUIVALENT BENDING END LOAD AS A FUNCTION OF TUBE DIAMETER AND DESIGN PRESSURE

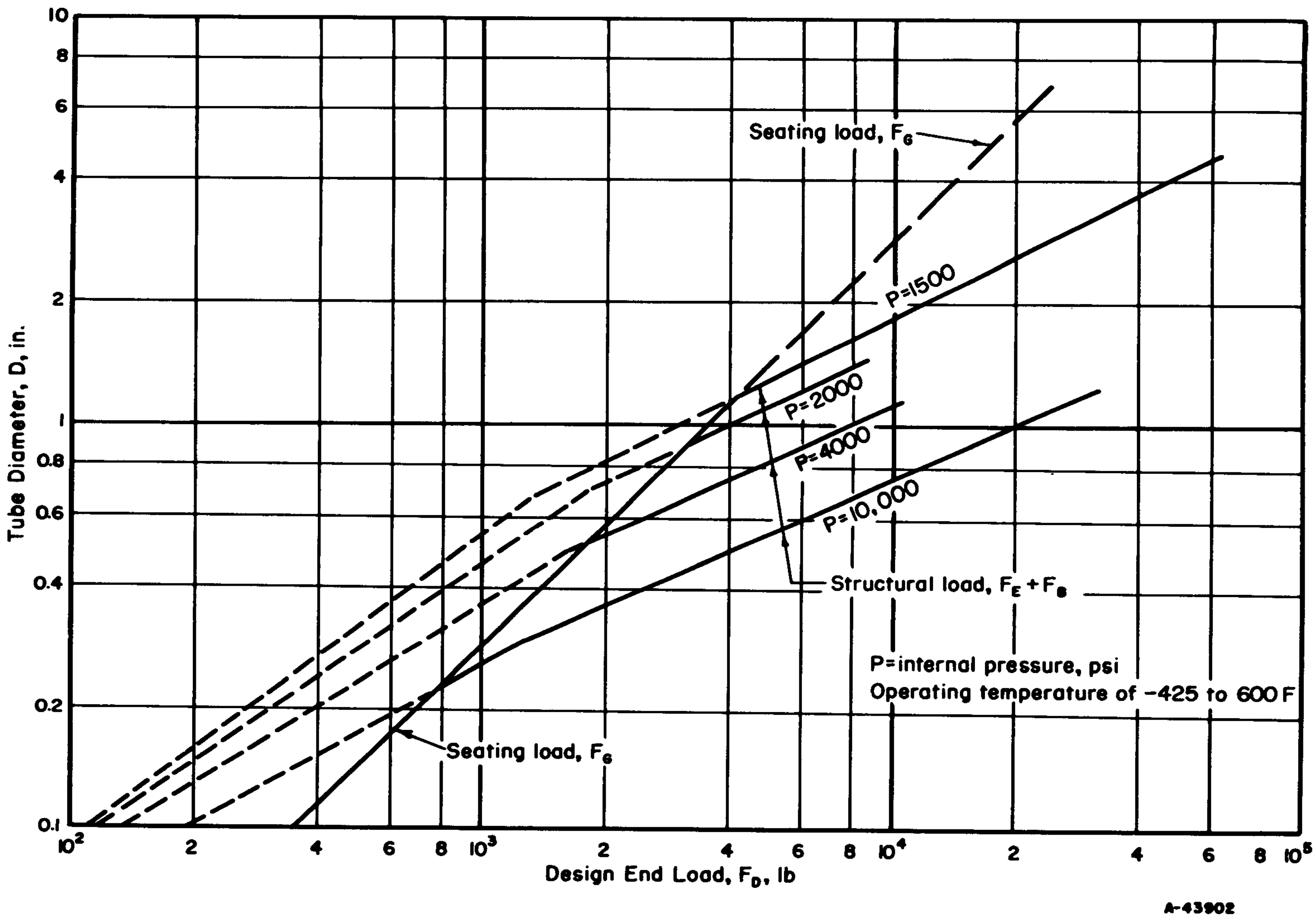

FIGURE 15. DESIGN END LOADS (GREATER OF F_G OR $F_E + F_B$) AS A FUNCTION OF TUBE DIAMETER AND DESIGN PRESSURE

The total structural load the fitting must carry is at least equal to the sum of the pressure end load and the pressure equivalent of the bending loads. However, the total structural load may not be the controlling design load since the load required to seat the gasket may be greater. The load required to seat the gasket given by Equation (9) and the total structural load are plotted in Figure 15. Figure 15 shows approximately the crossover point where either seating load or structural loads control the design. As an example, for a 3/8-in. fitting (D = 0.375), the seating and structural loads for different internal pressures are given in Table 4. The design load for each pressure is

TABLE 4. DESIGN LOADS FOR 3/8-IN. FITTING

(-425 to 600 F Operating Temperature)

Design Pressure, psi	Seating Load, lb	Structural Load, lb
1,500	1,300	600
2,000	1,300	750
4,000	1,300	1,000
10,000	1,300	2,100

underlined. For the 3/8-in. fitting the seating load is greater for design pressures of 1500, 2000, or 4000 psi, and only for a design pressure of 10,000 psi is the structural load the controlling factor.

Preload

Mechanical connections in a piping system are usually tightened so that an axial preload force in excess of the design structural load is created. In flanged connections, determination and control of the preload is accomplished more easily than in threaded connection. In threaded fittings the need for attaining a desired or required preload is often neglected although the principles involved apply as well to threaded connections as to flanged connections.

In service the action of the imposed axial loads is to "pull" the mating parts of the fitting apart. Any degree of separation generally will lead to early failure. Therefore in order to counteract this action it is necessary to prestress the flange members of the fitting in compression an amount greater than the expected strain relaxation caused by the tensile axial loads. Of course, preloading causes an initial tensile stress in the bolts or threaded nuts. This tensile stress may increase when the service loads are applied, and a balance must be achieved between a preload which is sufficient to prevent flange separation and a preload so large as to cause eventual tensile stress failure of the bolt or threaded nut. The factors that must be considered in determining the required preload are: (1) the spring constants of the compression and tension members, (2) the minimum compressive load on the flange members needed to prevent leakage, (3) the maximum allowable stress in the tensile members, (4) the magnitude of the structural loads, and (5) the effects of the thermal gradients.

The problem of a preloaded joint is statically indeterminate; hence, it must be solved on the basis of displacements of the structure. Calculations of displacements become quite complex where stretching and bending of structural parts, changes in moment arms, and radial effects of internal pressure are involved. A basic understanding of the problem, however, can be obtained by disregarding the effects of moment-arm changes and the radial components of internal pressure. The following discussion is therefore limited to a simple case analogous to that shown in Figure 16, where only tensile and compressive displacements are considered.

In threaded fittings, the nut is the tension member, analogous to the bolt in Figure 16. The stub ends and seal are the compression members analogous to the rings and seal of Figure 16. In flanged fittings, the bolts are analogous to the bolt and the flanges and seal are analogous to the rings and seal of Figure 16.

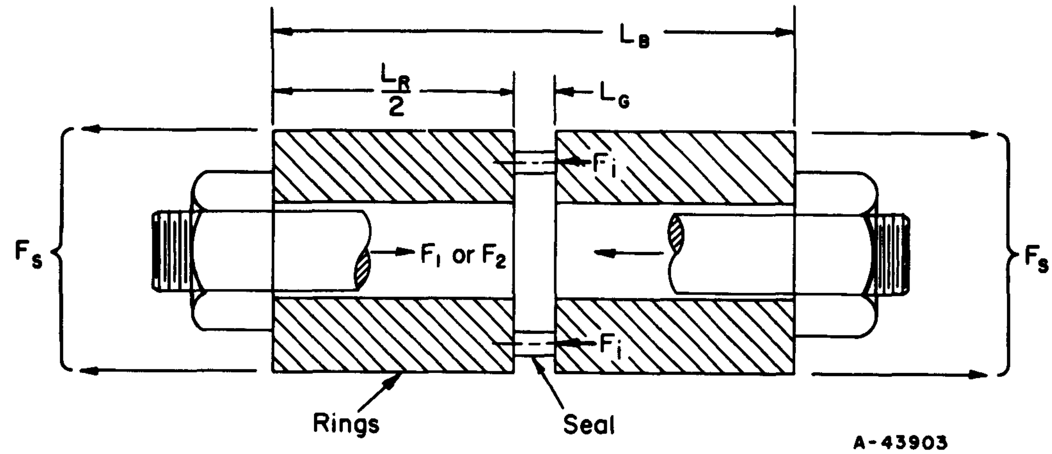

FIGURE 16. MODEL OF SIMPLIFIED PRELOAD THEORY

When the nut on the bolt is tightened, there will be an increase in bolt length and a decrease in the length of the rings and seal, given by

$$\delta_B = \frac{F_1 L_B}{E_B A_B}, \quad \delta_R = \frac{F_1 L_R}{E_R A_R}, \quad \delta_G = \frac{F_1 L_G}{E_G A_G},$$

where subscripts B, R, and G refer to the bolt, rings, and seal, respectively, and

F_1 = initial bolt axial force, lb
L = free axial length, in.
E = modulus of elasticity, psi
A = cross-sectional area, in.^{2}

When a load F_s is applied (as from the attached tube in the actual fitting), the force in the bolt in Figure 16 changes to F_2 and

$$\delta_{B2} = \frac{F_2 L_B}{E_B A_B}, \quad \delta_{R2} = (F_2 - F_s)\frac{L_R}{E_R A_R}, \quad \delta \quad = (F_2 - F_s)\frac{L_G}{E_G R_G}.$$

The change in length of the bolt must remain equal to the combined changes in lengths of the rings and gasket:

$$\delta_{B2} - \delta_B = (\delta_R + \delta_G) - (\delta_{R2} + \delta_{G2}) \tag{13}$$

or

$$(F_2 - F_1)\frac{L_B}{E_B A_B} = (F_1 - F_2 + F_s)\left(\frac{L_R}{E_R A_R} + \frac{L_G}{E_G A_G}\right). \tag{14}$$

Defining $\frac{L_B}{E_B A_B} = R_B$ and $\frac{L_R}{E_R A_R} + \frac{L_G}{E_G A_G} = R_G$ as the spring constants (in. /lb), and collecting terms in Equation (14),

$$F_2(R_B + R_G) = F_1 (R_B + R_G) + F_s R_G, \tag{15}$$

or

$$F_1 = F_2 - \frac{F_s}{1 + \frac{R_B}{R_G}} \quad . \tag{16}$$

If F_2, the maximum allowable load, and R_B and R_G, the spring constants, can be determined or closely approximated, the analytical determination of F_1 the preload is relatively simple by means of Equation (16). However, this simple case, if changed into a graphical representation, can be handled more easily when thermal effects are subsequently introduced. In a later discussion of the proposed fitting-to-fitting connections, the graphical presentation has been used extensively.

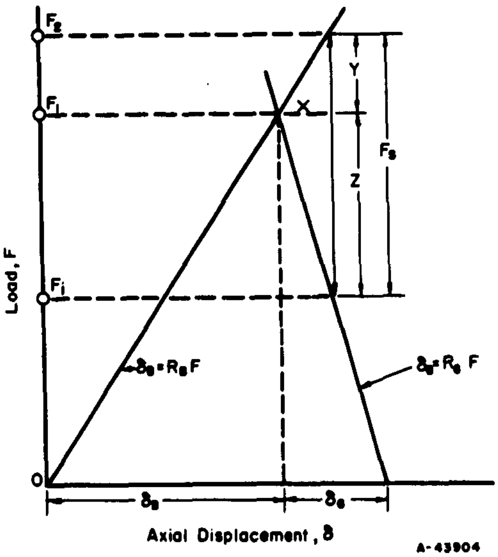

FIGURE 17. GRAPHICAL ILLUSTRATION OF SIMPLIFIED PRELOAD THEORY

The graphical representation of the basic relationships is shown in Figure 17. A line is drawn from the origin with a slope $\frac{\delta_B}{F} = R_B$. A second line, with slope $\frac{\delta_G}{F} = R_G$, is drawn to intersect the first line at $F = F_1$. The force applied, F_s, is drawn between the two intersecting lines as shown in the figure. As can be seen in the construction, $F_2 = F_1 + Y$. Since $\frac{X}{Y} = R_B$ and $\frac{X}{Z} = R_G$ and $Y + Z = \frac{X(R_B + R_G)}{R_B R_G} = F_s$:

$$X = \frac{F_s R_B R_G}{R_B + R_G}, \text{ and with } Y = \frac{X}{R_B}$$

$$F_2 = F_1 + Y = F_1 + \frac{R_G F_s}{R_B + R_G} = F_1 + \frac{F_s}{1 + \frac{R_B}{R_G}} .$$

Accordingly, the construction shown by Figure 17 is a graphical presentation of Equation (16).

The load existing at the gasket, F_i, can be obtained from static equilibrium:

$$F_i = F_2 - F_s . \tag{17}$$

From a fitting-design standpoint, it is necessary that the average stress on the seal contact area be at least equal to the internal pressure to prevent leakage.* This stress is simply the load at the seal, F_i, divided by the seal contact area. Equations (16) and (17) give means of calculating the required preload, F_1, in order to maintain a required residual seal load, F_i, after application of the structural load, F_s. Equations (16) and (17) may be combined to give

$$F_1 = F_i + \frac{\frac{R_B}{R_G}}{1 + \frac{R_B}{R_G}} F_s . \tag{18}$$

In the preceding discussion, the seal has been considered as not pressure energized. When considering a typical metal pressure-energized seal, reduction of F_i to a low value has a different but equally significant implication in the fitting design. A characteristic of many metal pressure-energized seals is that in order for the seal to be flexible enough to give any appreciable seal follow-up from internal pressure, its flexibility is such that it will withstand only a negligible amount of preload; almost all of the preload is supported by the fitting faces adjacent to the seal, or, in some designs, by a rigid part of the seal itself. With this type of seal, reduction of F_i to zero implies a separation of the fitting interface. In this case, leakage may not result under static conditions because of pressure-generated seal follow-up; however, vibration of the tube system may produce sufficient movement to cause flexing of the metal seal, thus possibly leading to leakage by abrasion of the sealing surfaces, or fatigue failure of the metal seal. Accordingly, even with a pressure-energized seal, the lower limit on F_i is an important design consideration.

In actual fitting design, other factors which influence the preload requirements are:

(1) Rotation of flanges

(2) Moment-arm changes as the load is transferred from the seal to the tube

(3) Radial effect of internal pressure.

*This is a theoretical lower limit on residual seal-contact-area stress and presumes a "perfect match" between sealing surfaces. This "perfect match" between sealing surfaces is, in practice, never really achieved but may be approached by adequate seal-seating load. In designs discussed later herein, a lower limit of 3 times the internal pressure has been used as a minimum residual seal-contact-area stress.

An equation for calculating F_2, including these factors, is

$$F_2 = F_1 + \alpha P, \tag{19}$$

where

P = internal pressure, psi

$$\alpha = \frac{\pi h_G}{4Q}\left\{\left[\frac{q_G}{h_G} - 2q_F(h_T - h_G)\right] G^2 - 2q_F B^2(h_D - h_T) - \frac{8}{\pi} q_r\right\}.$$

Equation (19) and the definition of α are taken from Wesstrom and Bergh[19] and Rodabaugh[20]. Symbols used are defined in Appendix I. The definition of α is directly applicable to a flanged fitting in which the flanges are identical. It may readily be adapted to a flanged fitting in which the two flanges are not identical. It may also be adapted to design of threaded fittings.

Equation (19), of course, reduces to Equation (16) when only tensile and compressive deformations are considered. Equation (17) can be used with Equation (19) to determine the relationship between F_1, F_s, and F_i.

Temperature Effects

In the preceding sections only design loads essentially at ambient temperature were discussed. When the effects of temperature change are considered, the design problem becomes more complex.

Creep or Relaxation.

At high temperatures, the strain in a metal part under stress cannot be considered as independent of time. In a mechanical connection, where creep produces a reduction in preload and in turn a reduction in stress, the problem becomes one of relaxation with variable stress.

An accurate theoretical method for calculating the performance of a threaded or flanged fitting under creep or relaxation conditions has not been developed insofar as the authors are aware. The problem is very complex because of the variable stress field in the structure, nonlinear relationships that are a result of elastic-plastic deformations, and the introduction of time as an additional parameter.

In view of the necessity for design under creep or relaxation conditions, an approximate theoretical design procedure has been established, as shown and discussed in Appendix II. This design method has the virtue of relative simplicity and is believed to be conservative.

Thermal Gradients.

If a cold fluid, like liquid oxygen, is suddenly introduced into a piping system, the temperatures of metal parts in direct contact with the fluid will decrease rapidly. The temperatures of those parts not in direct contact, such as the nut of a threaded fitting or the bolts of a bolted fitting, change less rapidly because of the air-film resistance between parts. Accordingly, there is a period during which the average temperature of the interior parts of the fitting is lower than the average temperature of the exterior parts. During this time effective preload decreases because of the relative thermal expansion of the fitting nut or bolts.

When a hot fluid is introduced into a piping system the internal parts may become hotter than the external parts. This increases the preload, since a relative thermal contraction of the nut or bolts occurs. However, there is also the possibility of yielding of some member of the fitting, and if temperature equality were later re-established, the preload might be partially or completely removed, with consequent leakage.

The temperature difference is a function of the fluid properties and flow velocity, as well as the properties of the fitting and its material; hence, a numerical value for this temperature difference can be calculated only for each specific case. To facilitate fitting design, the following limits have been set for the permissible temperature gradients:

Service Temperature, F	Maximum Design Temperature Difference*, F
-100 to 600	50
-425 to 1500	200

A relatively thin-wall tube will change in temperature more rapidly than will the more massive fitting parts. Therefore, the tube will exert either a radially inward or outward force on the flanges or stub ends, depending on whether cooling or heating is occurring. In either case a consequent tendency for parts to rotate relative to each other will be a design factor. Although this factor has not been evaluated in the preliminary design, it should be considered when final designs are established.

A nonsymmetrical temperature condition exists when some types of hot or cold fluids are introduced into a horizontal pipeline. The colder liquid tends to flow along the bottom half of the tube while the relatively warm vapor is near the top. This heterogeneous flow pattern causes "bowing" of the pipeline, with resulting high bending moments transmitted to the mechanical fitting. This condition is specific to a given piping system and when it is present its effect should be considered by the designer as a beinding moment which should be held within the bending-moment limits established previously.

Modulus of Elasticity. When the temperature of a fitting changes, there is a corresponding change in the modulus of elasticity and in the effective preload, F_1, to a new value, $(F_1)_T$. For AM-355 and René 41 in the temperature range under consideration, this effect is shown in Table 5.

With decreasing temperatures, the structure must retain a sufficient strength margin to prevent overstress by the consequent load increase. For the two materials considered, the yield strength increases more rapidly than does the modulus of elasticity and, therefore, the change in preload is not a design problem. However, for increasing temperatures, the structure must be endowed with extra preload to maintain an adequate residual load at temperature. As an example, for AM-355 for service at 600 F, this requires about 11 per cent extra preload.

*If in actual service the design limits are exceeded, use of a thermal shield is suggested. This could be simply a cylindrical sleeve at the bore of the fitting which provides a stagnant space between it and the fitting bore to retard heat transfer from the fluid to the fitting.

TABLE 5. CHANGE IN EFFECTIVE PRELOAD AS FUNCTION OF TEMPERATURE

	$(F_1)_T/F_1$ at Indicated Temperature				
	-425 F	-100 F	70 F	600 F	1500 F
AM-355	(a)	1.00	1.00	0.90	(a)
René 41	1.10	1.03	1.00	0.92	0.75

(a) Not used at these temperatures.

Threaded Versus Bolted Fittings

Considering pipe and tubing systems in general, threaded fittings are generally used in small sizes (1/8 to 1/2 in.). There is an overlapping size range of about 1/2 to 4 in. in which selection of threaded or bolted fittings depends upon the detailed service requirements of pressure, temperature, reliability, and installation conditions. For sizes larger than 4 in., bolted fittings are generally used.

Perhaps the most significant factor involved in the choice between threaded or bolted fittings is the torque required for preloading. In contrast to threaded fittings, in which the preload is applied by tightening a single threaded element, the preload is applied to bolted fittings by means of several comparatively small threaded elements, so while the preload is approximately the same, the required assembly torque is much lower for bolted fittings of comparable size and rating. The torque required to preload threaded fittings may be approximated by the equation

$$T = 0.2\, dF_1, \tag{20}$$

where

T = required preload torque, in-lb

d = nominal thread size, in.

F_1 = required preload, lb.

For preliminary evaluation purposes, d may be taken to be 1.30 D. As discussed in the next sections on design procedures, F_1 can be established only after detailed dimensions of the fitting are selected. However, for preliminary evaluation of torque requirements, F_1 may be taken as equal to F_D. The design load, F_D, is shown in Figure 15. With these assumptions, torque requirements have been calculated and are plotted in Figure 18.

The torque that can be applied to a fitting depends on numerous factors; e.g., the type of tool being used, the precision with which torque must be applied, the space around the fitting as initially installed and, as might be the condition for subsequent disassembly and reassembly, the space for a workman to stand and brace himself while applying the torque. Obviously, in designing a line of fittings for general use, any maximum torque limit is necessarily somewhat arbitrary. However, based on general experience with pipe and tube fittings, an upper limit of 2000 in-lb of torque appears

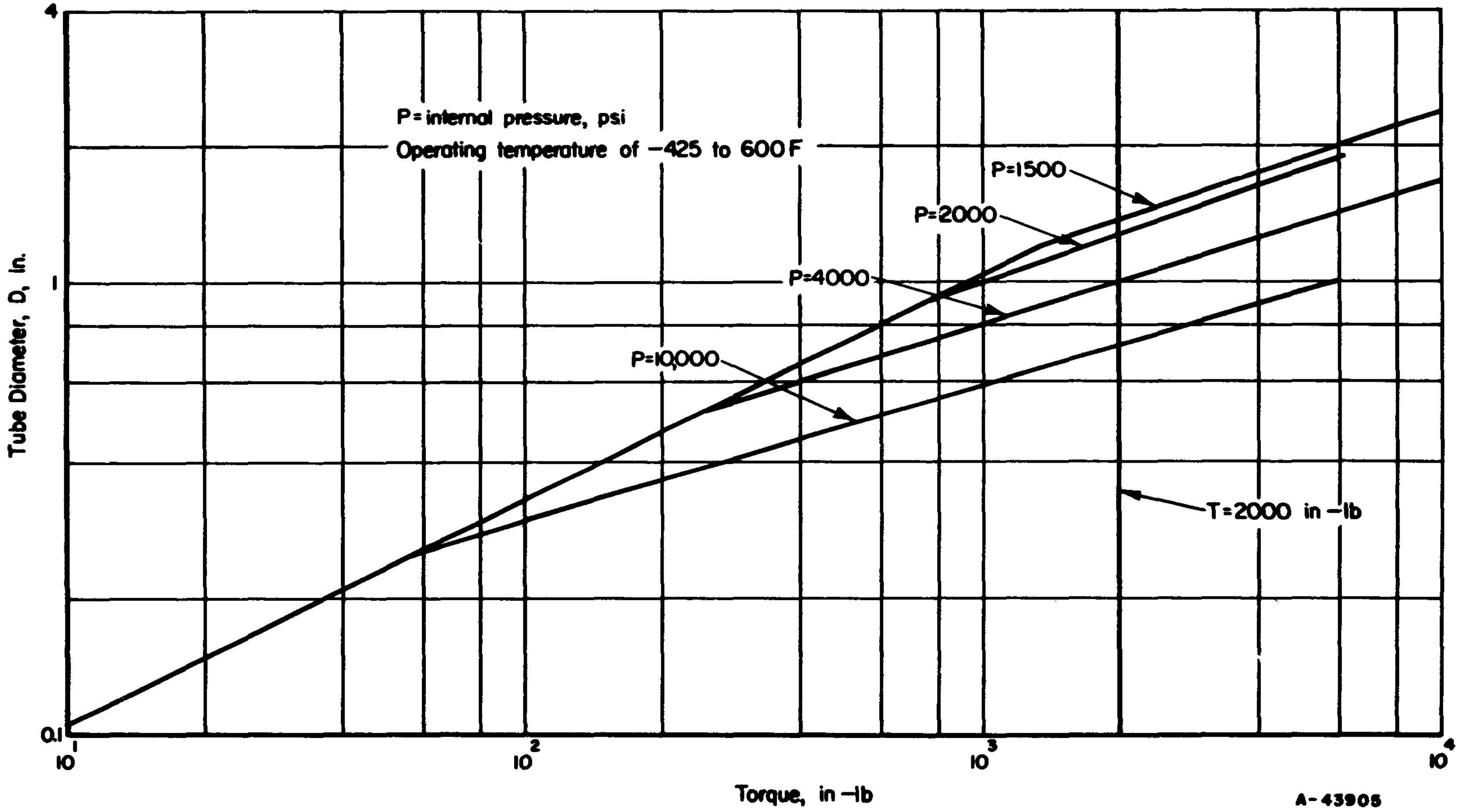

FIGURE 18. PRELIMINARY ESTIMATE OF PRELOAD TORQUE FOR THREADED FITTINGS

reasonable. This torque limit, when transferred to Figure 18, subdivides the fittings into threaded and bolted as shown in Table 6.

TABLE 6. DIVISION OF FITTINGS INTO THREADED AND BOLTED, BASED ON A MAXIMUM TORQUE OF 2000 IN-LB

(-425 to 600 F Operating Temperature)

Design Pressure, psi	Threaded-Fitting Sizes, in.	Bolted-Fitting Sizes, in.
1,500	1/8 through 1-1/4	1-1/2 and larger
2,000	1/8 through 1	(a)
(4,000)(b)	1/8 through 1	(a)
10,000	1/8 through 1/16	3/4 through 1

(a) Larger sizes are not included in these pressure classes.
(b) The design pressure of 4000 psi is shown for information only. Fittings for 4000 psi and 30-minute life at 1500 F will probably be similar to the 10,000 psi-fittings at 600 F.

A more detailed analysis, in which actual fitting geometry is established, will shift this division, but Table 6 may be taken as a preliminary indication of the division between threaded and flanged fittings based on torque requirements. Table 3 shows slightly smaller-size divisions between threaded and bolted fittings in Classes I and II than shown in Table 6, reflecting an anticipation that preloads (F_1) will be somewhat higher than design loads (F_D).

Fatigue

In general, tube or pipe fittings are subject to fatigue damage due to cyclic bending (vibration) of the piping system. When the fitting is properly preloaded, the cyclic stress in the fitting-to-fitting structure will be low and fatigue failure of the fitting-to-fitting is not anticipated. Fatigue failure, with cyclic bending of the attached pipe, is more likely to occur at the tube-to-fitting juncture. With the details shown later herein, and assuming an adequate brazed or welded tube-to-fitting joint, fatigue failure will occur first in the tube at the end of the hub socket. The stress-intensification factor at this juncture, however, will be fairly low if the socket wall thickness is not too large; i.e., the change in crosssection is not too great. The stress-intensification factors can be further reduced by tapering the end of the socket.

Seal Interaction

For detail design of the fitting-to-fitting connection, presented in the next two sections, it was assumed that the seal considered of a flat metal ring gasket 0.010 in.

thick, with appropriate diameters and width. It is expected that one or more of the seal types suggested for further investigation will reduce the requirements for the fitting structure, particularly in the realm of temperature gradients.

Tube-to-Fitting Interaction

Insofar as fitting-to-fitting design is concerned, the tube-to-fitting connection should be such that it does not distort the fitting structure, particularly the seating surface for the seal. Distortions produced at the tube-to-fitting connection can be prevented from distorting the sensitive parts of the fitting structure, such as threads in threaded fittings or seal-seating surfaces in both threaded and flanged fittings, by using a sufficiently long, relatively thin hub on the fitting stub ends (threaded fittings) or on flanges (flanged fittings). The designs shown later in Figures 20, 26, 27, 30, and 33 have fairly long hubs; depending upon details of the tube-to-fitting joining process, it may be possible to decrease the hub length. However, if the tube-to-fitting joining process produces severe distortions particularly of an axially nonsymmetric type, it may be necessary to increase the hub lengths.

Designs Considered

During the early stages of Phase I many possible methods of securing the fitting-to-fitting connection were considered. These ranged from exotic concepts like "Chinese finger grips" to the simple and everyday nut and bolt. Four methods which were considered worthy of consideration were (1) ring clamps, (2) snap or overcenter clamps, (3) differential threads, and (4) ball-and-socket joints.

Ring Clamps

Ring clamps were devised in an attempt to duplicate a flanged connection without using a great number of bolts. Generally the ring clamp is made of two mating flanges with tapered outer surfaces. A split hoop whose inside surfaces are tapered at the same angle as the flanges is fitted over the mating flanges. Small projections with bolt holes are provided where the two halves of the hoop are mated. Generally only two bolts are used. When these bolts are tightened a clamping force normal to the tapered faces is imposed. The axial component of the clamping force is the only force available for sealing and preloading. A typical ring clamp is shown in Figure 19a. This type of clamp is used extensively for many commercial applications and has been used in missile systems. Three major considerations ruled out this type of flange for an improved fitting.

(1) It is difficult to attain the required preload and it is also difficult to control initial preload within the limits necessary for the proposed service conditions.

(2) The weight of a fitting of this type would far exceed that of standard-type flanges for high-pressure applications.

(3) It is exceedingly difficult to secure this type of joint when the tubing is misaligned.

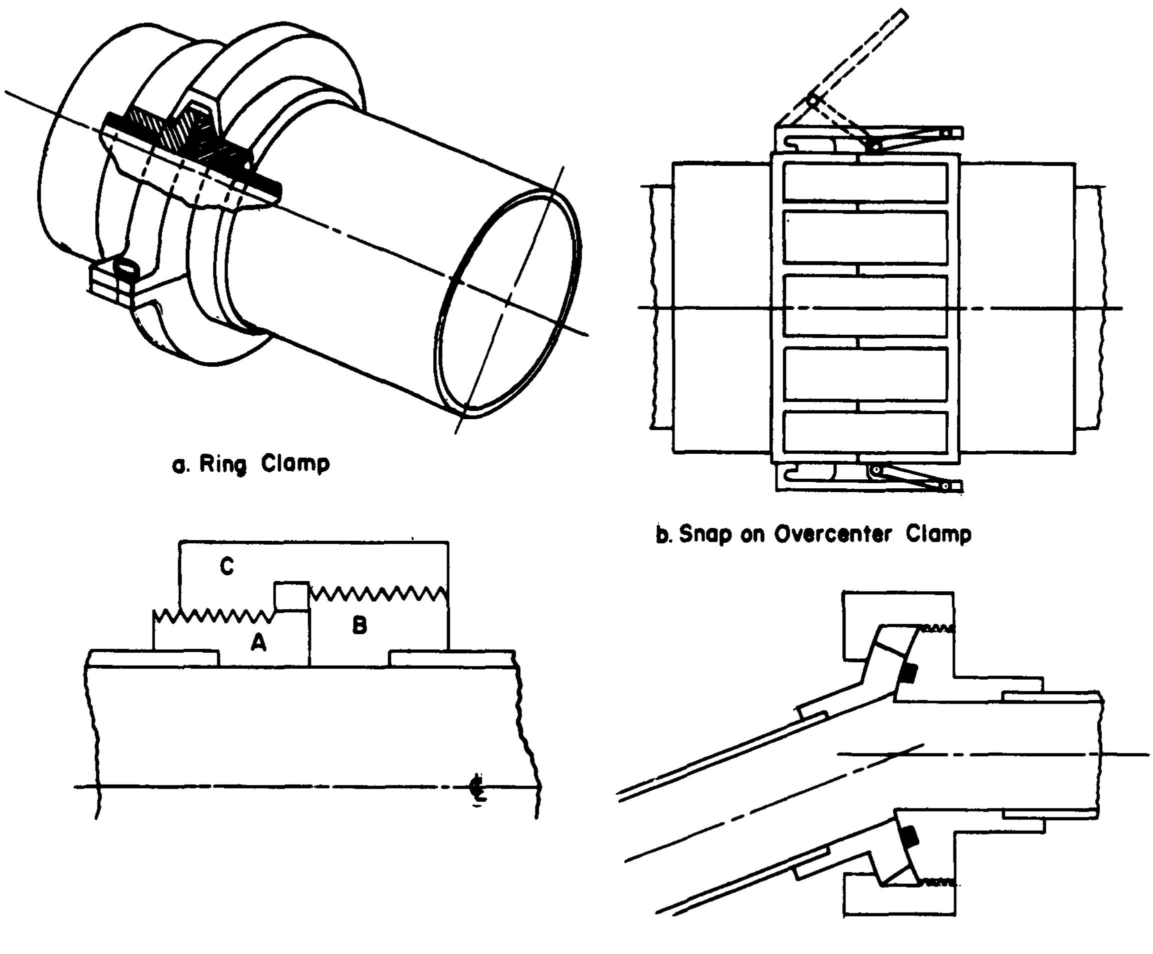

a. Ring Clamp

b. Snap on Overcenter Clamp

c. Differential Threads

d. Ball and Socket Joint

FIGURE 19. FITTING-TO-FITTING DESIGNS CONSIDERED

Snap Clamps

Snap clamps, or overcenter clamps, like those in Figure 19b, would be placed circumferentially around the tube and would act like a circle of bolts. However, unlike bolts, snap clamps once closed cannot be further tightened unless a take-up screw is provided. Such a clamp would be complex in construction and would be less reliable than a simple bolt-and-nut arrangement. Snap clamps cannot compensate for misalignment, cannot be readily preloaded, and are subject to early fatigue failure due to working of the parts.

Differential Threads

The coupling shown in Figure 19c is a typical application of a differential thread. Because the threads on parts A and B have a different pitch, each will travel a different linear distance relative to coupling C as the coupling is rotated. An arrangement of this type can produce high preload forces but it is difficult to assemble, it is heavy, and it is susceptible to thread seizure.

Ball and Socket

A ball-and-socket-type joint (Figure 19d) is probably the most widely accepted means of joining two misaligned tubes. Because this type of joint can be made rugged, a design which can operate reliably is possible. However, in order to accommodate the seal in any angular position within the range of misalignment specified, it is probable that the seal would have to be placed at the ball-and-socket interface. Probably the best approach would be to machine a seal-retaining cavity in the ball and to make the socket sufficiently large that it could overlap the seal in any given position. A joint of this type is necessarily large and heavy because of the oversized socket and the oversized nut. This type of joint should not be used unless it is absolutely essential that the fitting compensate for misalignment. Although initial misalignment can be overcome with the ball-and-socket joint, bending moments due to vibration will still exist during operation. This type of joint is more likely to fail due to these bending moments.

Threaded and Bolted Flange Connections

Threaded and bolted flange connections have been used so universally that too often they are taken for granted. Many times when structural failures occur in threaded or bolted fittings it is concluded too rapidly that the failure can be ascribed to the method of connection. Rather, the failure is more probably the result of "insufficient" design; i.e., the fitting was not designed to take full advantage of the interacting physical phenomena inherent in the design. Battelle's choice of threaded and bolted flange connections as the best means at present of securing the fitting-to-fitting connection is based on the following:

(1) Preloading of the connection, which is considered essential for successful operation of the system, is easily attained.

(2) The effects of transient thermal gradients can be overcome by judicious choice of the spring constants R_B and R_G* in conjunction with the preload phenomena.

*See pages 35 through 39.

(3) Although assembly of the connection requires care, the technique is definitely within the capabilities of the average mechanic and the completed joint can be easily reassembled many times.

(4) In terms of load capability, the connection is probably lighter than other comparable designs.

(5) The reliability of threaded and bolted connections has been demonstrated conclusively.

It is recognized that such considerations as torque relaxation and preload control by means of torque-wrench readings are two disadvantages inherent in these connections, especially with threaded fittings. However, because of the vast amount of experimental work already accomplished in these areas it is possible to adequately overcome the ambiguity these factors introduce into the design process.

Conclusions

The four designs shown in Figure 19 represent only a fraction of the number of concepts considered. They do represent, however, the better designs possible. Ring clamps and overcenter clamps are simple and easy to assemble. They probably can be used successfully for light duty operation. Differential thread devices appear to be too unreliable for missile applications. A review of all possible means conceived of securing the fitting-to-fitting connection revealed that none can compete with the threaded or bolted flange connections when the factors of simplicity, ruggedness, reliability, and weight are considered in combination.

Design Procedure for Threaded Fittings

Two preliminary designs of minimum-weight threaded fittings are presented in Figures 20 and 26. The first (Figure 20) is a Class Ia fitting designed for a 1-in.-diameter tubing system which operates at a maximum internal pressure of 2000 psi between -100 and 600 F. The second (Figure 26) is a Class IIIa fitting designed for a 1/8-in.-diameter tubing system which operates at a maximum internal pressure of 10,000 psi between -425 and 600 F.

Figures 20 and 26 show the basic structure of the fitting when used to connect one tube to another tube. In many applications the threaded stub end will be integral with or welded to a piece of equipment such as a compressor, pump, pressure vessel, manifold, elbow, or tee. In such applications, the attached equipment is expected to hold the fitting while the nut is being tightened, or, in the case of elbows or tees, there will be a place on the elbow or tee body which can be held by a wrench. When used simply as a connector, a wrench flat or suitable reinforced knurled sections must be provided on the threaded stub end.

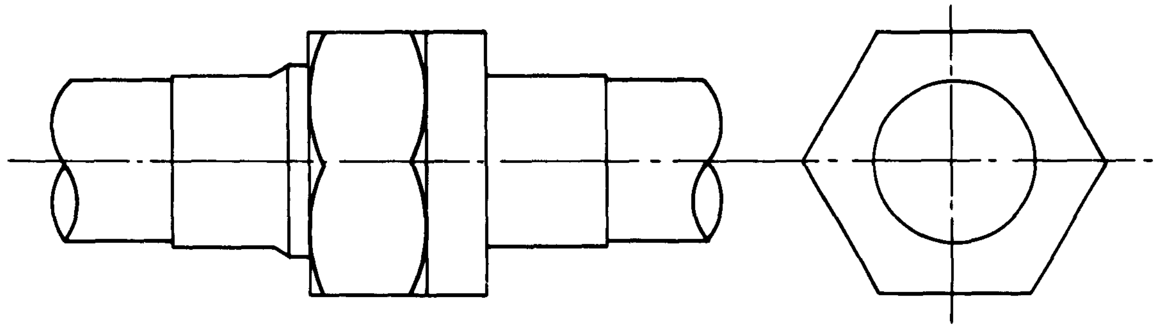

Actual size

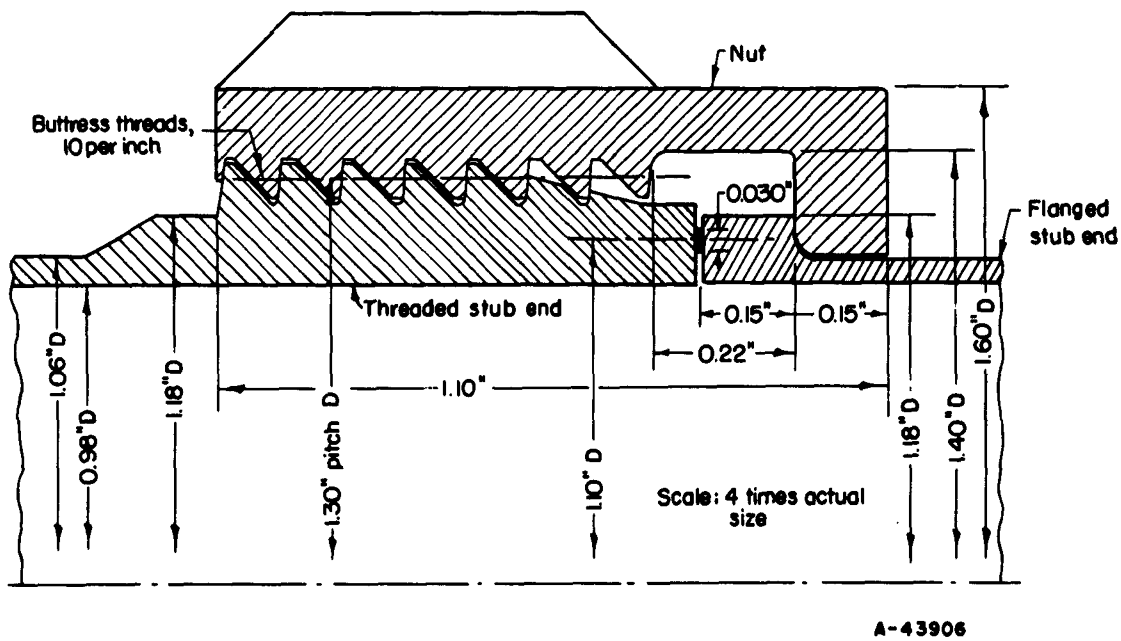

FIGURE 20. PROPOSED 1-IN. CLASS Ia THREADED FITTING, 2000 PSI AT -100 TO 600 F, AM-355

The following basic features should be noted in the proposed designs:

(1) The fittings contain a seal which is not part of the tubing. This gives relative freedom in seal design, material choice, surface finish, and tolerances. In contrast, standard AN- fittings produce a seal on the flared tubing material. Difficulties exist at present with austenitic stainless steel material, and increased difficulties would be expected if higher strength tubing material were used.

(2) A modified buttress thread form is used in the 1-inch fitting, thereby substantially eliminating the radial thrust that exists with 60° form threads. A discussion of thread profile in relation to fitting design is given in Appendix III.

(3) The inwardly projecting flange on the fitting nut is designed to act as a spring, thereby adding substantially to the elastic follow-up available for temperature gradients.

Class Ia 1-In. Threaded Fitting

The service conditions upon which the design is based are presented in Table 7. The design properties of the AM-355 alloy, chosen as the fitting material for Class Ia fittings, are given in Table 8.

TABLE 7. SERVICE CONDITIONS FOR DESIGN OF 1-IN. CLASS Ia THREADED FITTING

Design Pressure	2000 psi
Design Temperature	-100 to 600 F
Proof Pressure	3000 psi at 70 F
Structural Loads	
Hydrostatic, F_E	1900 lb (Equation 1)
Bending, F_B	1900 lb (Equation 12)
Seating, F_G	3460 lb (Equation 9)
Temperature Gradient (Nut to Body)	50 F (See page 39)
Creep	None

TABLE 8. DESIGN PROPERTIES OF AM-355

Temperature, F	Yield Stress, 1000 psi	Modulus of Elasticity, 10^7 psi	Thermal Coefficient of Expansion, in./in./F
-100	170	3	
70	165	3	7×10^{-6}
600	127	2.7	

After the basic design requirements and the general geometrical shape have been established, the detailed dimensions can be determined by an iterative procedure. An estimate of dimensions is first made and the strength and displacement characteristics are calculated. If these characteristics are not satisfactory, a second set of dimensions, based on the first approximation, is selected and the process repeated until a fitting of satisfactory design is obtained. The final calculations on the basis of the dimensions shown in Figure 20 are summarized in a series of four steps:

(1) Determine the stresses for a basic imposed load, hydrostatic plus bending, of 3800 lb.

(2) Determine the displacements on the basis of a unit load.

(3) Establish preload requirements.

(4) Select from the above calculations the controlling preload condition and recalculate the corresponding stresses.

As an aid in understanding how the various load conditions, evaluated in Step (3), influence the establishment of the necessary preload at room temperature, a series of preload diagrams are included. These diagrams, Figures 21 through 25, are all drawn to the same scale and if superimposed would result in a complete preload diagram which compares directly the maximum and minimum operating limits.

(1) Determine the stresses for a basic imposed load, hydrostatic plus bending, of 3800 lb.

Shear stress at thread pitch diameter, $S_a = 2300$ psi

Nut flange and hub maximum stress, $S_b = \pm 60,500$ psi

Stub end maximum stress, $S_c = \pm 73,600$ psi.

(2) Determine the displacements on the basis of a unit load*.

Spring constant, $R_B = 2.47 \times 10^{-7}$, composed of:

Tensile strain in the hub on the nut, $\left(\frac{\delta}{F}\right)_a = 4.01 \times 10^{-8}$

Rotation of flange on nut, $\left(\frac{\delta}{F}\right)_b = 2.06 \times 10^{-7}$

*Stress and displacement calculation methods are shown in Appendix I. Because of the length of the detailed calculations, they are not shown.

Spring constant, $R_G = 5.483 \times 10^{-8}$, composed of:

Compression of flange stub end, $\left(\frac{\delta}{F}\right)_c = 1.37 \times 10^{-8}$

Compression of threaded stub end, $\left(\frac{\delta}{F}\right)_d = 3.78 \times 10^{-8}$

Compression of seal, $\left(\frac{\delta}{F}\right)_e = 3.33 \times 10^{-9}$

Displacement characteristics are shown in Figure 21. The spring constant of the tension member, R_B, is drawn with a positive slope from the origin. The spring constant of the compression members, R_G, is drawn with a negative slope and intersects R_B at the required preload. This intersection point is determined in the next series of calculations. Also shown in Figure 21 is F_i, the minimum compressive load needed to maintain the seal.

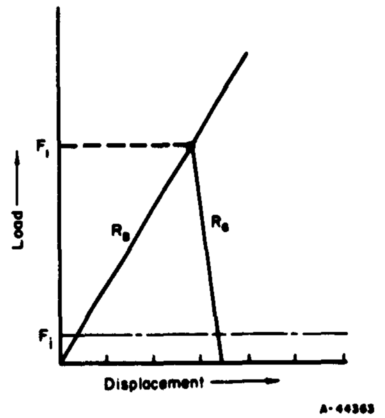

FIGURE 21. BASIC PRELOAD DIAGRAM FOR 1-IN. CLASS Ia THREADED FITTINGS

(3) Establish preload requirements.

Five design conditions are to be considered:

(a) Proof pressure of 1.5 times design pressure at 70 F
(b) Steady (temperature) state at design pressure and 70 F
(c) Minus* thermal gradient of 50 F
(d) Plus thermal gradient of 50 F
(e) Steady (temperature) state at design pressure and 600 F

The maximum preload required for those five design conditions is determined. This preload is then used in combination with the thermal gradient producing the highest load to determine the maximum stress condition.

*A "minus" temperature gradient is defined as a design condition in which the inner portions of the fitting are colder than the outer portions of the fitting.

Proof Pressure at 70 F

The design bending load and 1.5 times the hydrostatic load are imposed. The total structural load is then(1900 x 1.5) + 1900 = 4750 lb. A preload F_1 of 4500 lb is calculated by Equation (18) as required to maintain a residual seal load F_i of 600 lb after the proof pressure and design bending moment are applied. With a seal contact area (see Figure 20) of $\pi \times 1.06 \times 0.030 = 0.100$ sq in., the residual seal stress is 6000 psi, which is three times the design pressure and therefore in accordance with the suggested minimum residual seal stress.

Graphically, the total structural load of 4750 lb is measured vertically from the intersection of R_G and Fi in Figure 22. From the top of this line, R_B is drawn and the origin is established where R_B intersects the abscissa. The preload is 4500 lb and the maximum load on the nut is 5350 lb.

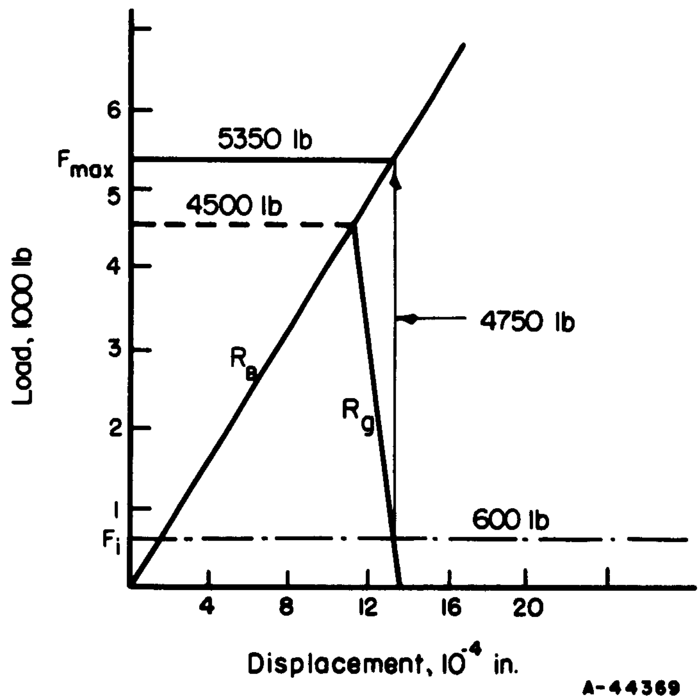

FIGURE 22. PRELOAD DIAGRAM FOR PROOF PRESSURE AT 70 F

Steady State at 70 F

At 70 F, only a preload of 3700 lb is required to maintain the residual seal load, F , of 600 lb when a structural load of 3800 lb is applied. The maximum load on the nut is 4400 lb. These relationships are shown in Figure 23.

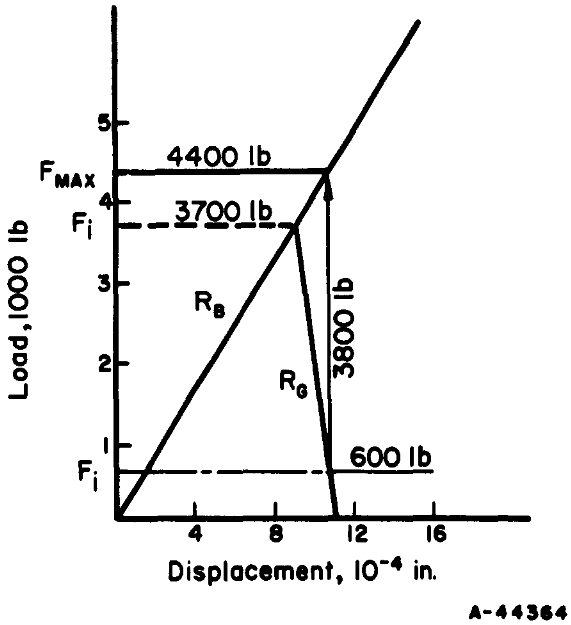

FIGURE 23. PRELOAD DIAGRAM FOR STEADY STATE AT 70 F

Minus Temperature Gradient

When a cold fluid is introduced and the average temperature of the nut is 50 F (design limit) higher than the average temperature of the stub ends, the relative expansion of the nut is:

$$\Delta T = 50 \times 0.7 \times 7 \times 10^{-6} = 2.45 \times 10^{-4} \text{ in.}$$

When a minus temperature gradient giving a differential expansion of ΔT occurs, the preload required to maintain a given residual seal load F_i is given by:

$$F_1' = \frac{\delta_B + \delta_G + \Delta T}{\delta_B + \delta_G} F_1 , \tag{21}$$

where

F_1' = preload required with differential expansion, ΔT

F_1 = preload required without differential expansion

δ_B , δ_G = displacements corresponding to preload F_1

when

F_1 = 3700 lb (steady state at 70 F), the corresponding

$\delta_B + \delta_G = (R_B + R_G)\ 3700 = 11.15 \times 10^{-4}$ inches, and

$$F_1' = \frac{13.60}{11.15} \times 3700 = 4510 \text{ lb.}$$

The effect of the minus temperature gradient is to displace R_G to the left as shown in Figure 24 because of the relative contraction of the compression members. When the structural load of 3800 lb is measured vertically from the intersection of R_G and F_i, the maximum load on the nut is less than the required room-temperature preload. The preload at room temperature needed to maintain the seal is 4510 lb, which is slightly greater than the previous preload at proof pressure.

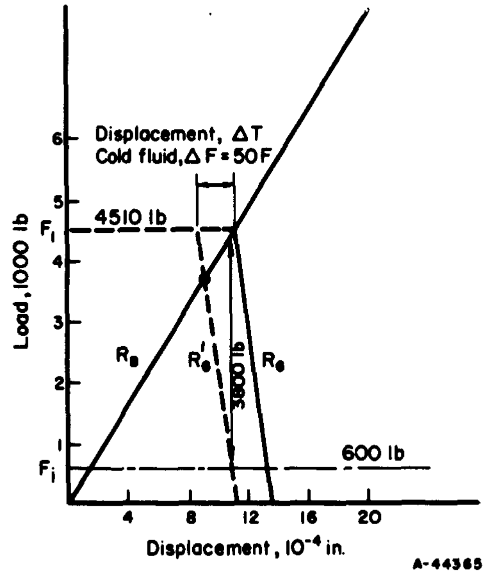

FIGURE 24. PRELOAD DIAGRAM FOR MINUS TEMPERATURE GRADIENT

Plus Temperature Gradient

When a hot fluid is introduced and the average temperature of the nut is 50 F lower than the average temperature of the stub ends, ΔT is again 2.45×10^{-4} in. However, in this case, the preload is proportionately increased. On the basis of a preload of 4510 lb required to handle cold fluids, the total load now carried by the fitting nut becomes, by Equation (16):

$$F_2 = \left(4510 \times \frac{16.05}{13.60}\right) + \frac{3800}{5.48} = 6030 \text{ lb.}$$

As shown in Figure 25, R_G is displaced to the right due to expansion of the compression members. The room temperature preload of 4510 lb established in the previous case for a minus temperature gradient is still valid. The structural load of 3800 lb represented by a vertical line is measured between R_B and R_G''. The actual residual seal load F_i' is approximately 2150 lb and the maximum load on the nut is 6030 lb.

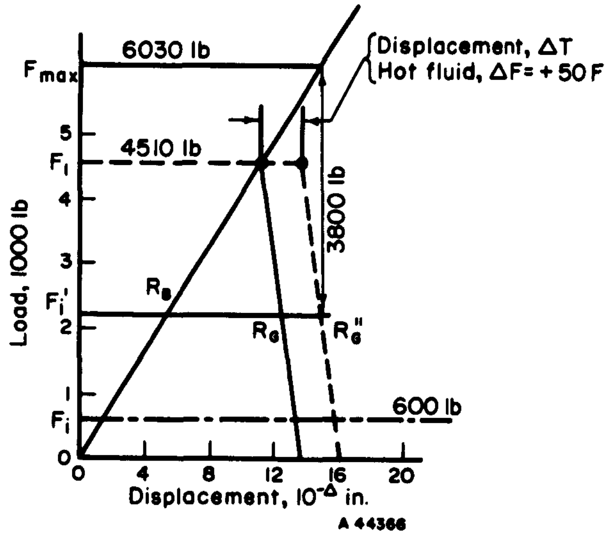

FIGURE 25. PRELOAD DIAGRAM FOR PLUS TEMPERATURE GRADIENT

Steady State at 600 F

At a uniform temperature of 600 F, the modulus of elasticity of the fitting material will decrease to 90 per cent of its room-temperature value. This loss reduces the effective preload from 4510 to 4060 lb. After application of the structural load of 3800 lb, the residual seal load is 950 lb, which is well above the design minimum of 600 lb.

(4) Select from the above calculations the controlling preload condition and recalculate the corresponding stress.

An initial preload of 4510 lb is necessary to provide sufficient residual gasket load when a thermal transient in which the nut temperature is 50 F higher than the stub-end temperature is present. This preload is sufficient for proof-pressure conditions and for steady-state conditions at 600 F. The highest stress conditions will occur when the nut is 50 F colder than the stub ends (plus temperature gradient). The stresses during this transient thermal state will be:

Actual size

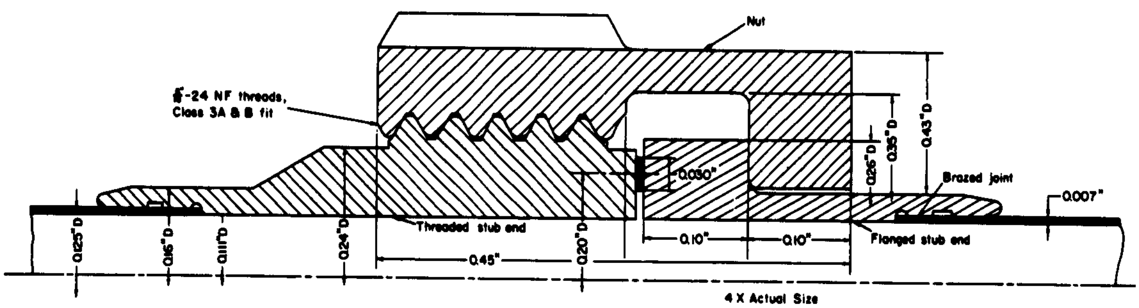

4 X Actual Size

FIGURE 26. PROPOSED 1/8-IN. CLASS IIIa THREADED FITTING, 10,000 PSI AT -425 TO 600 F, RENÉ 41

	70 F	600 F
Max Stress in Nut, psi	96,000	86,200
Max Stress in Flanged Stub End[a], psi	87,500	73,600

(a) The stresses in the flanged stub end arise directly from the structural loads. At preload conditions, before application of structural loads, the bending stress in the flanged stub end is essentially zero, since the seal and point of load application from the nut are opposite each other. The maximum stress occurs at the proof-test conditions at 70 F.

The yield strength of AM-355 is 165,000 and 127,000 psi at 70 F and 600 F, respectively, and therefore a factor of safety of at least 1.47 is evident.

Class III 1/8-In. Threaded Fitting

The detail design procedure for the 1/8-in. threaded fitting shown in Figure 26 is analogous to that of the 1-in. threaded fitting described above, with one important exception. In the 1/8-in. size, the seal-seating load is 628 lb because of the need to plastically yield the seal material. The structural load, even at 10,000-psi design pressure, is only 666 lb. Accordingly, there is little or no advantage to be gained in designing for operating pressures less than 10,000 psi.

Additional Design Considerations

Accuracy of Preloading. In the calculations presented above, it was assumed that the desired preload could be accurately applied. In practice, accurate preloading may be difficult. If a torque wrench is used, a preloading accuracy of about ± 25 per cent is the best to be expected.

Torque Relaxation. Experience with flared and flareless threaded fittings indicates that part of the initial torque applied to the fitting is lost with passage of time. It is not known if the axial load also decreases, but presumably it does. At elevated temperatures this relaxation is intensified. Although use of high-precision buttress threads will probably reduce thread relaxation, some relaxation may still exist, especially at elevated temperatures. Additional preloading may be required, therefore, to compensate for thread relaxation. Available test data on torque relaxation and a discussion thereof are given in Appendix IV.

Overtightening Factor. Unless installation procedures are carefully controlled, threaded fittings may be overtightened. This leads to higher stresses in the fitting and the possibility of yielding. To prevent yielding, a substantial margin must be available in the threaded fitting for overtightening allowance. For example, MIL-F-5509A, "Fittings; Fluid Connections", requires that steel fittings be able to withstand a torque equal to 1-1/3 times the required torque. The 1-in. threaded connection is designed to provide at least this overtightening margin. (The factor of safety is 1.47.)

Plastic Deformations. The three factors discussed immediately above indicate that the design preload may be increased above the theoretical 4510 lb for the 1-in. Class Ia threaded fitting. This would imply higher stresses in the fitting, which are already quite close to the yield strength of the fitting material. There is, however, a substantial factor of safety in the structural design in that the calculated stresses are localized bending stresses. The fitting, as a gross structure, will not yield appreciably when these stresses reach the yield strength of the material. Rather, there will be a redistribution of stresses due to local yielding. In approximate terms, the imposed load has to be 1.5 to 2 times the theoretical load required to produce a stress equal to the material yield strength before gross yielding of the structure will occur. This approximation will be better defined during the Phase II development of the threaded fitting.

Design Procedure for Bolted Fittings

Three preliminary designs of minimum-weight bolted fittings are presented. A major reduction in size and weight of the proposed flanged connections, as compared with standard pipeline flanges, is achieved by:

(1) Use of high-strength materials for both flanges and bolts

(2) Use of a proper number and size of bolts as required for specific design conditions

(3) Use of socket-head or similar bolts to eliminate or reduce wrench clearance between the nut and the flange hub.

Although the proposed designs represent a departure from standard pipeline practices in many ways, other elements of the design are quite similar to conventional flange designs, as in the use of raised faces and tapered hubs. Raised faces partially convert the flange rings into springs which can compensate for temperature gradients. The tapered hub provides maximum reinforcement, per unit weight, to the flange ring. In addition, the tapered hub provides a gradual transition in thickness between the flange rings and the attached tube for optimum fatigue-resistance to cyclic bending loads.

Class Ia 1-In. Bolted Fitting

The service conditions on which the design is based have been given in Table 7. The design properties of the AM-355 alloy chosen as the fitting material have been given in Table 8. According to the conditions listed in Table 3 in the section "Recommended Fitting Classes", a Class Ia 1-in. fitting would be threaded, while a Class Ib fitting would be flanged. However, the design shown in Figure 27 is for Class Ia service to provide a direct comparision with the threaded connection designed for the same conditions.

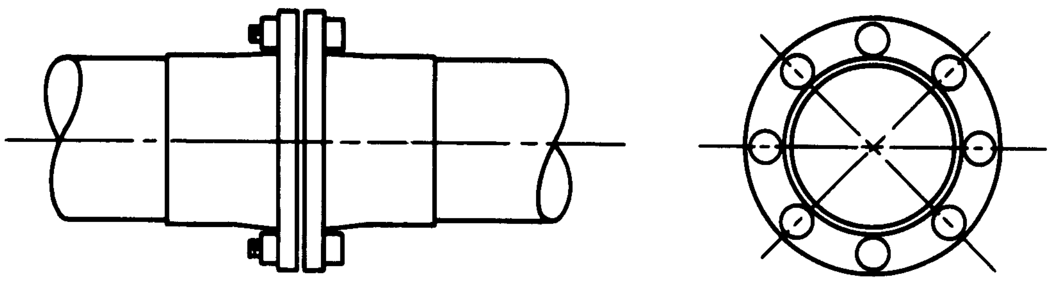

Actual size

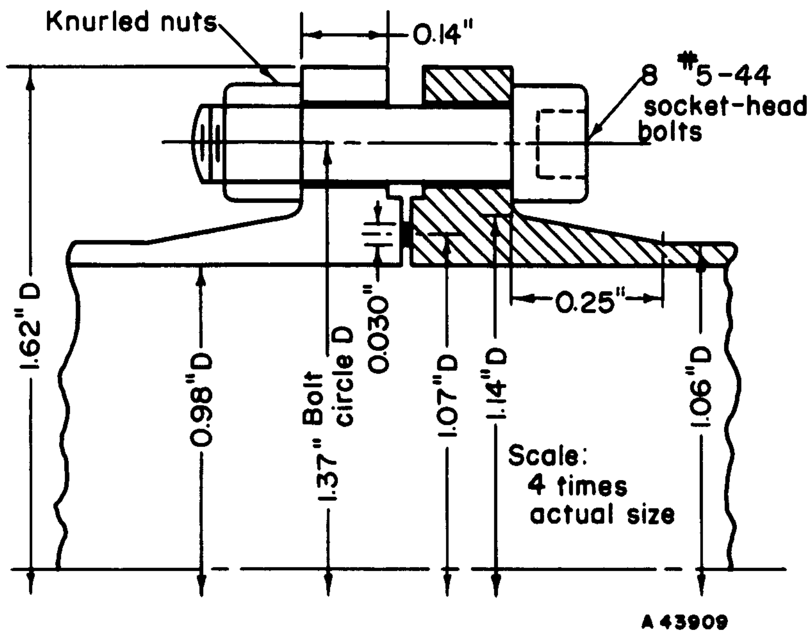

FIGURE 27. 1-IN. CLASS Ia BOLTED FITTING, 2000 PSI AT -100 TO 600 F, AM-355

Essentially the step-by-step analytical and graphical procedure used in analyzing the Class Ia 1-inch bolted fitting is the same as the step-by-step procedure presented for the Class Ia 1-inch threaded fitting. An iterative procedure is used to establish the detailed dimensions. The final series of calculations on the basis of the dimensions shown in Figure 26 are summarized in a series of four steps:

(1) Determine the stresses for a basic load, hydrostatic plus bending, of 3800 lb.

(2) Determine the displacements on the basis of unit load.

(3) Establish preload requirements.

(4) Select from the above calculations the controlling preload condition and recalculate the corresponding stresses.

The preload diagrams presented in conjunction with these calculations do not depict the effect of thermal gradients since subsequent analysis indicates that the required preload is not determined under thermal load conditions.

(1) Determine the stresses for a basic load, hydrostatic plus bending, of 3800 lb*.

Tensile stress in bolts, $S_b = 66{,}700$ psi

Maximum stress in flanges, $S_f = 73{,}000$ psi

(2) Determine the displacements on the basis of unit load*.

Spring constant, $R_B = 7.775 \times 10^{-7}$, composed of:

Tensile displacement of bolts $\left(\frac{\delta}{F}\right)_a = 2.335 \times 10^{-7}$

Rotation of flanges, $\left(\frac{\delta}{F}\right)_b = 5.44 \times 10^{-7}$.

Spring Constant, $R_G = 3.213 \times 10^{-8}$, composed of:

Compression of flanges, $\left(\frac{\delta}{F}\right)_c = 2.88 \times 10^{-8}$

Compression of seal, $\left(\frac{\delta}{F}\right)_d = 3.33 \times 10^{-9}$

The spring constants listed above describe the behavior of the flanged connection as the bolts are tightened and the preload is applied. Subsequent application of structural loads in an axial direction causes the bolt load to increase slightly. Since changes in moment arms are small when the axial load is transferred from the seal to the flange hub, the effect of this change can be neglected. The radial effect of internal pressure, however, is significant and must be included in the analysis. The decrease in initial bolt load due to the radial effects of internal pressure is

$$\Delta F = \frac{2q_r h_G}{Q} = 0.174P \, . \qquad (22)^{**}$$

*Stress and displacement calculation methods are shown in Appendix I.

**This expression follows from Equation (19), in particular the last term in the definition of α.

(3) **Establish preload requirements.**

Proof Pressure at 70 F

The design bending load and 1.5 times the hydrostatic load are imposed. The total structural load is then

$$(1900 \times 1.5) + 1900 = 4750 \text{ lb.}$$

The preload to maintain a minimum seal load of 600 lb is 5700 lb. This includes an allowance for reduction in bolt load due to the radial effect of internal pressure (Equation 22) of 0.174 x 3000 = 522 lb. With a seal contact area of 0.100 sq in., (see Figure 27) the residual seal stress is 6000 psi, three times the design pressure.

In constructing the preload diagram (Figure 28) it is first necessary to establish the effective preload, F_i', at operating pressure. The structural load of 4750 lb is measured vertically from the intersection of R_G' and F_i. From the top of this line, R_B is drawn until it intersects the abscissa. The effective preload of 5178 lb is established where R_B intersects R_G'. To determine the true preload at no-load conditions, it is necessary to take into account the radial effect of the internal pressure. This value of 522 lb is added to the effective preload. The no-load spring constant R_G is established by the intersection of F_i and R_B.

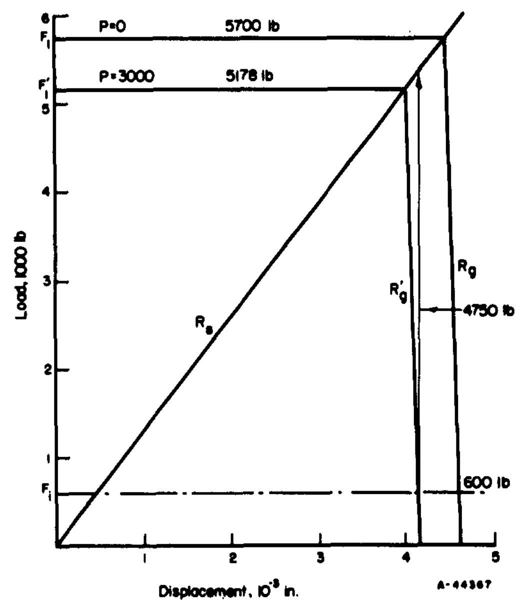

FIGURE 28. PRELOAD DIAGRAM FOR PROOF PRESSURE AT 70 F FOR 1-IN. CLASS Ia BOLTED FITTING

Steady State at 70 F

At 70 F, a preload of 4590 lb is required to provide the residual seal load of 600 lb after application of a structural load of 3800 lb, including the radial effect of the application of 2000-psi internal pressure, reduces the preload by 0.174 x 2000 = 350 lb.

The preload diagram is constructed in the same manner as the preload diagram for proof-pressure conditions. This diagram is shown in Figure 29 and is used to evaluate the effects of thermal gradients on the preload.

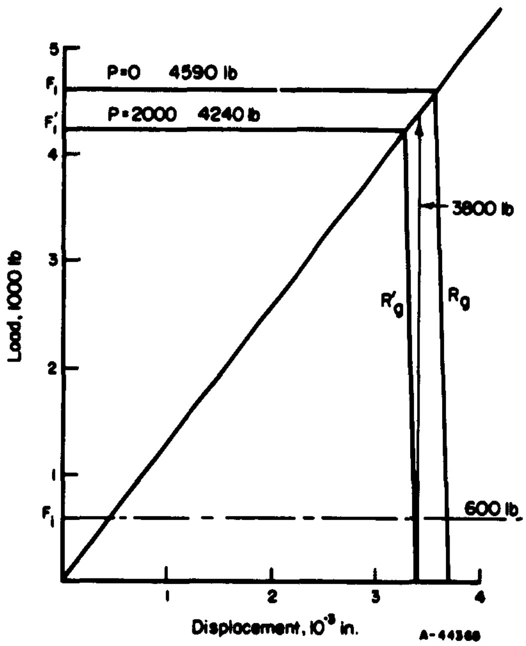

FIGURE 29. PRELOAD DIAGRAM FOR STEADY STATE AT 70 F

Minus Thermal Gradient

When the cold fluid is introduced and the average temperature of the bolts is 50 F (design limit) higher than the average temperature of the flanges, the relative expansion of the bolts is:

$$\Delta T = 50 \times 0.4 \times 7 \times 10^{-6} = 1.40 \times 10^{-4} \text{ in.}$$

When a minus temperature gradient giving a differential expansion of ΔT occurs, the preload required to maintain a given residual seal load F_i, is given by

$$F_1' = \frac{\delta_B + \delta_G + \Delta T}{\delta_B + \delta_G} F_1 + \frac{2q_r h_G}{Q} ,$$

where

F_1' = preload required with differential expansion, ΔT

F_1 = preload required with no differential expansion and without the radial effect of internal-pressure term

δ_B, δ_G = displacements corresponding to F_1.

Since $F_1 = 4590 - 350 = 4240$ lb (steady state at 70 F), and the corresponding $\delta_B + \delta_G = (R_B + R_G)\ 4240 = 34.2 \times 10^{-4}$ in.,

$$F_1' = \frac{35.6}{34.2} \times 4240 + 0.174 \times 2000 = 4760 \text{ lb} \quad .$$

Plus Thermal Gradient

When hot fluid is introduced and the average temperature of the bolts is 50 F lower than the average temperature of the flanges, ΔT is again 1.40×10^{-4} in. In this case, the preload is proportionately increased. When a preload of 5700 lb for the proof test has been applied, the maximum load carried by flanges and bolts becomes

$$\left(5700 \times \frac{47.4}{46.0}\right) + \left(\frac{3800}{25.2}\right) - (0.174 \times 2000) = 5670 \text{ lb} \quad .$$

Steady State at 600 F

At a uniform temperature of 600 F, the modulus of elasticity of the material will decrease to 90 per cent of its room-temperature value. The effective preload is reduced to 5700 x 0.90 = 5130 lb. Because the radial effect of internal pressure will further decrease the effective preload by 350 lb, the residual preload is 4780 lb. The residual seal load, after application of structural loads, is 1140 lb, which is more than ample to meet the minimum design criterion of 600 lb (6000 psi seal-contact-area stress).

(4) Select from the above calculations the controlling preload condition and recalculate the corresponding stresses.

A preload of 5700 lb is necessary for proof-pressure conditions and is ample to handle thermal transients of +50 F and also steady-state conditions at 600 F. With an initial preload of 5700 lb, the maximum stresses occur when the full design pressure and bending moment are applied, while the temperature difference is such that the bolts are 50 F colder than the flanges. The maximum stresses are:

	70 F	600 F
Tensile stress in bolts, psi	99,600	89,600
Bending stress in flanges, psi	109,000	98,000

The yield strength of AM-355 is 165,000 psi at 70 F and 127,000 psi at 600 F. Therefore, the design provides a minimum safety factor of 1.30.

An important consideration in the design of a bolted connection is the question of bolt selection and spacing. There are no analytical means of determining optimum choices. However, there are some empirical guides which on the basis of past experience can be used to closely approximate a satisfactory design. These guides are discussed on pages 72 and 73.

Classes III and IV 1-In. Bolted Fitting

The bolted fitting shown in Figure 30 generally illustrates the dimensions of a 1-in. bolted fitting suitable for 10,000 psi at temperatures up to 600 F when made of AM-355 (Class III pressure and maximum temperature), and at the same time, when made of René 41 is suitable for 4000 psi for 30 minutes at 1500 F (Class IV) with about 100 F maximum thermal gradient. These designs were made to help establish the classes shown in Table 3. While design conditions do not correspond exactly to Table 3, they are sufficiently close to illustrate the design procedure and resulting dimensional proportions.

Design of the bolted fitting shown in Figure 30 for 10,000 psi at -100 to 600 F follows the same procedure as discussed for the 1-in. bolted fitting for 2000 psi at -100 to 600 F. Establishing ratings for this bolted fitting at 1500 F, however, illustrates the design procedure for fittings where creep or relaxation occurs, and this aspect will be discussed in the following.

The design procedure at temperatures where creep or relaxation is a dominant factor is discussed in Appendix II. The procedure is essentially one of establishing pressure-time ratings at a specified temperature for a given fitting; i.e., a fitting with all dimensions established and made of a specified material. In this discussion, the "given fitting" is shown in Figure 30.

Data on René 41 for Creep Design. As noted previously, René 41 was selected as the recommended material for high-temperature design. The design analysis uses creep data from Figure 3.042 of Reference (15), "Master Curves for Creep and Creep Rupture for Sheet and Bar". Specifically, the data for bar stock, heat treated at 2150 F for 2 hours, air cooled and aged at 1650 F for 4 hours, were used. These data are given in the form of stress versus the Larson-Miller parameter $(T+460)(20+\log_{10}t)$, for the 0.2 per cent creep condition. With the assumption that $d\epsilon/dt$ is independent of time, the data can be converted to a graph of $d\epsilon/dt$ versus stress at 1500 F, as shown in Figure 31.

The relationship between creep rate and stress in the creep-stress range of 10,000 to 60,000 psi can be conservatively approximated by the equation

$$\frac{d\epsilon_p}{dt} = 1.3 \times 10^{-26} S^{4.82} \quad , \tag{24}$$

where

ϵ_p = strain, in./in.

t = time, hr

S = stress, psi.

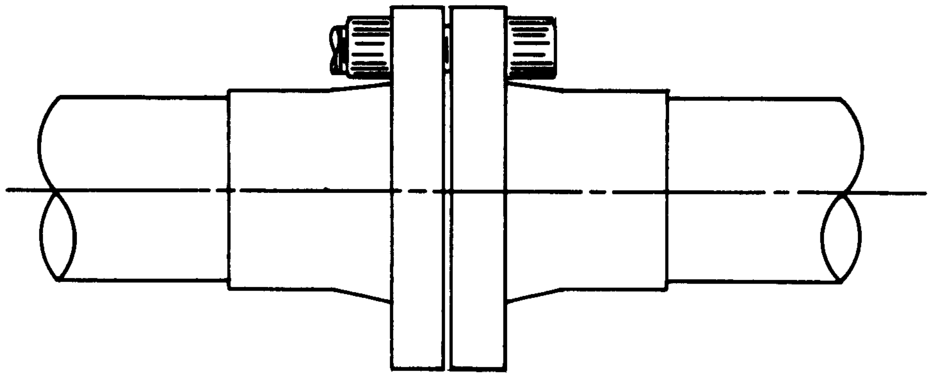

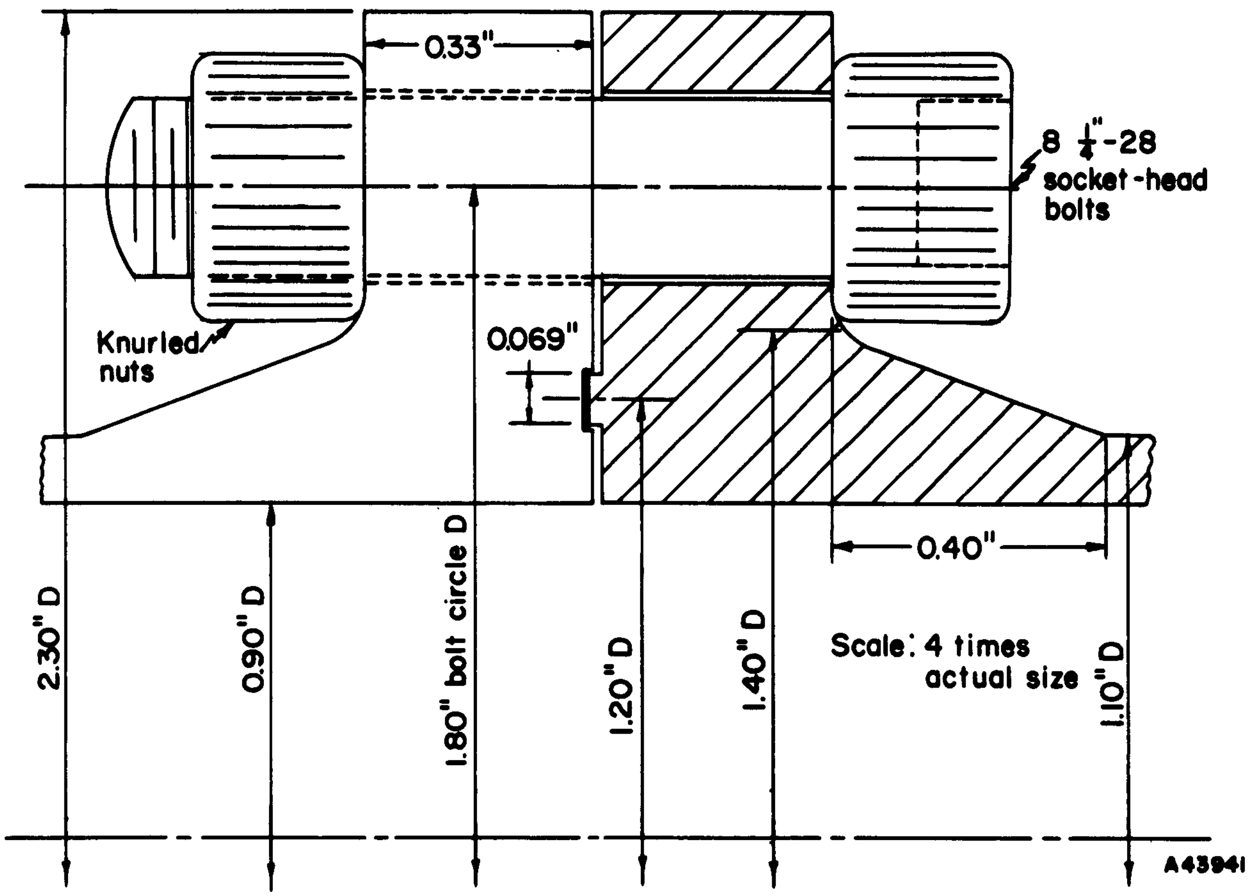

FIGURE 30. 1-IN. BOLTED FITTING, APPROXIMATELY CLASS III (10,000 PSI UP TO 650 F) AND CLASS IV (4,000 PSI AT 1500 F, 30-MINUTE LIFE)

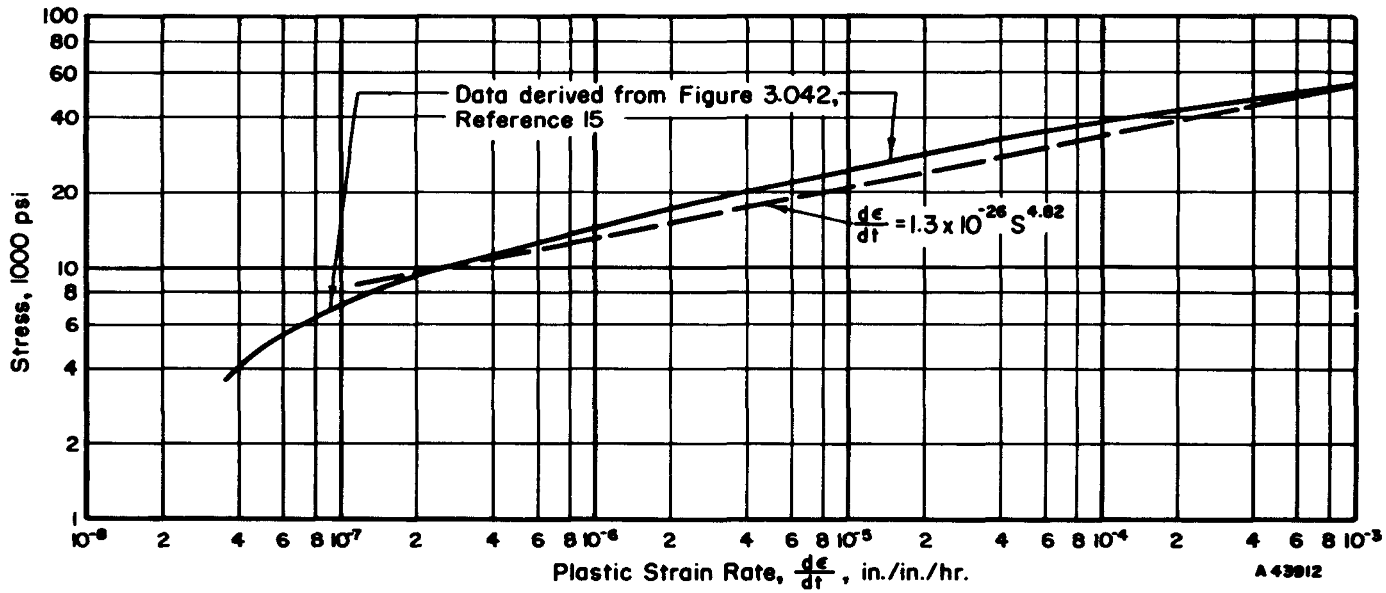

FIGURE 31. CREEP RATE OF RENÉ 41 BAR AT 1500 F

Equation (24), plotted in Figure 31, is of the form $\frac{d\epsilon_p}{dt} = C_1 S^n$, which forms the basis for the development in Appendix II. Additional data on René 41 needed for the analysis is presented in Table 9.

TABLE 9. DESIGN PROPERTIES OF RENÉ 41

	70 F	1500 F
Yield Strength[a], psi	120,000	97,000
Modulus of Elasticity, psi	3.2×10^7 (E_r)	2.4×10^7 (E_T)
Coefficient of Thermal Expansion, per F	6.8×10^{-6}	8.5×10^{-6}
Pseudo-Modulus[b], E^1, psi, at S_o = 60,000 psi and 1500 F	Approximately 1.6×10^7	

(a) From Reference (21).
(b) From Reference (22).

Application of Creep Design Procedure. The creep design procedure established in Appendix II will be applied to the bolted flanged joint with the dimensions shown in Figure 30. The procedure is characterized by the following steps: (1) determine maximum preload at room temperature,(2) determine effective preload at 1500 F, steady state,(3) compute a time-versus-residual-bolt-stress curve, and (4) consolidate maximum operating pressure corresponding to the residual bolt stresses for both steady state and transient thermal conditions.

Because maximum service life is obtained with the application of maximum initial preload, the bolts are considered to be initially tightened to their yield strength of 120,000 psi. The flanged-joint shown in Figure 30 has eight 1/4-28 bolts, each bolt having a cross-sectional area at the root of the threads of 0.0326 square inch. The total cross sectional area of the bolts of the flanged joint shown in Figure 30 is therefore 8 x 0.0326 or 0.261 square inch. The total bolt load corresponding to 120,000-psi bolt stress is then 120,000 x 0.261 = 31,400 lb. By using the stress-calculation methods shown in Appendix I, it can be shown that a total bolt load of 31,400 lb, applied to the flanged-joint shown in Figure 30, produces a controlling stress in the flanges of 116,500 psi. Since this stress is almost equal to the bolt stress of 120,000 psi, it will be assumed that the initial stress in both the bolts and the flanges is 120,000 psi. This assumption permits the use of Equation (81) of Appendix II to calculate service life, t, rather than the more complex Equation (82). In the following, the decrease in bolt stress as a function of time will be determined; it should be kept in mind that this decrease in bolt stress is due to creep of all parts of the joint, not the bolts alone.

As the temperature is increased from ambient to 1500 F, the initial preload is reduced by a factor E^1/E_r, where E^1 is the pseudo-modulus of elasticity at 1500 F (derived as indicated in Appendix II), and E_r is the modulus of elasticity at room temperature. Gross yielding does not occur, since the yield strength decreases at a lesser rate than does the modulus of elasticity.

The values of the constants in Equation (81) for René 41 at 1500 F are: $C_1 = 1.3 \times 10^{-26}$, n = 4.82, and $E_T = 2.4 \times 10^7$. The bolt preload at 1500 F is one-half the initial preload of 120,000 psi; that is, S_o is 60,000 psi. By substitution of these values, Equation (81) becomes

$$t = \frac{1 - \left(\frac{S_t}{60,000}\right)^{3.82}}{(1.19 \times 10^{-18})(S_t)^{3.82}} , \qquad (25)$$

where S_t = residual stress in the bolts after t hours of service life.

The effective residual bolt load at any time is simply S_t multiplied by the bolt area of the flanged-joint shown in Figure 30:

$$F = A_B S_t = 0.261\ S_t . \qquad (26)$$

Arbitrary values may be assigned to S_t and the corresponding time required for the stress to relax from 60,000 psi to the chosen value can be calculated from Equation (25). The corresponding residual bolt load given by Equation (26) can also be calculated for each assigned valus of S_t. The structural loads carried by the connection, with this effective residual bolt load, can then be computed by the method outlined earlier, where temperature effects did not involve creep.

As an example, assume that S_t is assigned a value of 40,000 psi. From Equation (25), t is found to be 1.74 hours; i.e., it will take 1.74 hours for the bolt stress to decrease from 60,000 psi to 40,000 psi. From Equation (26), with S_t = 40,000, the residual bolt load at the end of 1.74 hours is 10,430 lb.

The residual bolt load of 10,430 lb at the end of 1.74 hours may now be considered as if it were an initial applied bolt load F_1. By using the method discussed earlier in designs in which creep was not a factor, a design pressure P corresponding to an initial load F, can be obtained. For the bolted fitting shown in Figure 30, the significant factors may be expressed by the equation

$$F_1 = F_i + \frac{\frac{R_B}{R_G} F_s}{1 + \frac{R_B}{R_G}} + \frac{2qh_G}{Q} P , \qquad (27)$$

where

F_1 = 10,430 lb (in this particular example).

F_i = seal load which, in the design procedures, is required to be such that the seal stress is not less than 3 times the pressure. On this particular bolted fitting, the seal area (See Figure 30) is 0.281 sq in., hence, a minimum value of F_i is 0.281 x 3 x P = 0.783 P.

R_B and R_G = spring constants of the bolted fitting discussed in the section "Preload".

F_s = structural load. This load is the sum of the hydrostatic end load, which is proportional to the pressure, and an external bending-moment load*, which, while not necessarily proportional to the pressure, is considered as such in this evaluation.

* The bending-moment design limits at high (over 600 F) temperatures should be further investigated before final designs are established.

$\frac{2qh_G}{Q}$ = displacement characteristic of the bolted fitting giving bolt-load decrease due to the radial effect of internal pressure [See last term in definition of α under Equation (19).]

When the displacement characteristics are evaluated for the bolted fitting shown in Figure 30, and taking F_s as 1.9 P (its value in the temperature range -425 to 600 F), and using the design limit F_i = 0.783 P, Equation (27) becomes

$$F_1 = 0.783\ P + 1.585\ P + 0.206\ P \quad . \tag{28}$$

For F_1 = 10,430 lb, Equation (28) gives P = 4050 psi. This means that the maximum design pressure for the bolted fitting shown in Figure 30, operating at 1500 F for 1.7 hours, is 4050 psi. A series of such calculations has been made for different values of S_t; the results are shown graphically in Figure 32.

The above analysis assumed that there were no temperature gradients in the flanged joint which, in general, probably is not a correct assumption. A critical condition occurs when the bolt load relaxes to 10,430 lb near the end of the service life along with a temperature fluctuation at that time which causes the flanges to be 200 F (design limit) cooler than the bolts. Under these conditions there will be a relative bolt expansion of:

$$\Delta T = 200 \times 0.86 \times 8.5 \times 10^{-6} = 1.46 \times 10^{-3} \text{ in.}$$

The residual bolt load, F_1, is further reduced by this thermal gradient from 10,430 lb to 4900 lb; the corresponding design pressure, P_1, must therefore be limited to 1900 psi. Figure 25 shows P_1 plotted against service life, P_1 being the maximum design pressure where the design procedure includes a 200 F thermal gradient.

Class Ib 3-In. Bolted Fitting and Larger Bolted Fittings in General

The general configuration of a 3-in. bolted fitting for service with internal pressure up to 1500 psi, temperature from -100 F to +200 F is shown in Figure 33. The material used is AM-355. The detailed design procedure is analogous to that discussed for the 1-in. Class Ia bolted fitting.

The comparison of the structural loads with the seating loads for the 3-in. fitting illustrates a general consideration in the design of larger bolted fittings. The basic structural load for the 3-in. Class Ib bolted fitting is 29,000 lb, whereas the seating load needed to yield the seal material is only 10,400 lb. The structural load is proportional to the pressure; hence, by designing for a lower pressure the weight of the fitting would be substantially reduced. In contrast, for a 1-in. Class Ia fitting, the structural load is 3800 lb, the seating load is 3460 lb; hence, there is little to be gained by designing for a pressure lower than 1500 psi.

In many piping systems in a missile, particularly in sizes over 3 in. , the actual operating pressure may be only a fraction of the design pressure of 1500 psi specified for Class Ib and Class IIb fittings. In these large sizes, the structural load rather than the seal-seating load controls the design. Since the structural load is, in large part,

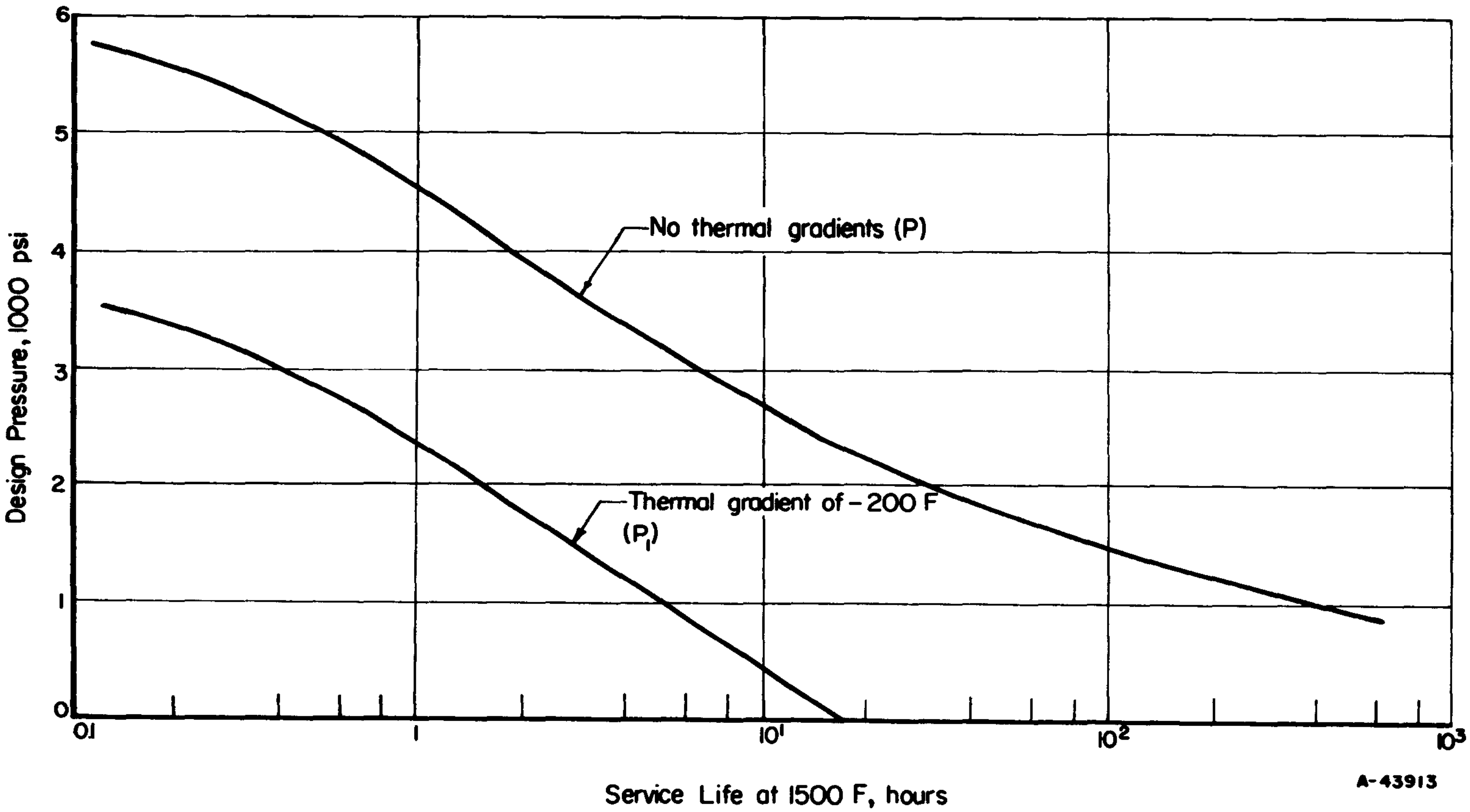

FIGURE 32. PRESSURE-SERVICE LIFE RATINGS OF THE BOLTED FITTING SHOWN IN FIGURE 30

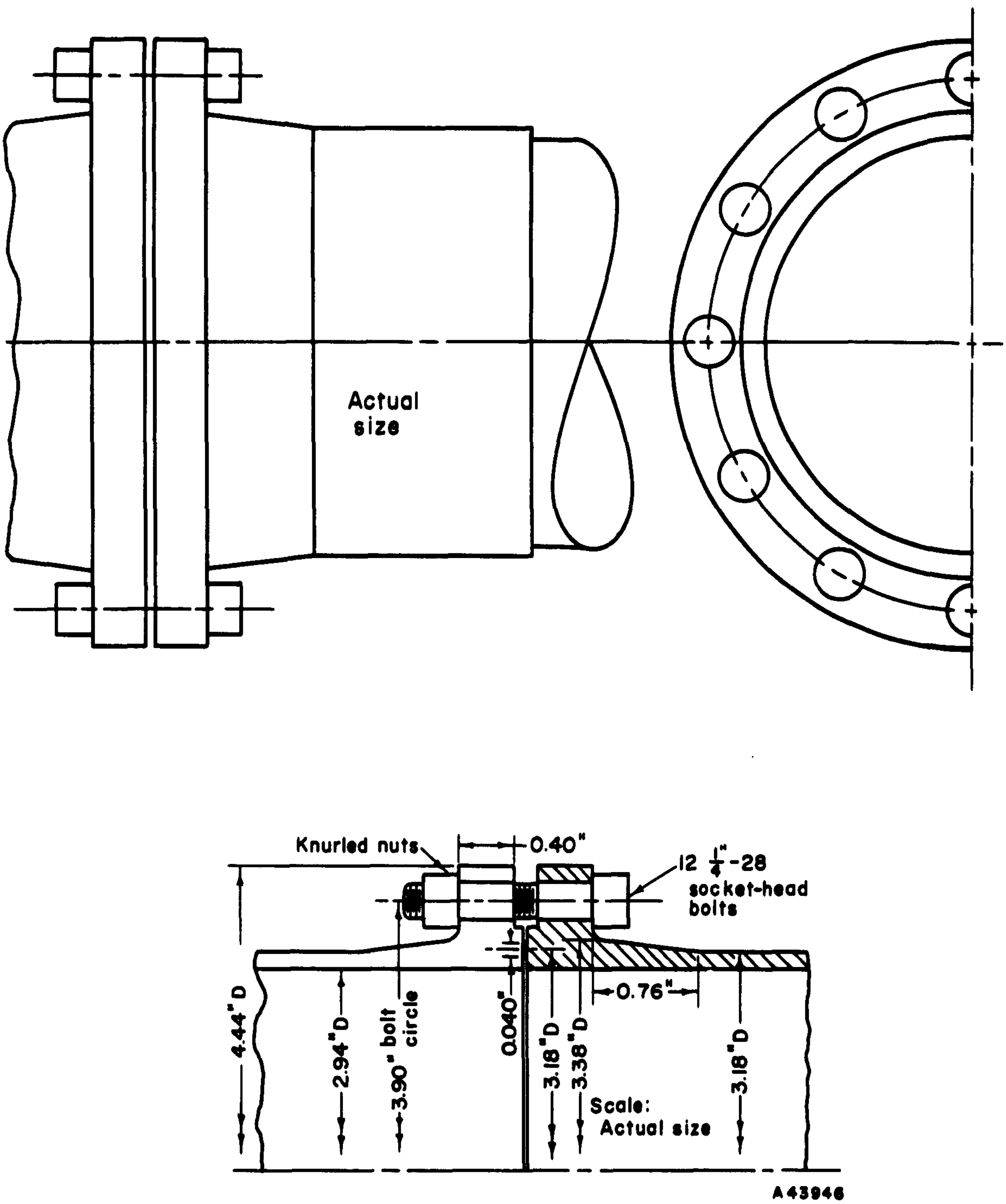

FIGURE 33. 3-IN. CLASS Ib BOLTED FITTING, 1500 PSI AT -100 TO +200 F, AM-355

proportional to the design pressure, a large weight penalty will be imposed by designing for 1500 psi when a lower operating pressure is to be used. As an example of the weight penalty involved, a 16-in. fitting for 1500 psi might weigh about 200 lb, whereas a 16-in. fitting designed for 150 psi might weigh only about 30 lb.

In view of the relatively small number of large size fittings required in missiles, and in view of large weight penalties for overdesign in such large fittings, it does not appear reasonable to establish arbitrary detailed dimensional standards for such fittings. Instead, it would seem more desirable to establish a standardized design procedure, by which means larger fittings could be readily designed for a specific application.

Additional Design Considerations

Accuracy of Preloading. As in the case of threaded fittings, accuracy of preloading may be limited to ±25 per cent if torque wrenches are used in tightening bolts. With a multiplicity of bolts, the probability of achieving a prescribed preload is better than for a threaded fitting in which a single nut is tightened.

Torque Relaxation. While the problem of axial-load relaxation exists in bolted fittings, such behavior is usually ascribed to creep of nonmetallic gaskets rather than to local deformations of the bolt threads. In the process of assembling a bolted fitting, it is good practice to tighten the bolts in steps, using a symmetrical tightening sequence. In this process, each bolt is tightened not once but several times so that short-time yield effects are taken up in the assembly process. In addition, where service conditions are critical, it is good practice to retighten the bolts some 24 hours after initial tightening or, better yet, to retighten the bolts after a short period under service conditions.

Overtightening Factor. As discussed under threaded fittings, some allowance is necessary to prevent damage due to inadvertent overtightening. The 1-in. Class Ia bolted fitting has about a 30 per cent margin for flanges and 42 per cent margin for bolts.

Plastic Deformations. In the case of bolted fittings, maximum calculated stresses in the flanges are localized bending stresses and, hence, the design contains a reserve against gross yielding. On the other hand, the bolts are loaded essentially in tension, and accordingly this margin does not exist. From this standpoint, allowable stresses for bolts should be somewhat more conservatively based than allowable stresses for flanges.

Selection and Spacing of Bolts. For minimum-weight design, it is desirable to locate the bolts rather close to the flange hub, since this decreases the moment on the flange ring by decreasing the moment lever arm. Use of standard hex-head bolts with either regular or heavy hex nuts requires excessive clearance, particularly if additional space is required for use of a box wrench. Standard socket-head cap screws require a minimum of radial clearance and appear generally acceptable for bolted fittings using small (about 1/4 in. or smaller) bolts. In larger sizes, socket-head cap screws do not have adequate bearing surface, and bolts such as those given in NAS-624, "High Strength Air Frame Bolts"(23) are suitable.

The minimum spacing between bolts is controlled by necessary bolt-head clearances and by the "rule-of-thumb" that the ligament between bolt holes should be at least equal to the bolt diameter. The maximum spacing between bolts must be limited to prevent excessive bowing of the flanges between bolt holes, with consequent nonuniform seal loading. The maximum spacing is a function of flange thickness, bolt size, and seal characteristics, along with other factors. Several practical rules for maximum bolt spacing have been proposed; some of these are discussed by Lake and Boyd[24]. A theoretical approach is given by Roberts[25], considering the flange as a beam on an elastic foundation consisting of the seal. This theoretical approach, however, is not applicable to a flange with an integral hub. A review of these developments resulted in the following equation for establishing maximum bolt spacing for bolted fittings with metal seals:

$$C_{max} = 2(d + t) \quad , \tag{29}$$

where

C_{max} = maximum spacing between bolts, in.

d = bolt diameter, in.

t = flange thickness, in.

Equation (21) was used in designing the flanged joints shown in Figure 27 and 30.

Alternative Types of Bolted Fittings. The raised-face, welding-neck type of bolted fitting is, of course, only one of several commonly used types of flanges. A flanged joint with a full-face gasket, as illustrated in Figure 34a, is often used. It has the advantage that both initial bolt loads and structural loads produce less stress than on a raised-face flange. The disadvantages are that the full-face flange has less tolerance against thermal gradients, and there is a much greater tendency for the stress on the gasket to be concentrated at the bolt holes and on the part of the gasket outside of the bolt holes. For this reason, bolted fittings using full-face gaskets generally require higher bolt loads than do comparable fittings using raised faces (gasket entirely inside the bolt holes). In commercial pipeline practice, flanges with full-face gaskets are widely used for mild service conditions (e. g. , water or gas distribution lines at or near atmospheric temperature) but are seldom used for severe service conditions involving either high or low (cryogenic) temperatures or high pressures (above 300 psi).

Use of weld-neck flanges, in which the flange is permanently attached to the tube, may involve problems in aligning bolt holes. The use of a loose-ring flange, as illustrated in Figure 34b, will alleviate this problem. The loose-ring type of flange may, under some conditions, have a further advantage in that greater freedom of choice is available in selecting the flange-ring material since it need not be weldable or brazable to the tube material and it need not be compatible with the fluid. Disadvantages are (1) in general, the loose-ring type flange will be somewhat heavier than the welding-neck-type flange, since it lacks the reinforcement of the integral hub, and (2) the joint is more susceptible to bending-fatigue failure at the juncture of the cylindrical shell with the lap; this disadvantage can be at least partially overcome by increasing the stub-end thickness over that of the mating tube wall, as indicated in Figure 34a.

The flange-ring cross section, except at the bolt holes, consists of a solid metal rectangle. Several other possible cross sections were investigated to see if significant weight reduction could be achieved. Cross sections investigated were (1) coned (Bellville washer shape), (2) tapered, (3) composite (surface of one material, core of a lighter

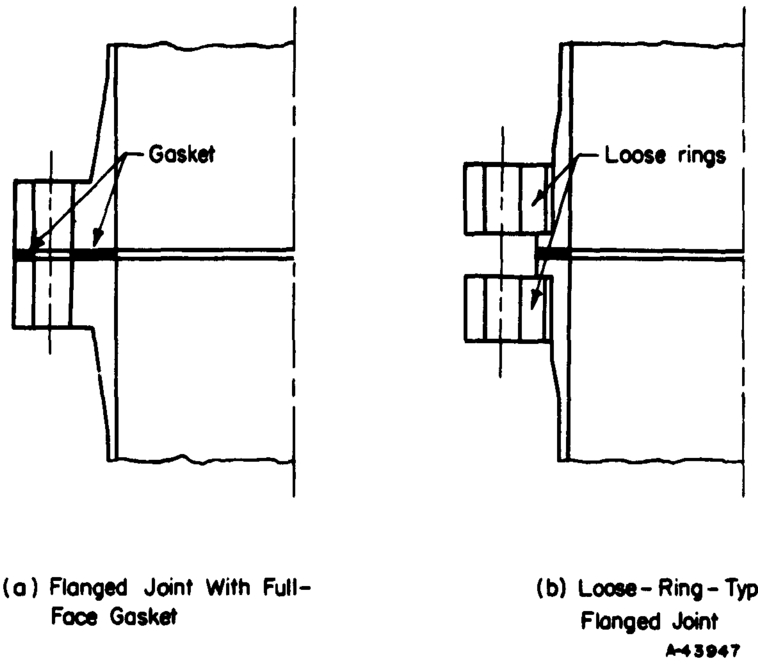

(a) Flanged Joint With Full-Face Gasket

(b) Loose-Ring-Type Flanged Joint

FIGURE 34. ALTERNATIVE TYPES OF BOLTED FITTINGS

material), (4) honeycomb construction, and (5) boxed or internally ribbed construction. The conclusion from the preliminary studies of these alternative ring cross sections was that while minor reduction in weight can be achieved by their use, the resultant disadvantages of increase in costs of design and manufacturing, limitations of temperature range and gradients, and problems of bolt-load distribution are such as to exceed the advantage of a minor weight reduction.

Application of Computers for Optimization of Design

In discussing designs of threaded and bolted fittings the design method was briefly described as the process of selecting a set of dimensions and then checking if these dimensions were satisfactory; if not, a second set of dimensions were selected and the computations repeated. This was repeated as often as necessary to obtain a "satisfactory" design, but not necessarily an "optimum" design. To be of "optimum" design, a fitting for use in missiles must meet two requirements:

(1) The fitting must have the required degree of reliability for the specified service conditions.

(2) Of the infinite number of fitting designs meeting requirement (1), the optimum fitting must be of minimum weight.

Since digital computers can do no more than that which can be done on a desk calculator, the advantage of a computer lies entirely in its speed and accuracy. It is therefore pertinent to consider the design time required for fittings in the absence of a high-speed digital computer and the appropriate computer program. For a specific example, assume that the designer is to establish the dimensions for a bolted fitting of the type shown in Figure 35. He will be furnished the required design parameters:

(1) Maximum and minimum operating temperature and pressure

(2) Matching tube diameter, wall thickness, and material

(3) Thermal gradients

(4) External loadings (bending, axial, and torsional)

(5) Contained fluid or fluids.

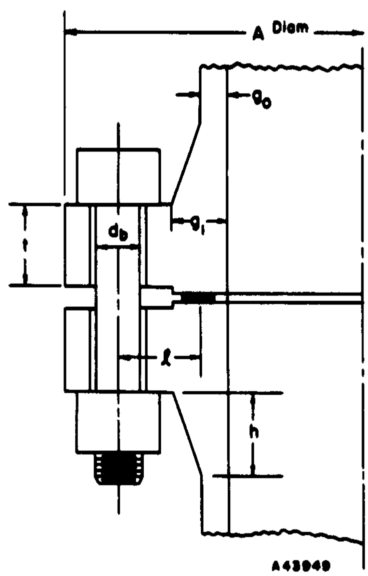

FIGURE 35. ILLUSTRATION OF INDEPENDENT DIMENSIONAL VARIABLES IN A BOLTED FITTING

From the above the designer may select suitable materials for flanges, bolts, and seal, based on suitability for the operating temperatures, compatibility with the fluids, and possibly from the standpoint of weldability or brazability to the matching tube. Having selected materials, the designer may now choose suitable allowable stresses for the flanges and bolts. The next step requires the selection of seven more-or-less independent variables; i. e., on Figure 35 the dimensions t, g_1, g_o, h, ℓ, A, and d_b.

Having selected these dimensions, the designer may proceed with the following calculations, with a rough estimate of the time required (using a desk calculator or slide rule) shown for each calculation:

Stress calculations	1 hour
Displacement calculations	2 hours
Preload calculations	2 hours
Creep design calculations	3 hours

Upon completion of from about 5 to 8 hours' work (depending on whether creep is involved), the designer will know whether the dimensions he has selected will provide a satisfactory fitting, as indicated by the maximum calculated stresses being less than the pre-established allowable stresses or, in the case of creep design, that the calculated service life is adequate. If the fitting meets the design criteria (and after some experience, most designers can readily select dimensions so that the criteria are met) the question arises: Is the fitting of minimum weight? That is, is there some other combination of the variables t, g_1, g_o, h, ℓ, A, and d_b which would also meet the design criteria and would be of less weight? Unfortunately, there are no established analytical relationships between the seven independent variables, the design parameters, and the fitting weight. In order to answer the question, it is necessary to vary each of the seven variables while holding the other six constant. Even for a very limited investigation of the variable ranges, it is apparent that hundreds of calculations are involved, each of which requires some 5 to 8 hours of design time. (For example, if only two steps are used for each variable, the total calculations number 128.)

The value of the digital computer at this stage is obvious, since the computation time involved could be reduced from hundreds or thousands of hours to a few hours. (A reduction factor by use of high-speed digital computers of 1 to 100 is readily obtainable.)

Several degrees of sophistication in a computer program could be used. At one extreme, a program which appears technically feasible would entail feeding into the computer only the design parameters of tube size, design pressure and temperature, external loads, thermal gradients, and material properties, the program being such that the computer would automatically perform a series of iterations with various step values of the independent variables, compute and compare weights, and eventually print out the values of the independent dimensional variables which give a fitting of minimum weight and its weight. While technically feasible, preparation of such a program is a formidable undertaking.

On the other hand, a much simpler program could be developed in which the design parameters and independent dimensional variables would be fed into the computer. The computer would then compute and print out the stresses and weight for the particular set of variables fed into the computer. Independent dimensional variables could then be step-varied by the designer, each step reintroduced into the computer and successive steps varied as indicated by the results of previous computations. This type of program would be expected to give general indications of the relationships between the independent dimensional variables, the design parameters, and the fitting weight, in addition to specific optimization of a given fitting design. In the present state of the art, the simpler program approach appears to be more practical.

Although the design of a bolted fitting was used as an illustration in explaining the use of a computer, threaded fittings are not excluded from this consideration. However, it must be recognized that design of a threaded fitting by a computer is more difficult and the results will probably be less reliable in the absence of experimental verification. This is true because such variables as thread friction, torque relaxation, and preload control enter into the design process, and their varying behavior is not known as accurately for a threaded connection.

References

(14) "Strength of Aircraft Elements", Military Handbook 5 (March, 1961).

(15) "Air Weapons Materials Application Handbook, Metals and Alloys", ARDC TR 59-66 (December, 1959).

(16) "Fittings, Flareless, Fluid Connection", Military Specification MIL-F-1280A (A56) (April 24, 1956).

(17) "Mechanical-Drive Steam Turbines", National Electrical Manufacturers Association (NEMA) Standards Publication No. SM20-1958 (revised November, 1959).

(18) Rossheim, D. B., and Markl, A. R. C., "The Significance of and Suggested Limits for the Stress in Pipe Lines Due to the Combined Effects of Pressure and Expansion", ASME Trans. (July, 1940).

(19) Wesstrom, D. B., and Bergh, S. E., "Effect of Internal Pressure on Stresses and Strains in Bolted-Flanged Connections", ASME Trans. (July, 1951).

(20) Rodabaugh, E. C., Discussion of Reference (19), ASME Trans. (July, 1951).

(21) Engineering Data Bulletin VM-107, René 41 (May, 1958), Metallurgical Products Dept., General Electric Co., Detroit 32, Michigan.

(22) "Effect of Creep-Exposure on Mechanical Properties of René 41", University of Michigan, ASD TR 61-73 (August, 1961).

(23) National Standards Association Standard NAS-624, "High Strength Air Frame Bolts".

(24) Lake, G. F., and Boyd, G., "Design of Bolted, Flanged Joints of Pressure Vessels", Proc. Institute of Mechanical Engineers (1957).

(25) Roberts, Irving, "Gaskets and Bolted Joints", ASME Journal of Applied Mechanics (1950).

TUBE-TO-FITTING DESIGN

Design Parameters

Brazing and Welding

High-Energy-Rate Welding

References

TUBE-TO-FITTING DESIGN

The tube-to-fitting connection must satisfy two major requirements: it must contain the fluid with no leakage, and it must maintain structural integrity throughout the design life of the system. The structural loads which the tube-to-fitting connection must withstand are similar to many loads discussed in the section on fitting-to-fitting connections and hence will not be discussed here in detail. The other design parameters will be described.

Design Parameters

Reliability

Reliability of the tube-to-fitting connection is of such prime importance that the method chosen by which this connection is made must assure repeatable joint integrity within close limits. Ideally, reproducibility as established by statistical evaluation should be adequate to preclude preliminary tests. However, some provision for visual inspection is desirable to guarantee that all parts are assembled in their correct position.

Weight

A permanent connection would be the most reliable type of joint and would result in a mechanical fitting of least weight. This is especially true when the effects of the connection on the tubing wall thickness are considered. Because the tubing may constitute as much as 90 per cent of the total system weight, it is essential that its wall thickness be kept as low as possible. If the tube-to-fitting connection is not a permanent connection, as is the case with the flareless fitting, additional tubing strength must be provided at the point of connection because of the stresses caused by the clamping of the tubing wall. Practically speaking, this can be done only by increasing the wall thickness, with a resulting over-all weight increase.

Assembly

The tube-to-fitting connection must be simple to enhance its reliability and it must also be easily assembled. The method of making the connection must therefore be relatively independent of tubing tolerances, surface finishes, surface cleanliness, and operator skill. If this is not possible, a suitable technique or piece of equipment must be developed which will satisfactorily reduce these to minor considerations.

Misalignment of the tubing within the system must be compensated for. The program objectives were to provide a fitting which would tolerate 4° included angle misalignment for fitting sizes up to and including 4 in.; 1-1/2° for size up to and including 6 in.; and 1/2° for sizes up to and including 16 in. An axial misalignment capability 1/4 in. from center line was desired for all fitting sizes greater than 1 in.

One approach was to use a ball-and-socket joint at the fitting-to-fitting connection. Any such joint conceived, however, was excessively heavy. Within the fitting structure the tube-to-fitting connection is the only other choice for misalignment compensation. The misalignment of the tubes to be joined might be measured and compensated for in the process of joining the tube to the fitting. Because the system will probably be fabricated from a high-strength heat-treated material, not easily deformed or modified, it is possible that misalignment can best be compensated for by means of adjustable tubing supports. In any case the tube-to-fitting connection must be designed to withstand these imposed loads.

Material

Recent advances in metallurgy have provided alloys with very good strength-to-density ratios. In the future, even better materials probably will be available. The assembly method, therefore, should be such that new materials can be used with a minimum of development work. Furthermore, the assembly method should not cause degradation of the mechanical properties of the tube or fitting materials. Many of the newer alloys, including the three selected for the improved fittings, attain their high strength-to-density ratios because of heat treatment. This strength advantage is minimized when excessive temperatures are applied to local areas. The thickness and hence the weight of the fitting must then be increased in proportion to the reduction in material strength.

Candidate Joining Methods

Two kinds of joints were considered, namely, "hot" and "cold". Hot joints are those which require an external source of heat, e.g., soldering, brazing, and the many types of welding. Cold joints are those which require only mechanical energy, e.g., swaging, roll bonding, friction welding, and high-energy welding.

Of the many types of joints considered, three are recommended for the tube-to-fitting connection: brazed, hot welded, and explosive welded. However, unlike the fitting-to-fitting connection, a configuration for the tube-to-fitting connection cannot be derived readily by analytical methods within the present state of the art. Experimentation is necessary to define the critical parameters. Therefore in the following discussion instead of presenting preliminary designs, the recommended methods for making the tube-to-fitting connection will be described and the effect of these methods on the final configuration will be discussed.

Brazing and Welding

Considerable work has been done by North American Aviation* on welded and brazed joints for tubing for aerospace applications. The results of this work have been reviewed in detail and have been found to be directly applicable to the problem of making a satisfactory tube-to-fitting connection for improved missile mechanical fittings. Many of the NAA procedures are illustrated in a paper by G. R. Barton, et al., (26)** and a full description will soon appear in an official report. The possible application of these concepts to a mechanical fitting is discussed below.

* AF Contract No. 04(611)-8177.

** Numbers in parentheses refer to references on page 92.

Choice of Materials

Materials that are compatible with the welding and brazing operations must be chosen. North American Aviation has reported that the materials recommended by Battelle for mechanical fittings have been successfully brazed and welded by NAA as part of their joint development effort. Therefore, no difficulties should arise because of the materials selected.

Source of Heat

Heat sources selected by NAA include a modification of the standard induction heating system for the brazed joint and the tungsten, inert-gas (TIG) process for the fusion-welded joint. Although other heat sources may be used, the ones chosen offer the advantages of being clean, neat, versatile, and, most important, easily controlled. Very close control is necessary when heat-treated materials such as AM-350 are used, to prevent the heat-affected zone from extending outside the fitting envelope.

Joint Fit-Up

Because OD tolerances of purchased tubing are too liberal, the tubing must be sized before joining to insure correct braze capillary action and proper weld penetration and heat transfer, and to insure the proper fit of the tube and fitting to withstand external bending loads. Typically, total diametrical tolerances of 0.002 to 0.005 in. are required.

Filler Material

In the NAA brazed joint, illustrated in the Barton paper(26), brazing alloy reservoirs are provided to obtain optimum capillary flow during brazing. The brazing alloy must be selected for structural strength, service temperature, and corrosion resistance to the contained fluid. Nominally, its eutectic temperature should be at least 300 to 500 F above the expected service temperature(27). Fluid compatibility is unimportant in fusion welding because there is no alien filler material present(26).

Cleanliness

To insure highly reliable joints, whether brazed or welded, all components must be specially cleaned. It is also necessary to purge with a specially prepared inert gas before, during, and after the application of heat because of the detrimental effect of surface oxides.

Conclusions

In spite of some apparent drawbacks associated with North American Aviation's hot-joining techniques, the probability of successfully satisfying the stringent requirements of joint integrity are much better for the immediate present with these methods than with other methods or concepts suggested or studied. The need for sizing the tube for joint fit-up will necessitate a quality-control program. Special handling and assembling procedures are also serious limitations. However, it is believed that such limitations can be sufficiently overcome to make the brazed or welded joint a practical tube-to-fitting connection. Furthermore, extensive field experience and experimentation should lead to further refinements and simplifications.

High-Energy-Rate Welding

High-energy-rate welding is a process which utilizes high pressures for extremely short periods of time to obtain a metallurgical union between two metallic parts. High-energy-rate welding differs from high-energy-rate forming only in the magnitudes and time-variant characteristics of the applied forces.

Two basic energy sources presently being utilized for high-energy-rate forming are (1) the electrical energy stored in a bank of high-voltage capacitors, and (2) chemical explosives. No data have been found on the use of capacitor discharge for welding metal, although the operation is theoretically possible. On the other hand, considerable work has been done by several companies on the use of chemical explosives to weld different metal shapes. Much of this work appears pertinent to the problem of making satisfactory tube-to-fitting connections.

Chemical Explosives

Chemical explosives are classified into two general categories: low explosives and high explosives. Low explosives, such as smokeless powder and black powder, have a burning rate or deflagration velocity ranging from a few inches to a few feet per second and can produce pressures in the order of 30,000 to 300,000 psi, depending on the degree of confinement. High explosives, such as TNT, PETN, and dynamite have a detonation velocity in the order of 6000 to 28,000 ft/sec and can produce pressures up to about 4-million psi. Low explosives are normally used in enclosed systems where the containment helps increase the impulse imparted to the workpiece. High explosives are normally fired as bare charges in open systems because the peak pressure is relatively independent of the degree of confinement[28]. Some characteristics of high explosives are given in Tables 10, 11, and 12. From Table 11 the total energy available from 1 lb of PETN is approximately 1.74-million ft-lb ($4.35 \times 10^5 \times 4$). With a typical conversion time of 2 μ sec, this is equivalent to approximately 1.57-billion hp.

The total impulse imparted to the workpiece is represented by

$$I = \int_{t_o}^{t_f} P dt, \tag{30}$$

where

I = impulse, lb-sec/in.^{2}
P = pressure, psi
t = time, sec.

TABLE 10. CHARACTERISTICS OF HIGH AND LOW EXPLOSIVES[29]

Property	High Explosives	Low Explosives
Method of initiation	Primary high explosives--ignition, spark, flame, or impact Secondary high explosives--detonator, or detonator and booster combination	Ignition
Conversion time	Microseconds	Milliseconds
Conversion rate	6,000 to 28,000 ft/sec	A few inches to a few feet per second
Pressures	Up to about 4,000,000 psi	Up to about 40,000 psi

TABLE 11. CHARACTERISTICS OF HIGH EXPLOSIVES[29]

Explosive	Specific Gravity	Detonation Velocity, 1-1/4-In. Diameter, ft/sec	Energy[a], 10^5 ft-lb/lb	Maximum Pressure[b], 10^6 psi
RDX (cyclotrimethylene trinitramine)	1.7	27,500	4.25	3.4
PETN (pentaerythritol tetranitrate)	1.6	26,500	4.35	3.2
Pentolite (50 PETN/50 TNT)	1.6	25,000	3.17	2.8
TNT (trinitrotoluene)	1.6	23,000	2.62	2.4

(a) Based on ballistic-mortar comparisons. Total energy would be four times these figures.
(b) At 1-1/4-in. diameter. Based primarily on the calculations by the methods of Cook. By Taylor's methods, this pressure will be 10 to 20 per cent lower.

TABLE 12. PROPERTIES OF EXPLOSIVES[28]

Explosive	Specific Gravity	Detonation Temperature, C	Detonation Pressure, 10^6 psi
RDX	1.6	5450	375
PETN	1.6	5400	330
Tetryl	1.6	4400	290
Picric acid	1.6	3900	265
TNT	1.6	3900	225

For a given impulse, which is proportional to the energy imparted to the workpiece, the pressure-time relationship can take many forms. In explosive welding both the total impulse and the pressure-time relationship are important. For example, if the high-pressure loads are released too fast, the tensile stresses induced by the over-recovery of the material may tend to distort or fracture the piece[28]. Typical pressure-time curves for low and high explosives are shown in Figure 36. The conversion time, i.e., the time required to convert a working amount of explosive into gaseous products, is measured in microseconds for high explosives and milliseconds for low explosives[28]. To date, only high explosives have been shown to be applicable to welding operations[30].

Explosive-Welding Variables

The variables that must be controlled in explosive welding are primarily those affecting the velocity of the interface closure. If the developed interface angle and the closure velocity are correct, welding occurs. In the case of tubular or concentric components, interface angle and closure velocity can be varied by changing wall thickness, charge density (amount of explosive per unit of surface area being welded), or the initial clearance or separation at the interface. It is not necessary that all of these be variables if one or more can be changed to bring the system into proper balance[30].

Two explosive-welding techniques are possible[28]. In one method the parts are placed in contact and are then subjected to a load applied normal to the surface to be welded in an underwater standoff operation. This method is applicable mainly to flat plates. In the second method, which is applicable to flat plates and tubular components, the parts are not initially in contact. This is the method discussed below.

When an explosive detonates, there is a finite time during which the detonation travels symmetrically outward from the initiation point. For a line charge set off at one end, the detonation progression is, of course, along the length of the line. For example, Figure 37 shows a linear charge, consisting of a stick of dynamite, detonating under water. The V-shaped shock wave produced is essentially a conical front around the explosive[31]. The effect of the shock wave is apparent in the displacement of the suspended wire.

The principles of explosive welding can be illustrated by the system of plates shown in Figure 38. As the detonation progresses along the sheet of explosive, a shock wave and gas cloud are produced. For high explosives not in contact with the workpiece, the major portion of the usable energy is provided by the shock wave, whereas for low explosives the gas-cloud pressure provides a major portion of the usable energy. The velocity of the shock wave in the direction perpendicular to the plate is essentially the velocity of sound in the transfer medium between the explosive and plate. In the space immediately adjacent to the explosive the velocity will be much greater due to the rapid expansion of the gaseous products. With contact charges the gaseous expansion also adds to the usable energy transfered to the workpiece.

Figure 39 depicts the manner in which the peak pressure at the workpiece may be varied as a function of charge size and standoff distance. An explosive with a detonation velocity of 25,000 ft/sec was used in constructing these curves on the basis of the following equations[29]:

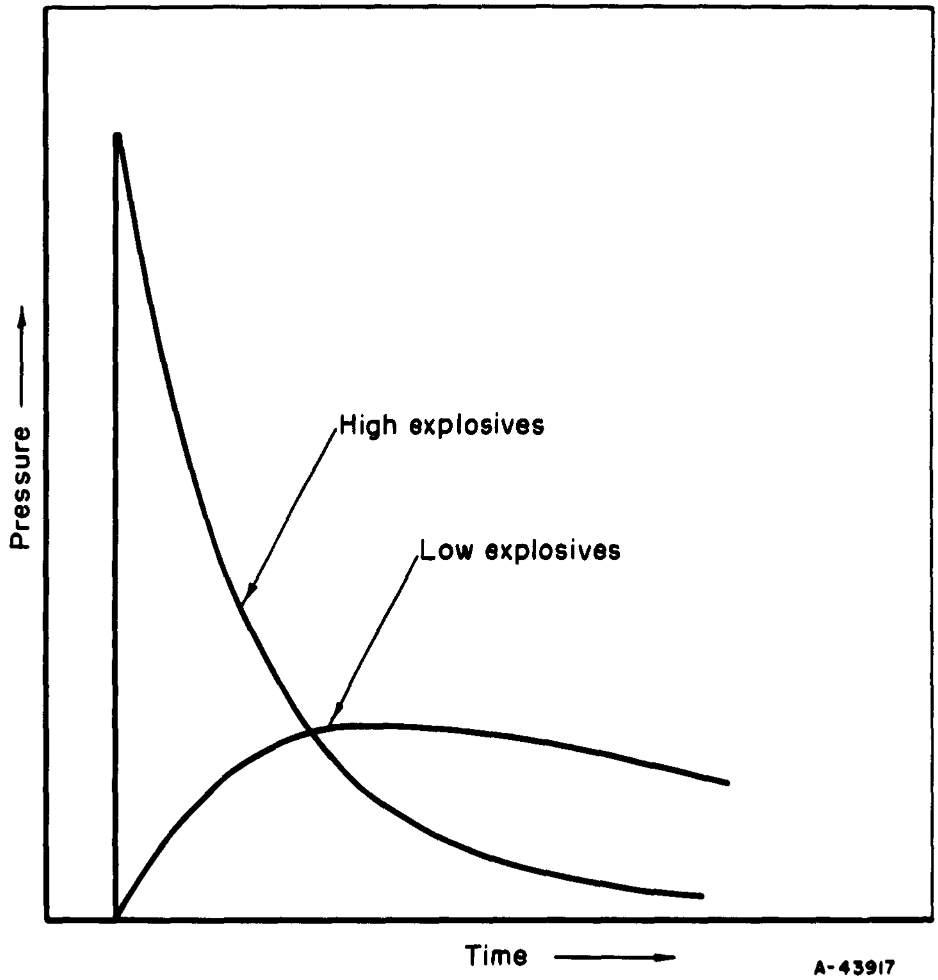

FIGURE 36. TYPICAL TIME-PRESSURE PROFILES FOR LOW AND HIGH EXPLOSIVES(29)

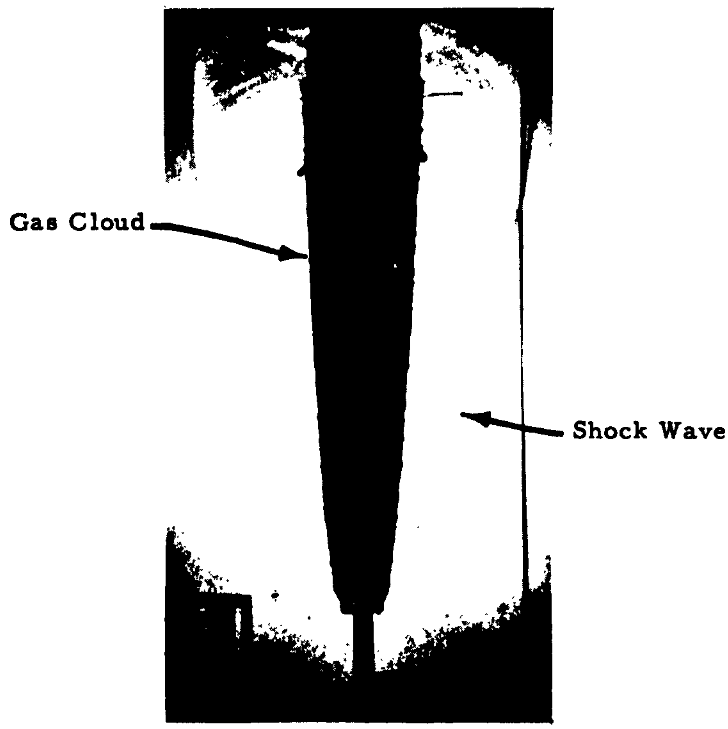

FIGURE 37. LINE CHARGE DETONATING IN WATER(31)

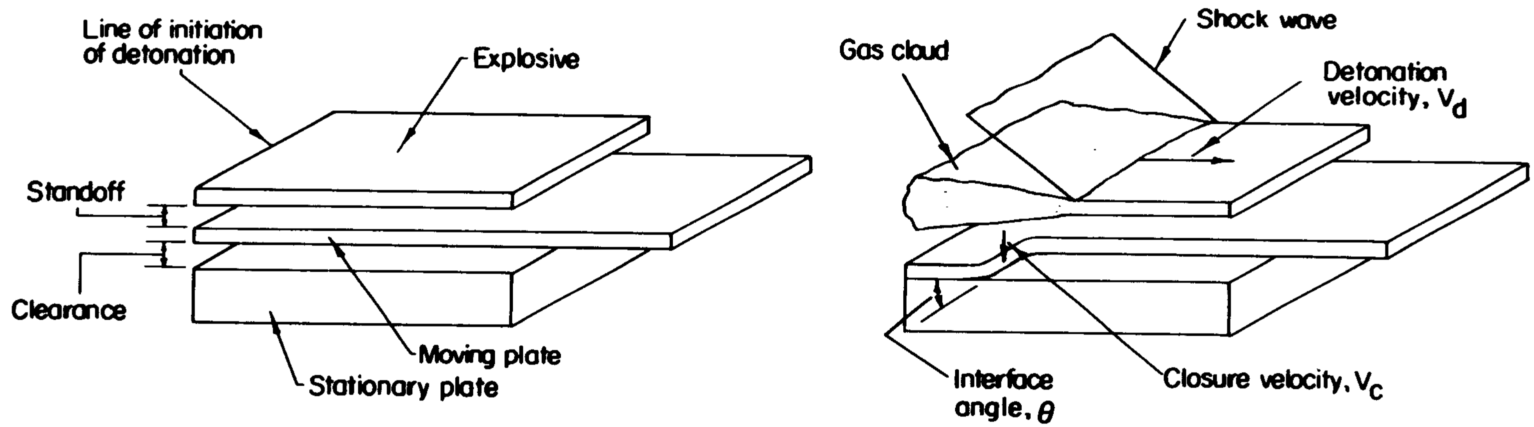

a. Before Detonation

b. After Detonation

A-43931

FIGURE 38. EXPLOSIVE WELDING OF FLAT PLATES

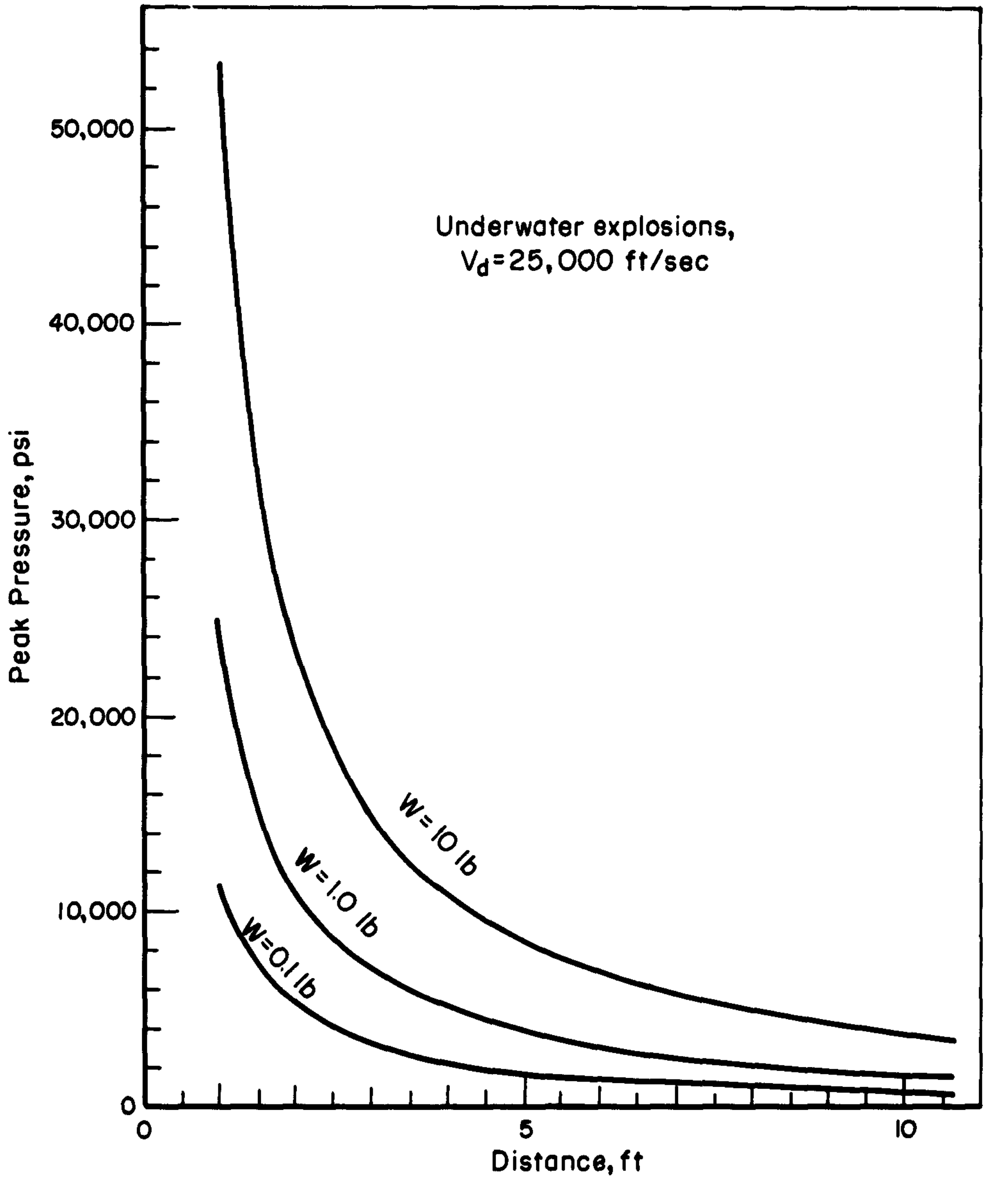

FIGURE 39. EFFECT OF CHARGE SIZE AND STANDOFF DISTANCE ON PEAK PRESSURE[29]

$$P = K_1\left(\frac{W^{1/3}}{R}\right)^{\alpha} \tag{31}$$

and

$$P = 155\left(\frac{W^{1/3}}{R^{1.15}}\right)\sqrt{V_d}, \tag{32}$$

where

P = peak pressure, psi
W = weight of explosive, lb
R = distance from explosive, ft
K_1 = constant which varies with the explosive
α = constant which is generally equal to 1.15
V_d = detonation velocity of explosive, ft/sec

It is not necessary to perform the welding operation in water. However, the constants in Equations (31) and (32) must be modified where air is the transfer medium. The peak pressure with air as the transfer medium will be approximately 30 per cent of the peak pressure with water as the transfer medium.

Figure 40 shows the effect of the transfer medium and the standoff distance on the peak pressure at the workpiece. If a charge were detonated at the end of a tube, the peak pressure would diminish along the length of the tube as shown. Therefore, a piece of equipment 3 ft from an explosive charge equal to 4 lb of TNT would be subjected to a pressure of only 500 psi in air.

The shock wave, as it progresses (Figure 38b), imparts an impulse load to the plate. The velocity of closure, V_c, is much smaller than the velocity of detonation, V_d, and hence the plate, as it deforms, forms the interface angle, θ, between the stationary plate and the moving plate.

The developed interface angle, θ, will depend on the relative magnitudes of V_c and V_d and the initial clearance between the two plates. As the initial clearance between the plates is increased, θ becomes larger. For a given type of explosive, the detonation of velocity, V_d, is a constant. The closure velocity, V_c, which is a function of the total energy delivered to the upper plate, can be varied over a wide range by changing the charge density, the upper plate thickness, and the charge standoff distance. The closure velocity also depends on the density and dynamic yield strength of the upper-plate material. Variations in the charge density and standoff distance change the peak pressure and hence also change the total amount of energy delivered to the workpiece.

The total energy delivered to the workpiece is expended in three ways. Part of the energy is used to overcome the material inertia, part causes deformation of the upper plate, and the remainder causes the plate to accelerate. The final closure velocity is a function of the acceleration of the plate. Any parametric change that affects the percentage of total energy left for acceleration of the plate will also cause a change in the closure velocity. Hence, an increase in plate thickness, material density, or dynamic yield strength will diminish the closure velocity.

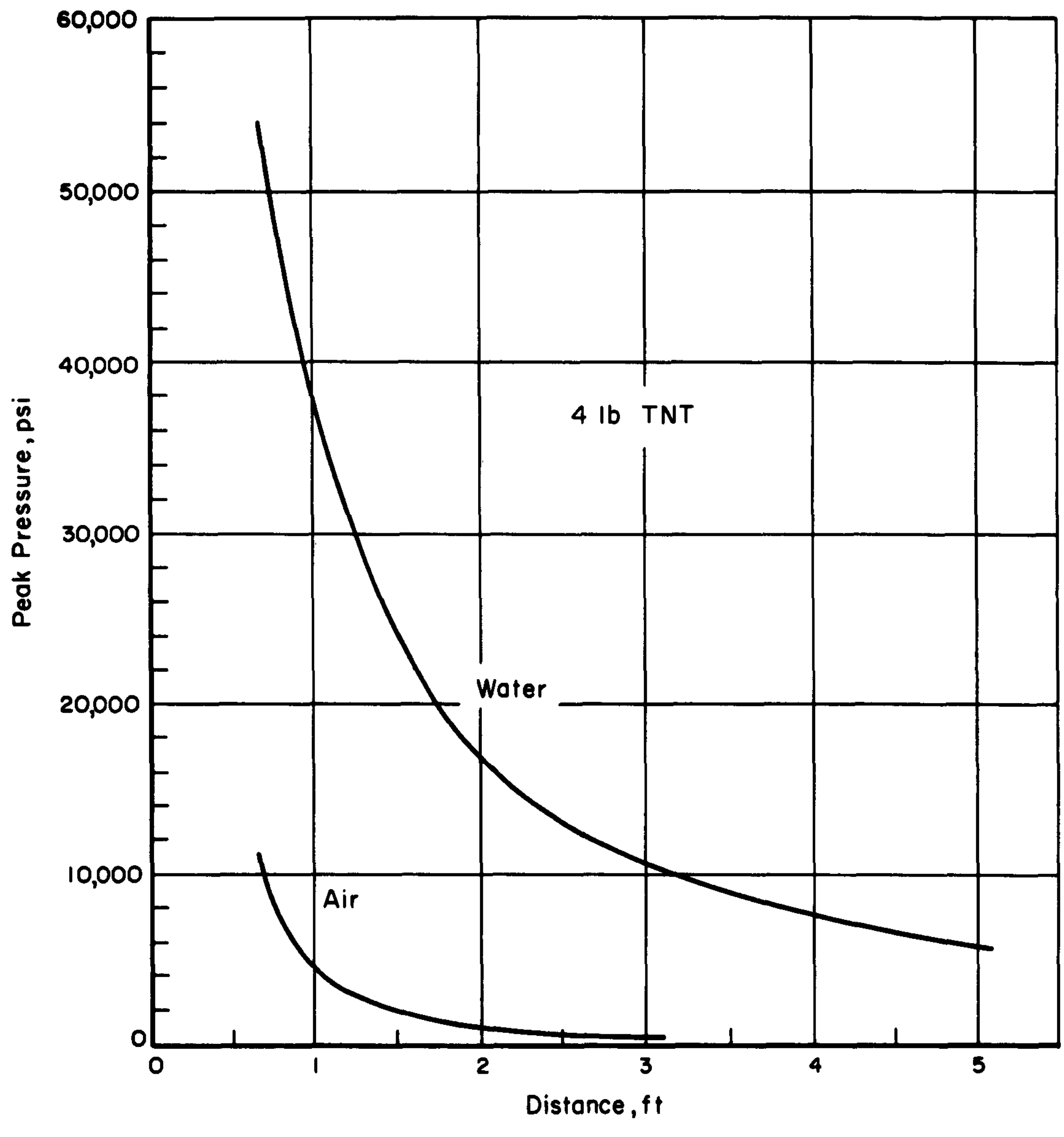

FIGURE 40. EFFECT OF TRANSFER MEDIUM AND STANDOFF DISTANCE ON PEAK PRESSURE[29]

In much of the past work on explosive welding, the interface between the two plates has been evacuated. However, it has been shown that evacuation is not necessary to obtain welding. The principal advantage to be gained from evacuation is the reduced compound formation when dissimilar materials are being welded. However, even in cases in which dissimilar metals are joined, the small amount of compound formation usually has little effect on the strength and integrity of the joint.

Experience has shown that the explosive welding process is not sensitive to surface cleanliness or roughness. Degreasing and wire brushing are usually the most stringent surface preparations necessary. Welds have been obtained even without the wire brushing, and it has been reported that degreasing is unnecessary[31, 32]. A series of experimental runs at Battelle on the explosive welding of Zircaloy-2 tubing to Type 410 stainless steel tubing indicated that changes in the surface finish in the range of 300 μin. rms to 1500 μin. rms had no effect on the accomplishment of a weld[33]. A Type 304 stainless steel sleeve with a 100-μin. rms finish was successfully welded to the inside of a Type 304 stainless steel ring with a surface finish of 30 μin. rms.

Characteristics of Explosively Welded Joint

Among the principal advantages of explosive techniques are the absence of heat-affected zones, the absence of excessive compound formation in cases in which the welded elements are dissimilar metals, the lack of effect on the mechanical characteristics of most materials, the ability to treat large areas and geometries which present difficulties with other processes, and the relatively small and simple equipment required[29,30].

Mechanical fittings which utilize a replaceable seal are particularly susceptible to the effects of heat applied near the seal surface because of the tendency for the seal surface to warp under nonuniform heating. A rule of thumb states that a fusion weld should be a distance of $2\sqrt{Dt}$ from the sealing surface, where D is the tube diameter and t is the tube-wall thickness. The temperature necessary to fusion weld or braze may also affect the strength of the material, as previously discussed. An explosive weld, because of the low amount of heat generated, and because of the symmetrical nature of the forming process, would minimize the warping problem.

When dissimilar metals are fusion welded the relatively large melted zone causes considerable compound formation. Again, because there is no melted zone with explosive welding, this problem is minimized.

Figure 41 shows four possible arrangements of tube, fitting, and explosive. Figure 41a shows the working explosive charge in contact with the inside of the tube. The working charge is set off by means of the detonating cap attached to an explosive leader, which is tented so that the detonation progression of the working explosive is symmetrical with the tube axis. Figure 41b shows a line charge placed on the axis of the tube. A modification of Figures 41a and 41b is shown in Figure 41c, in which the working explosive is wrapped on a mandrel centered in the tube. Variations in mandrel diameter would vary the charge standoff distance. With a given total explosive charge, the peak pressure at the tube would be a maximum in Figure 41a, and a minimum in Figure 41b. Any pressure between the maximum and minimum could be obtained by means of the configuration in Figure 41c. An externally placed explosive charge is shown in Figure 41d. Again, a tenting arrangement is provided to obtain the proper detonation progression.

In each of the configurations in Figure 41 it would be possible to make the explosive into a package that could be inserted and set off by semiskilled personnel. The only other equipment needed for all fittings would be a battery detonator no larger than a lunch pail and a length of wire to lead from the detonator to the detonating cap. For some fittings, depending on the tube wall thickness, the size of explosive charge, and the configuration, it might be necessary to provide internal or external backup dies to prevent excessive deformation of the tube and/or fitting.

Because of the possibility of developing a "package" for a particular size fitting, an explosively welded joint should be extremely reliable.

Conclusions

Although adaptation of the North American brazed or welded joint appears to be the best method of achieving a reliable tube-to-fitting connection in the next year or two, it is believed that an explosively welded joint might be a significant improvement for introduction at a later date. For this reason it is recommended that further research be pursued to determine the general problems of explosively welding AM-355, 17-4PH, and René 41, which are the materials selected for use in improved fittings. It is difficult to estimate the proper size range that future development should be concerned with because economic and logistic considerations are as important as the safety of the operation and the technical feasibility. At Battelle, a 3-in.-diameter Zircaloy tube with a wall thickness of 0.045 in. was successfully welded to a stainless steel header with a 45-gram charge of PETN. This appears to be a reasonable estimate of the conditions that might be encountered in making a 3-inch welded tube-to-fitting connection, and this size of charge probably represents the maximum that could be readily handled.

References

(26) Barton, G. R., et al., "Tubular Joining by Induction Brazing and Fusion Welding Methods", SAE Aerospace Manufacturing Forum, The Ambassador Hotel, Los Angeles, California, October 8, 1962.

(27) Personal communications with Robert M. Evans of Metals Joining Division, Battelle Memorial Institute.

(28) Pearson, John, "The Explosive Working of Metals", Navord Report 7033 (1960).

(29) Simons, Charles C., "Explosive Metalworking", DMIC Memorandum 71, OTS PB 161221 (November 3, 1960).

(30) Personal communication with Ronald J. Carlson and Charles C. Simons of the Department of Metallurgy and Physics, Battelle Memorial Institute.

(31) Douglass, John J., "Forming Practices With High Explosives", Du Pont Technical Bulletin (May 26, 1960).

(32) Yernow, Dr. Louis, "Explosive Welding", Paper presented at New Bonding Methods Symposium of Annual ASM Metals Show, New York, New York, October 30, 1962.

(33) Paprocki, Stan J., Porembka, Stanley W., et al., "Joining Zircaloy-Stainless Steel and SAP Alloys by Friction, Rolling, and Explosive Techniques", report BMI-1594 to the AEC (September 4, 1962).

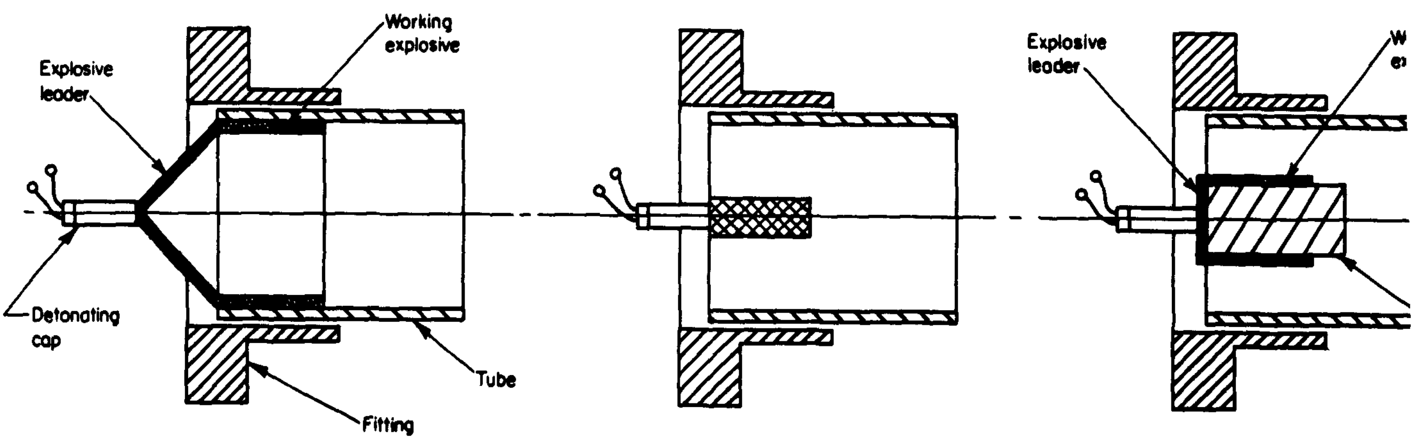

a. b. c.

FIGURE 41. EXPLOSIVE-WELDING ARRANGEMENTS

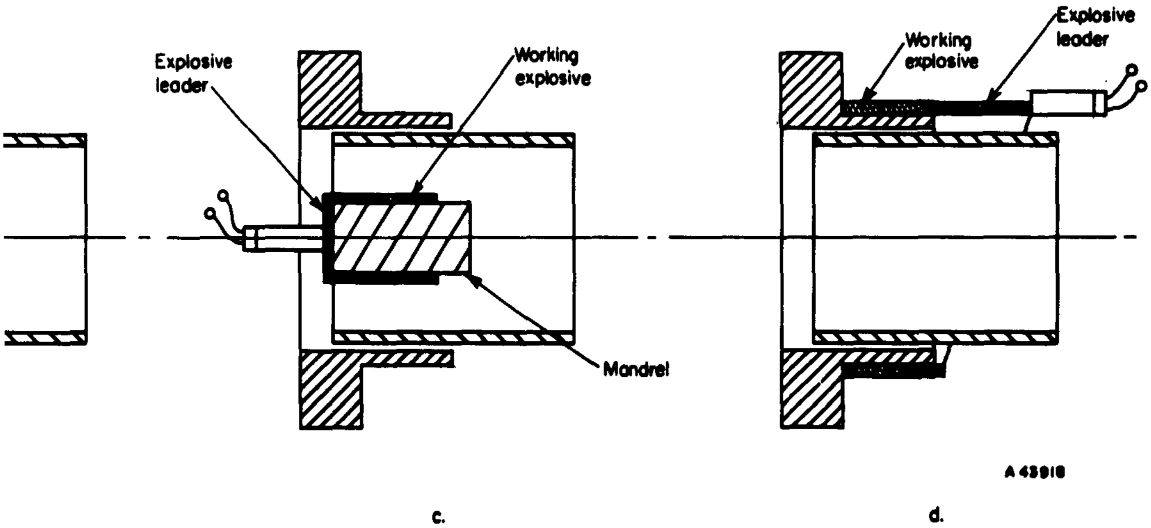
Explosive leader
Working explosive
Mandrel
Working explosive
Explosive leader
A 43918
c.
d.

NTS

2

SEAL DESIGN

SEAL DESIGN

The seal poses the most difficult design problem of the fitting. The required service-temperature ranges preclude the use of a nonmetallic seal except for Class I fittings, and experience with metal seals has not resulted in clearly defined understanding or agreement among designers on the sealing mechanism of metal seals. Unfortunately, analytical studies do not appear to provide the necessary information, and laboratory studies have not been conclusive because of the predisposition of the evaluators or because of the small sample sizes tested. The failure data from the field have been sufficiently limited that field experience has not contributed significantly to a solution of the sealing problem.

The studies and evaluations performed in Phase I have resulted in the selection of three types of seals which offer sufficient potential to be considered for Phase II:

- Pressurized O-ring
- High-energy-rate formed
- Mechanical toggle

The first is conceptual, and its feasibility is yet untested. Considerable experimental evidence exists to support the basic mechanism of the second, but a promising configuration has yet to be conceived. The third is available in commercial fittings, but the configurations have not met with wide acceptance. The seal-design parameters are first discussed and then the recommended seals are described.

Design Parameters

An understanding of the problems involved in attaining a helium-tight seal is dependent on the analysis of certain factors known to affect leakage when the seal is initially established as well as after the seal is established. These factors include (1) the geometry of the leakage path and the nature of the leakage flow, (2) the magnitude of the seating loads needed to produce an initial seal, (3) the plastic flow of the seal material, (4) the interaction of sealing members, and (5) the effects of temperature. Also in this section, a brief discussion is given of the design thinking in relation to pressure-energized seals.

Leakage Analysis

The flow of a viscous fluid through the seal interface can be analyzed on the basis of laminar flow if the mean free path of the fluid's molecules is less than the height of the smallest passage along the leak path. If the mean free path is the same order of magnitude as the passage height, molecular flow results, and a correction for slip flow along the wall must be applied to the laminar-flow analysis. A more detailed analysis is presented in Appendix V. In general, the flow may be considered laminar if

$$\frac{\lambda}{h} < 1.0 \quad , \tag{33}$$

where

$\frac{\lambda}{h}$ = Knudsen number

λ = mean free path of molecule

h = passage height.

If the Knudsen number approaches 1.0 it is still possible to analyze the flow on the basis of laminar flow by use of a correction factor which is a function of the Knudsen number.

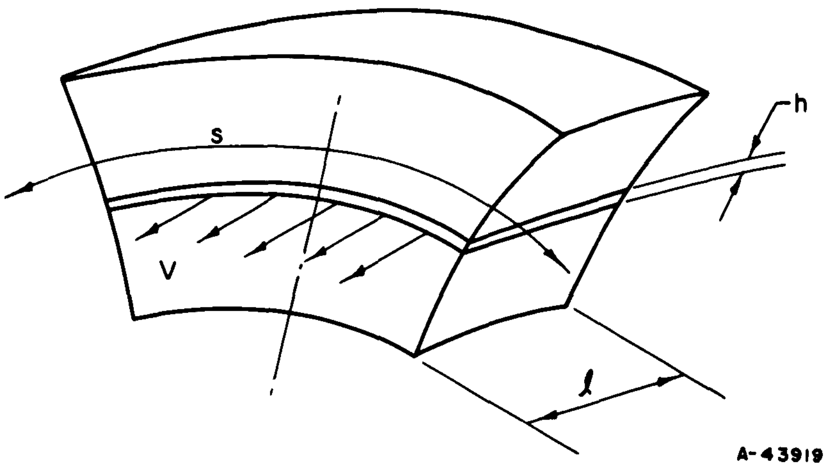

FIGURE 42. MODEL OF TYPICAL LEAKAGE PATH

The narrow slot in Figure 42 represents a typical flow passage. Flow takes place at velocity V in the direction of the length, ℓ. The width, s, corresponds to the periphery of a circular seal and h is the passage height. For the case where flow is laminar, the mass-flow equation in terms of the discharge pressure is

$$M_L = \frac{sh^3\left[\left(\frac{P_1}{P_2}\right)^2 - 1\right] P_2 \rho_2}{24 \eta \ell} , \tag{34}$$

where

M_L = mass rate of flow

P_1 = inlet pressure

P_2 = discharge pressure

ρ_2 = discharge-gas density

η = viscosity.

For molecular flow, the mass-flow equation is

$$M_m = \frac{16sh^2(P_1 - P_2)P_{avg}\lambda}{9\pi\eta RT} , \quad (35)$$

or more simply,

$$M_m = 6.8 \frac{\lambda}{h} M_L . \quad (36)$$

When the flow is neither laminar nor molecular, i. e., for Knudsen's number close to 1.0, the flow equation of state is defined as

$$M_T = M_L + EM_m , \quad (37)$$

where E is a constant found experimentally to be approximately 0.9 for single gases and 0.66 for gaseous mixtures(34). The total flow, by substitution of Equation (36) and the value of 0.9 for E, is

$$M_T = M_L (1 + 6.1 \frac{\lambda}{h}) . \quad (38)$$

This expression holds when the mean free path is evaluated at the average pressure in the passage.

The above expressions indicate the important effect the length and height of the leakage path have on flow rate. For both the laminar and molecular flow conditions, the rate of flow is inversely proportional to passage length. Therefore, one conclusion is that the seal passage should be of considerable length. However, increasing the length of the seal passage is a severe handicap from the viewpoint of seating loads and minimum assembly torque.

The effect of the second parameter, height, makes it obvious that the degree of surface conformity is extremely critical. In the case of laminar flow, mass rate of flow is dependent on the cube of the passage height, whereas in molecular flow it is dependent on the square of the passage height.

Because of the random variations in surface profile, the best measure of required average passage height for seals capable of sealing gases would be in microinches or angstroms, where one angstrom equals 3.937×10^{-3} μin. Extrapolation of leakage-rate charts(35) indicates that a passage height ranging between 0.25 and 25 A is required to seal helium gas at 10,000 psi, with a leakage rate no greater than 7.7×10^{-7} atm-cc/sec. This is the maximum allowable leakage as defined for the project.

Seating Loads

A basic problem in designing a metal-to-metal fluid seal is the determination of the "seating load", i. e., the load required to produce intimate contact between the sealing surfaces initially. The problem is essentially the same whether the seal is pressure energized or not and is independent of operating pressures or external loads.

*Numbers in parenthesis denote references listed on page 115.

Below are some of the factors that must be considered in determining seating loads:

(1) Seal Design. The seal width largely determines the magnitude of the seating load, since seating load is a function of sealing area.

(2) Metal Properties. The hardness, compressive yield strength, and strain-hardening characteristics of the seal material will determine the unit stress necessary to effect a seal.

(3) Surface Properties. The surface finish determines the total amount of yielding necessary to close all leak passages. Gross distortion such as waviness and warping is ordinarily a minor problem but can become serious when processes which cause distortion, such as welding, brazing, and swaging, are used to effect the tube-to-fitting connection.

(4) Contained Fluid. The viscosity, density, surface tension, and state of the contained fluid determine the maximum size of leak path which can be tolerated.

(5) Pressure. The pressure, which affects the rate of flow through a passage, also determines the maximum size of leak path acceptable.

(6) Allowable Leakage Rate. Obviously, as the allowable leakage rate is lowered, higher seating loads may be required to reduce the size of the leak paths.

A widely used set of gasket seating-stress constants are those given in the ASME Code for Unfired Pressure Vessels.

Material	Seating Stress[(a)], psi
Soft aluminum	4,400
Soft copper or brass	6,500
Iron or soft steel	9,000
Monel or 4 to 6 per cent chromium	10,900
Stainless steels	13,000

(a) Gaskets not over 1/2 in. wide.

These gasket constants are based on experience and rather limited test data and are justified[(36)] principally on the observation that flanged joints when designed on the basis of these constants almost always work satisfactorily.

In addition, it should be noted that the gasket stresses are interrelated with a comparatively low bolt design stress so that, in actual installations, considerably higher stresses can be and probably generally are applied.

A gasket stress of 30,000 psi is suggested for stainless steel flared fittings for sealing helium.[(37)] This is roughly double the ASME Code value. However, the Code value is possibly based on experience with liquids and gases for which low leakage rates were not objectionable. It might be noted that flared fittings, usually satisfactory with liquids, have seating stresses as follows:

Nominal Size	Seating Stress, psi
3	37,000
4	36,000
5	33,000
6	37,000
8	26,000
10	25,000
12	18,400
16	15,700

On the basis of the literature, the larger sizes of flared fittings, 8 and up, apparently are especially troublesome when attempting to seal helium.

The preceding discussion was concerned with seating stresses for flat metal gaskets. The axial load can be reduced by using a very narrow gasket until, as a limit, a line contact is obtained, at least initially. The question arises as to what seating load is required for line-contact gaskets. For stainless steel O-rings used for sealing helium, an average seating load of 1000 lb/lineal in. is suggested.[38] One design method for flanges with lens-ring gaskets is based on about 3000 lb/lineal in. Some approximate calculations on probable loadings on pipe unions also give seating loads in this general range.

Plastic Flow

The previous discussion of seating loads was based on gross effects and on data gathered from experience. Another approach to the problem is a consideration of microscopic effects at the seal interface. Because plastic deformation of the surface asperities is considered essential to achieve the surface conformity required to seal helium, an analysis of seating loads can be based on the phenomena of contact resistance and plastic flow of metals. Although the phenomenon of local plastic deformation of surface asperities has been investigated extensively, neither an exact nor consistent determination of the phenomenon is available. It has been shown, however, that the seating force applied should be greater than that obtained by merely multiplying the yield stress of the material by the surface contact area. Exactly how much greater this force should be is not known; estimates range up to 3 times greater.

Temperature Effects

Two temperature effects of particular importance are the steady-state effect at the temperature extremes and the transient effect during temperature changes. Dimensional changes due to temperature occur axially, radially, or both, depending on the configuration of the seal. Typical configurations are shown in Figure 43. Seals may contain variations or even combinations of these basic seal configurations.

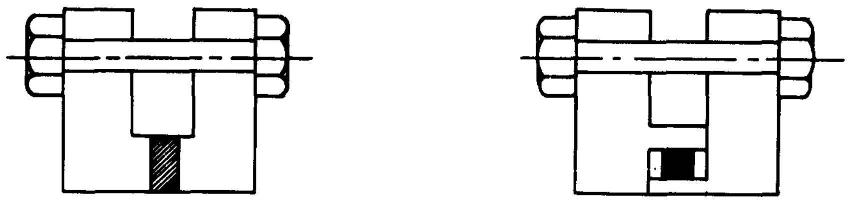

a. Axial Seal b. Radial Seal

A-43920

FIGURE 43. AXIAL AND RADIAL SEALING CAVITIES

At a temperature extreme, if the seal and the flanges are made of dissimilar materials, the sealing pressure may increase or decrease due to relative expansion or contraction of the seal and the structural components of the fitting. The actual changes depend on the location of the parts and their thermal coefficients or expansion. At elevated temperatures the effects of creep must be considered. The magnitude of the initial axial preload must be sufficient to compensate for these effects. Axial preload is a minor consideration in a radial seal, but the seal must be elastically deflected initially and must be able to follow up when dimensional changes occur.

Large thermal gradients, caused by transient thermal states, aggravate the problems described above. In addition, thermal gradients are more likely to cause a momentary shifting of the sealing surfaces, and this may destroy the surface mating which was achieved when the fitting was originally assembled and one material yielded against the other.

Pressure Energization

The concept of a pressure-energized metal seal has become increasingly popular. Many new seals and fittings have been designed which incorporate this principle. Basically, it is postulated that by elastically deflecting "cantilevered" legs a sufficient amount when the fitting is initially assembled, the seal can breathe with the system as the sealing load relaxes. Relaxation could be caused by pressure end loads, vibration or reverse bending, creep, thermal gradients, or torque relaxation. Further, as the system pressure increases, more force is applied to the deflectable leg by the pressurized fluid, thereby causing additional sealing force.

The major problems of using a pressure-energized seal for the improved fittings are related to the temperature range required, the fluids handled, and the low leakage requirement. While a nonmetallic material might be used as a seal in a Class I fitting, a major program objective is to obtain a seal for -425 F to 1500 F. Such a seal must be metal. Further, because of temperature problems and fluid-compatibility problems, it appears that the softer metals such as aluminum, copper, and gold may not be suitable. Thus, any candidate seal material, such as nickel, has a fairly high yield stress. As explained previously, the seal pressure needed to seal helium is estimated to be up to three times the yield stress of the softer material.

The strength necessary in a cantilever leg to seal helium can be provided with present materials only by designing a stiff leg with low deflection. In a commercially available seal using several such legs to increase the deflection, the total deflection is of the order of 0. 005 in. Manufacturing tolerances and thermal gradients make this low movement difficult to design for. The use of this and similar seals has resulted in difficulties for temperature ranges similar to Class I. For temperatures ranging from -425 to 1500 F it is believed that it will be exceedingly difficult, if not impossible, to apply a cantilever seal satisfactorily with acceptable manufacturing and assembly tolerances.

A further complication of the cantilever seal is its normal tendency to move slightly. For many applications this movement is not harmful. For sealing helium, a very slight movement of one surface relative to the other probably will destroy the minute surface conformity obtained by yielding one material against the other. It is believed that a satisfactory seal must be designed to be stationary and firmly clamped in place.

Conclusions

Of all the parameters discussed, the one which influences and predetermines the seal and fitting design most is that concerning plastic yielding at the sealing surface. Once it is concluded that plastic yielding is essential for sealing helium, the choices available as to the size of the sealing area, the amount of preload, and the choice of materials become limited. The conclusions drawn can be summarized as follows:

(1) The effective height of the sealing passage must be of the order of 0. 25 to 25 A. This surface contact can be achieved only by plastic yielding of one or both surfaces. To effectively reduce the seating load, a relatively low-yield-strength metal such as nickel might be used as a surface coating on the seal.

(2) An initial seating stress possibly as high as three times the yield stress of the gasket material is necessary to achieve the desired degree of yielding.

(3) A pressure-energized seal may not be necessary, or even desirable.

Pressurized Metallic O-Rings

Present Theory

The sealing force generated between the walls of a standard metallic O-ring and the walls of the flange is a function of the spring constant of the toroidal configuration of the O-ring and the properties of the material of the ring. The presently accepted theory defining this operation is that upon flange closure, the contacting surface of the O-ring is plastically deformed into the seal cavity. The combination of the spring-back resiliency of the ring and the action of the fluid pressure on the exposed surface of the ring (see Figure 44a) tend to further force this deformed surface against the flange walls. This produces a significant contact stress between these two surfaces which, being greater than the fluid pressure, acts as an efficient seal.

The spring-back resilience of this configuration can be increased by using the pressurized metallic O-ring (Figure 44b) or the self-energized metallic O-ring (Figure 44c). In both, pressure inside the O-ring increases the ring's spring constant and its spring-back resiliency after plastic deformation has taken place. The self-energized O-ring has the further feature of allowing an increase in pressure inside the ring as the pressure of the fluid to be sealed increases.

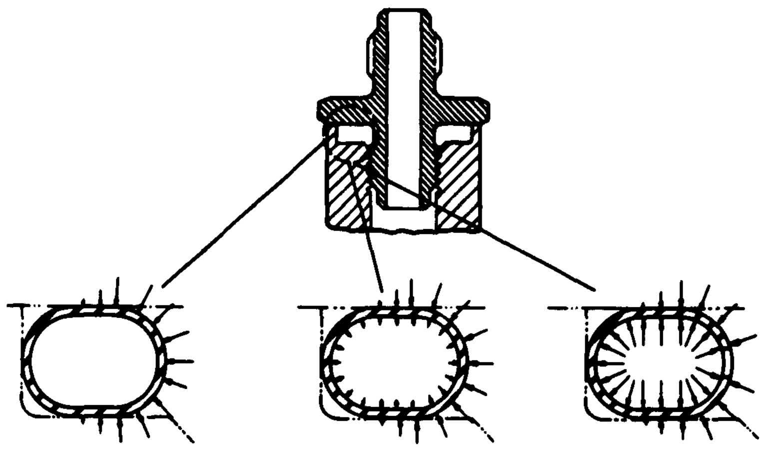

a. Standard Metallic O-Ring b. Pressurized Metallic O-Ring c. Self-Energized Metallic O-Ring

FIGURE 44. PRESSURE FORCES ACTING ON VARIOUS TYPES OF METALLIC O-RINGS

These sealing methods have been shown to be successful for many applications. However, where high temperatures or severe induced vibrations or bending loads are encountered, leakage will almost invariably occur. It would appear that in the case of elevated-temperature operation the change in material properties of the O-ring material becomes a definite parameter. As the temperature is raised, both the yield stress and the elastic modulus of the material are lowered. These changes have the effect of decreasing the spring constant and the spring-back resiliency of the ring. Such decreases will result in a reduction in the contact stresses found at the interface of the sealing surface and so reduce the sealing capabilities.

New Design Principle

With this in mind, a seal design is postulated which could operate successfully in the elevated-temperature range. This concept, which might be called a plastic-state O-ring (illustrated in Figure 45), utilizes to advantage the change in material properties of the ring at elevated temperature.

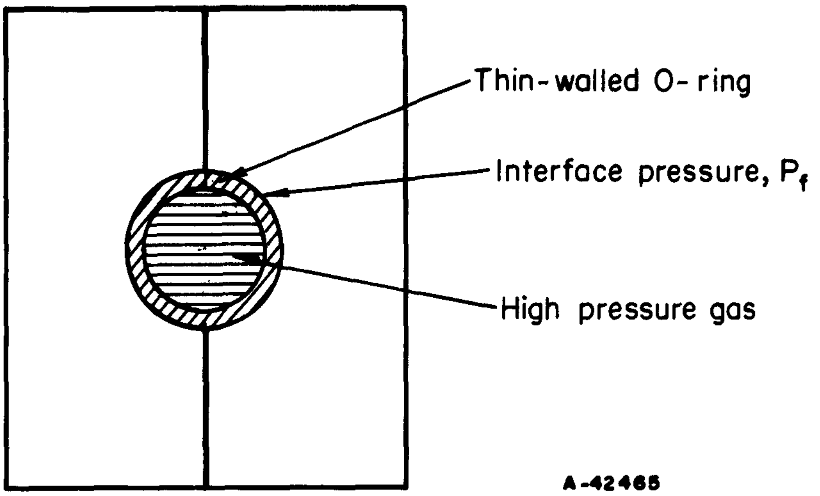

FIGURE 45. INTERNALLY PRESSURIZED O-RING

When assembled, the O-ring is fitted into a cavity which supports the torus in all directions. In order to compensate for tolerances it may be advisable to make the cavity and the torus dissimilar in cross section. When the flanges are assembled and the tightening preload is applied, the torus will be deformed to conform to the cavity geometry, and metal-to-metal contact will be obtained. Included inside the O-ring torus is a gas-emitting crystal or a low-energy pyrotechnic. The gas-producing reaction would be initiated after the fitting is completely assembled and torqued.

Since the gas in the ring is completely sealed in a fixed volume, the change in pressure of this gas would be a simple function of the operating temperature of the fitting (see Equation 40); a rise in temperature would induce a rise in pressure.

The material of the O-ring should be so chosen that when the operating temperature of the fitting is increased, its elastic-stress capability is drastically decreased. If the O-ring material and the type and volume of gas in the O-ring are carefully selected, a point somewhere below the normal operating temperature of the fitting will be reached where the O-ring is in a fully plastic state. This can be clearly seen if we consider the O-ring – flange configuration as a cylindrical pressure vessel with an infinite outside diameter and an inside diameter equal to that of the O-ring. In this consideration, of course, the curvature of the ring as well as the large but finite thickness of the flange wall as compared with the O-ring inside diameter are neglected. However, for a close approximation this assumption serves adequately. The point at which the inner fibers of the wall become plastic will be reached when the internal pressure equals 0. 577 σ_y (yield stress at any given temperature of the material as determined from a simple uniaxial tensile test). This criterion is derived from the maximum-distortion- energy-criterion of failure for material, sometimes called the Hencky-von Mises criterion.

Noting that the wall of the O-ring is very thin, we can further assume that the tube will be fully plastic when the pressure is slightly greater than 0. 577 σ_y.

The action is qualitatively illustrated in Figure 46.

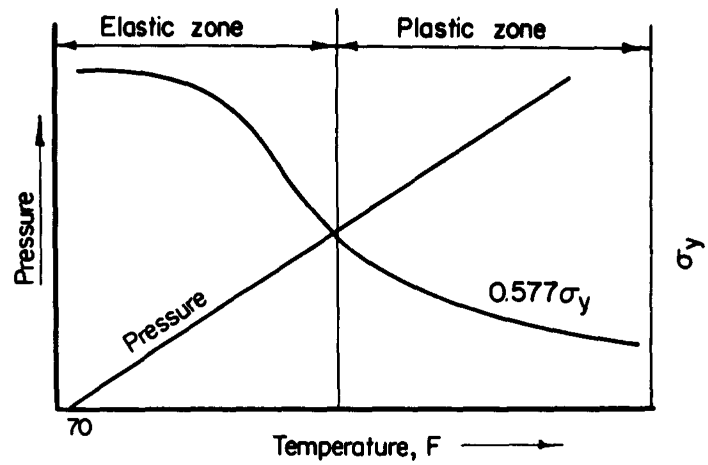

FIGURE 46. PRESSURE-TEMPERATURE-YIELD STRESS RELATIONSHIP FOR O-RING SEAL

The internal pressure, P, is defined as

$$P = \rho ZRT , \tag{39}$$

where

ρ = gas density

Z = compressibility factor

R = universal gas constant

T = absolute temperature.

Assuming that the internal volume is essentially unchanged and discounting the compressibility factor,

$$\frac{P_1}{P_2} = C \frac{T_1}{T_2} , \tag{40}$$

where C includes the ρ, Z, and R terms. Therefore the internal pressure increases linearly with the change in temperature ratio.

In this situation the high internal pressure is contained in a fully plastic O-ring which is in turn fully contained by the walls of the seal cavity of the flange. As long as a there is no separation of the flange faces the tube cannot blow out, since there is no place for the tube material to go. In fact, as long as the flange faces stay in contact the internal pressure in the ring could still be raised significantly (as would occur with a further increase in temperature).

The advantages of this concept are: (1), that in the fully plastic state the O-ring material, under the action of the high internal pressure, will flow into the small surface discontinuities of the seal-cavity walls, thereby forming a seal that should be effective in stopping even molecular leakages, and (2) with the advent of the relaxation of the flange prestress, which is encountered at elevated temperatures, the high contact stress required to maintain this close interface fit is achieved by the action of the internal pressure. A serious disadvantage would be encountered if this type of seal were to be exposed to conditions where the temperature variation would be cyclic, resulting in a condition where the O-ring would vary between the plastic and the elastic state. Such a condition could adversely affect the physical properties of the ring material, resulting in a low-cycle fatigue phenomenom and early ring failure.

Conclusions

As presently conceived, the O-ring would not become plastic until some elevated temperature was reached. The primary reason for this requirement is to prevent rupture at room temperature and to permit safe handling at assembly and disassembly of the pressurized O-ring. Therefore, the seal could be primarily of use for high temperatures and might be considered only in the role of a secondary seal. In the plastic zone there would be no significant time lag, as the seal breathes with the strain fluctuations and essentially a steady state condition would exist. Probably the most advantageous application would be in sealing hot gases for Class V fittings where temperatures range from 1000 to 3000 F. Development of an O-ring seal that could operate in this temperature range will require utilization of metals with very high melting points. Tantalum seems to be a possible choice. In the lower temperature range, 600 to 1500 F, nickel or copper could be used.

Aside from the temperature ranges, one other limitation must be emphasized. As previously indicated, when the O-ring is in the plastic zone the flange separation must be kept below a few thousandths of an inch to prevent rupture or blowout.

High-Energy-Rate Formed Seal

Considerable experimental evidence has been developed concerning the conformity of one metallic surface with another when caused by high-energy rate forming. As discussed in the section "Tube-to-Fitting Design", explosive energy has been used to achieve a good mechanical bond, equivalent to a weld, between several kinds of metals either flat or tubular in configuration. On the basis of an analysis of this work, it was believed that the surface conformity needed to seal helium could be easily provided by high-energy-rate forming.

Two basic configurations were envisoned as a means of applying explosive energy to the formation of a seal in a fitting. The first was an internal formed seal in which the expanding explosive force would be used to seal a sleeve against the inside of the fitting parts. This configuration would make the best use of the available energy, but a problem existed in the contamination of the fluid system by the explosive. The second configuration was an externally formed seal which would collapse radially or seal against the flange faces. Because it was difficult to postulate the energy needed to achieve adequate conformity for the possible configurations, preliminary laboratory experiments were made to obtain a general idea of the effect of different amounts of explosive on basic seal shapes.

Experiments Performed

Seal formation by means of an internal explosive charge was investigated with the configuration shown in Figure 47. The ferrules, representing the stub-end portion of the fitting attached to the tubing, were separated by a spacer ring which would be used to facilitate disassembly. The seal ring was expanded by means of an explosive charge to form a seal between the ferrules. The mandrel diameter upon which the explosive charge was mounted was changed in successive experiments to provide variations in the standoff distance.

Use of an external explosive for formation of the seal was investigated by means of the configuration shown in Figure 48. The explosive was contained in a groove machined on the outside diameter of the seal ring. The walls between the flanges and explosive were approximately 0.010 in. thick, and it was hoped that these walls would be sealed against the flanges.

Description of Results

For the internal explosive charge, five experiments were made with various size mandrels. The mandrel size determined both the total charge and the standoff distance. In all cases the seal ring was displaced slightly in the direction of the detonation progression, that is, from right to left as shown in Figure 47. Figure 49 is a photomicrograph of Area B in Figure 47, polished and etched. Excellent conformity was achieved between the seal ring and the spacer ring and ferrule. Figure 50 is a photomicrograph of Area C polished but not etched.

Eight experiments were made with the external explosive-charge configuration. The original attempt was to form a seal at Point A in Figure 51. However the best bond occurred at Point B. Evaluation will show that this is a reasonable result, since Poisson's effect is most pronounced at Point B when the seal ring is under a high external load, as shown in Figure 52. The thin seal flanges shrouding the explosive were too flexible and probably sprang back after the explosive pressure was dissipated.

However, when the force, w, is high, as in the case of an explosive charge, the actual strain, ϵ_2, is much greater than the elastic strain and a considerable seating load is applied from the seal to the flange face.

Possible Externally, Explosively Formed Seal

The design concept shown in Figure 53, although preliminary in nature, illustrates the basic premises on which an external high-energy seal might be based.

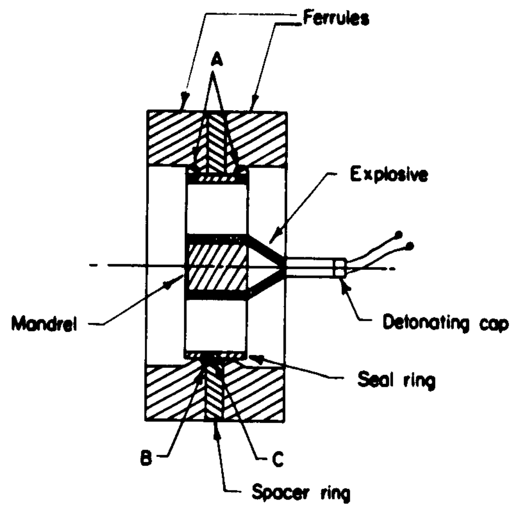

FIGURE 47. CONFIGURATION FOR INTERNAL-CHARGE SEAL EXPERIMENT

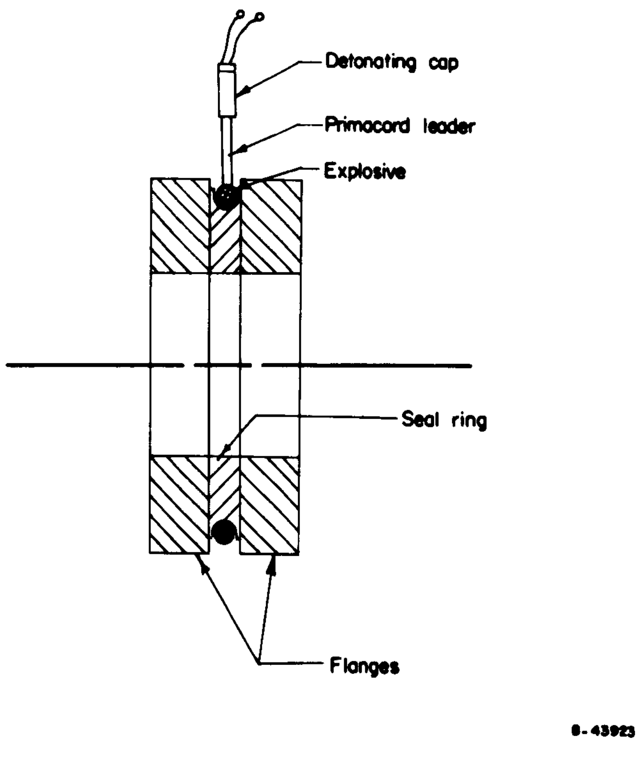

FIGURE 48. CONFIGURATION FOR EXTERNAL-CHARGE SEAL EXPERIMENT

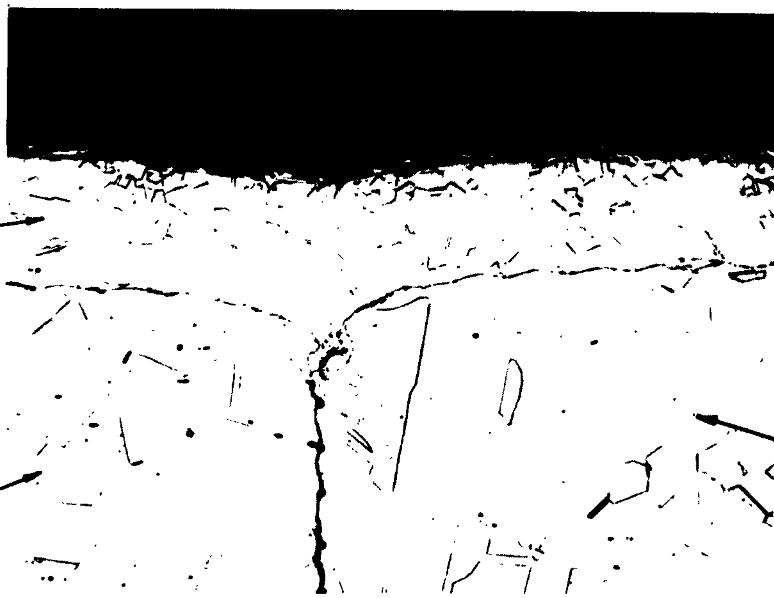

100X Etched RM22186

FIGURE 49. AREA B OF FIGURE 47

1000 X Unetched RM22256

FIGURE 50. AREA C OF FIGURE 47

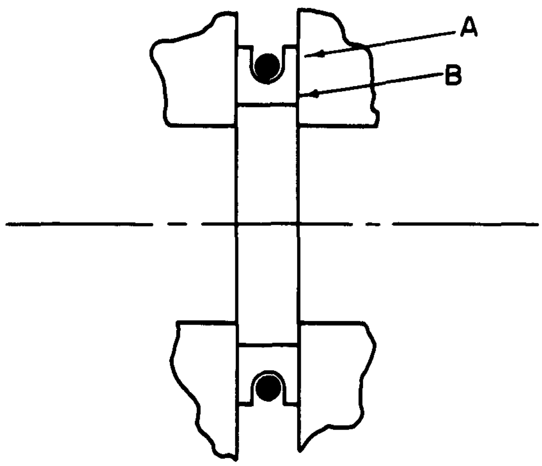

FIGURE 51. EXTERNAL-EXPLOSIVE SEAL

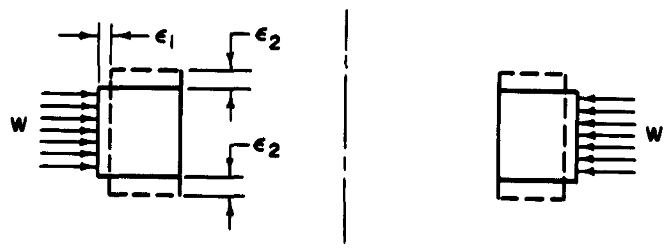

FIGURE 52. POISSON'S EFFECT ON SEAL RING

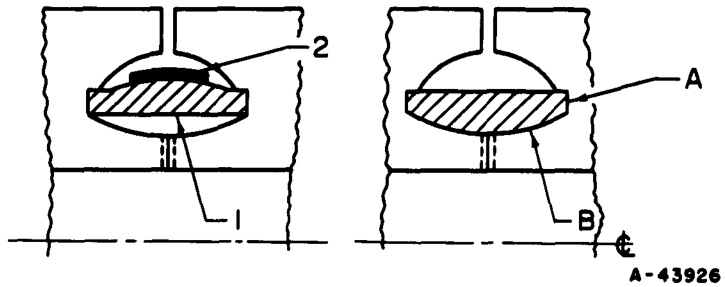

FIGURE 53. EXTERNAL EXPLOSIVE SEAL

A major consideration is the blowout effect of the internal pressure. The seal ring must be thick enough to withstand the developed hoop stress. Also, the initial strain on the seal interface must be sufficiently greater than the pressure-induced hoop expansion to maintain sufficient surface contact. The primary seal is developed at Point A because of the combined effects of initial preload, Poisson's ratio, and over-center tin canning. A secondary seal can be developed along Surface B. This secondary seal is highly desirable to reduce the force of the fluid acting on the seal and tending to blow it out. The overhanging lips at A also add structural support to the seal ring to prevent blowout.

Initially the seal ring is clamped between the flanges, which bottom out as in Figure 53. The ring can be made to bow under this clamping force to compensate for manufacturing tolerances and discrepancies. In the example illustrated a contact explosive charge, Point 2, is used.

The assembly preload is predicated on the eventual structural load requirements, since the effective seating load will result from the high-energy discharge. The seal ring is deformed by the high-energy discharge and is pushed over center. The insertion of a transfer buffer at Point 2 may be necesary. A support die might have to be assembled onto the fitting to prevent stretch and expansion of critical sections and subsequent distortions and strain relaxations.

Other energy sources such as capacitor discharge or magnetic pulse might be used as a means of applying more than one sealing impulse. With this arrangement, a leaking seal could be tightened without disassembling the fitting.

Conclusions

It would be possible to use an internal explosive charge to form a seal if a method could be found to initiate the detonation without the need for lead wires. An exceptionally intimate bond is possible along the seal-retainer interface when a reasonable amount of explosive is used. Moreover, the problem of personnel safety and possible damage to surrounding equipment can probably be overcome. However, a major problem for which no immediate solution appears likely is the degree of contamination of the internal surfaces caused by the explosive materials.

Although the use of external explosive charges to form a seal would eliminate the contamination problems and allow easy detonation, further experimentation is necessary on selected configurations before the feasibility can be shown.

Mechanical Toggle Seal

Unlike the self-energized O-ring or the high-energy-rate formed seal, which may be termed "exotic", the mechanical toggle seal is conventional in principle. Seals of this type are commercially available and have attained some measure of success in missile systems; especially in low-pressure gas ducts. Even the ferrule on the MS-flareless fitting may be termed a toggle type seal because of the elastic bowing of the ferrule.

A toggle seal can have many forms, but for illustrative purposes the standard Belleville-type disk spring will be considered as a typical case. The seal is strictly a mechanical device, and no auxiliary energy sources help actuate the seal. Because of this, considerations of torque and preload are major factors not only in the seal design but also in the subsequent design of the over-all fitting. Other design factors that must be considered are seating-force magnification and the amount of axial relaxation that the seal can accommodate.

Seating Action

In Figure 54a, a toggle seal is shown when the seating load is first applied. The position of the seal after assembly is shown in Figure 54b.

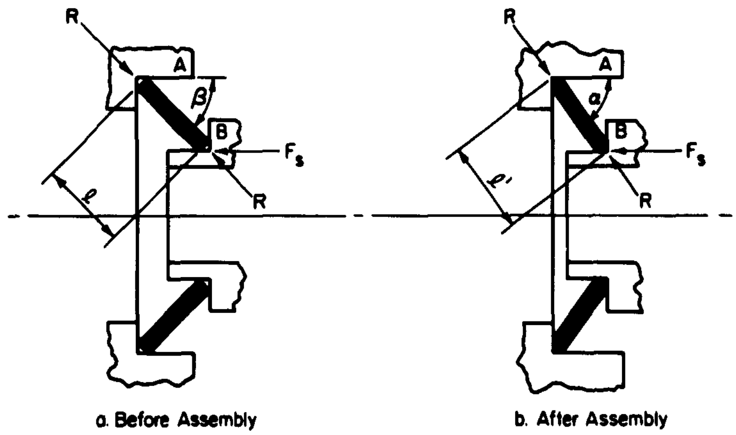

FIGURE 54. SEATING ACTION OF MECHANICAL TOGGLE SEAL

As member B travels axially from right to left the resultant seating force, R, rotates through the angle (α-β). The axial seating force, F_s, increases as the seal is rotated, first to create elastic strain and then to cause plastic yielding. However, after plastic yielding commences, the force, F_s, is relatively constant. Because the seal is fully restrained at both the inside and outside diameters, there will be plastic yielding along the length, ℓ, if the seal does not buckle or bow.

The elastic limit may be reached when the seal has rotated through only a few degrees, depending on the configuration and support of the seal element. Plastic yielding then can occur during the major portion of the travel. This feature is a distinct advantage because dimensional discrepancies can be overcome more readily. When finally assembled, the angle α should be less than 90° or removal of the seal will be difficult. The total angular rotation desired from the point of initial contact depends primarily on the manufacturing tolerances.

One problem encountered with this type of toggle seal is the rotation that occurs at the sealing surfaces. The area of contact shifts as the seal rotates. This means that the seal location is constantly changing as the rotation progresses, and the final contact area is determined only when the seal is seated in its final position. Moreover, the movement between the seal and the retainer is not pure rotation. Smearing of the sealing surfaces may occur because of sliding. This problem might be alleviated by designing the element to bend against the flange faces prior to yielding so that rotation takes place almost entirely within the seal element. Another means of counteracting the rotation problem might be to make both the seal lands and retaining cavities rounded. Neither of these techniques will probably completely overcome the smearing effect, but the plastic state of the seal face will probably cause it to fill the asperities adequately. This is especially true if one of the sealing surfaces is coated with a soft metal like nickel.

Force Magnification

The greatest advantage of the toggle seal for sealing helium is the effect of force magnification. In Figure 55 the force relationship on the toggle seal is compared to a flat metal washer. In the case of the flat washer the force, F_2, needed to exceed the elastic limit must be greater than $(\sigma_y \cdot A_2)$. Assuming that the toggle seal is of the same material and that A_1 equals A_2, then R must approximately equal F_2 at all times. However, F_1, the axial force, is only equal to R sin θ.* Therefore, the axial force needed to seat the toggle seal is less then the corresponding force needed with the flat washer, and the input torque is also less. In itself, this feature is significant only where preload is determined by seating-load rather than structural-load requirements. However, even when preload is predicated on structural loads, the additional axial force can be used effectively by increasing the seating area to its maximum limit. This can be beneficial since a longer seating surface will (1) improve the seal, according to leakage path analysis, and (2) minimize the effects of local, minute scratches and nicks on the sealing area.

Preload Torque

The significance of the force magnification possible with the toggle seal is best shown when the preload and torque are also evaluated. If the 1-in. threaded connection rated at 2000-psi internal pressure (Figure 20) is chosen as a typical fitting, the initial axial preload is 4510 lb**. This preload is possible with a torque of only 1200 in-lb. Referring again to Figure 54 and assuming the final angle α as 80°, the resulting force, R, is 25,800 lb. Assuming the yield stress of the toggle seal material at 150,000 psi, the seating area possible would be 0.172 in.^{2} Referring to Figure 55a it can be assumed

*It is assumed that the strength of the toggle seal as a ring is negligible.

**See page 51.

that the contact length, s, is $\frac{\pi r}{2}$ and the total seal area is $\frac{\pi^2 r}{2}$ G. The length of the seal contact, s, is therefore 0.050 in. and the thickness of the toggle, which is equal to 2r, is about 0.064 in.

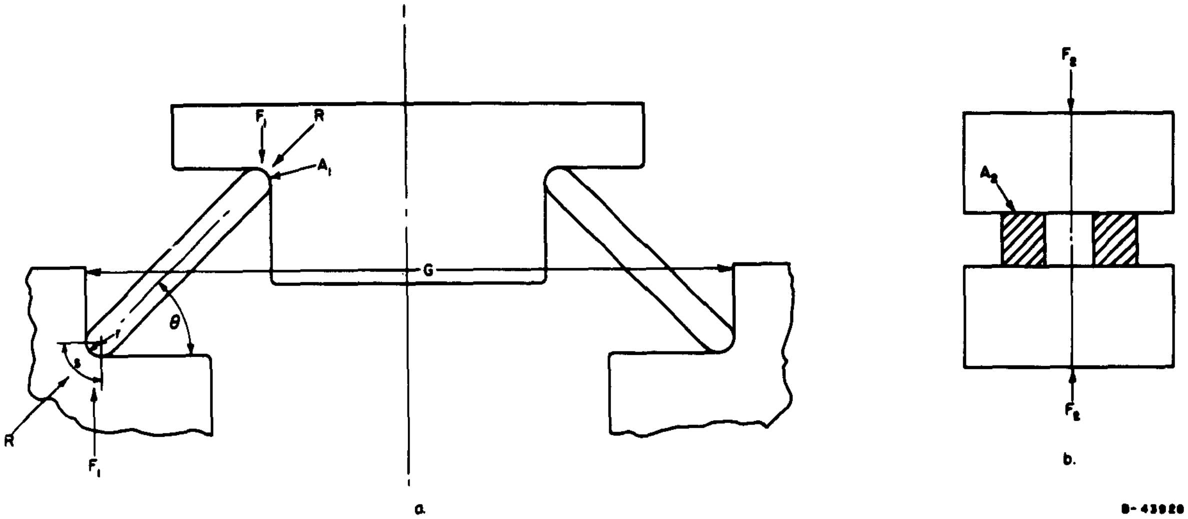

FIGURE 55. FORCE COMPARISON BETWEEN TOGGLE SEAL AND FLAT METAL WASHER

In contrast, the flat washer in Figure 55b would be subjected to a seating force of of only 4510 lb and its area would be much less if a high strength material were also used.

Axial Backoff

Axial backoff due to torque relaxation, creep, or elastic deformations under load was considered in determining the initial axial preload of 4510 lb for the 1-in. threaded fitting.* Because of the magnitude of the preload, some residual strain is always present, even under the most severe set of conditions. However, the elastic recovery on the part of the seal must be at least equal to the amount of strain relaxation expected.

The amount of elastic recovery which may be possible with a toggle seal fabricated from a material with a yield stress of 150,000 psi is indicated in the ideal force-deflection curve in Figure 56.

* See page 51.

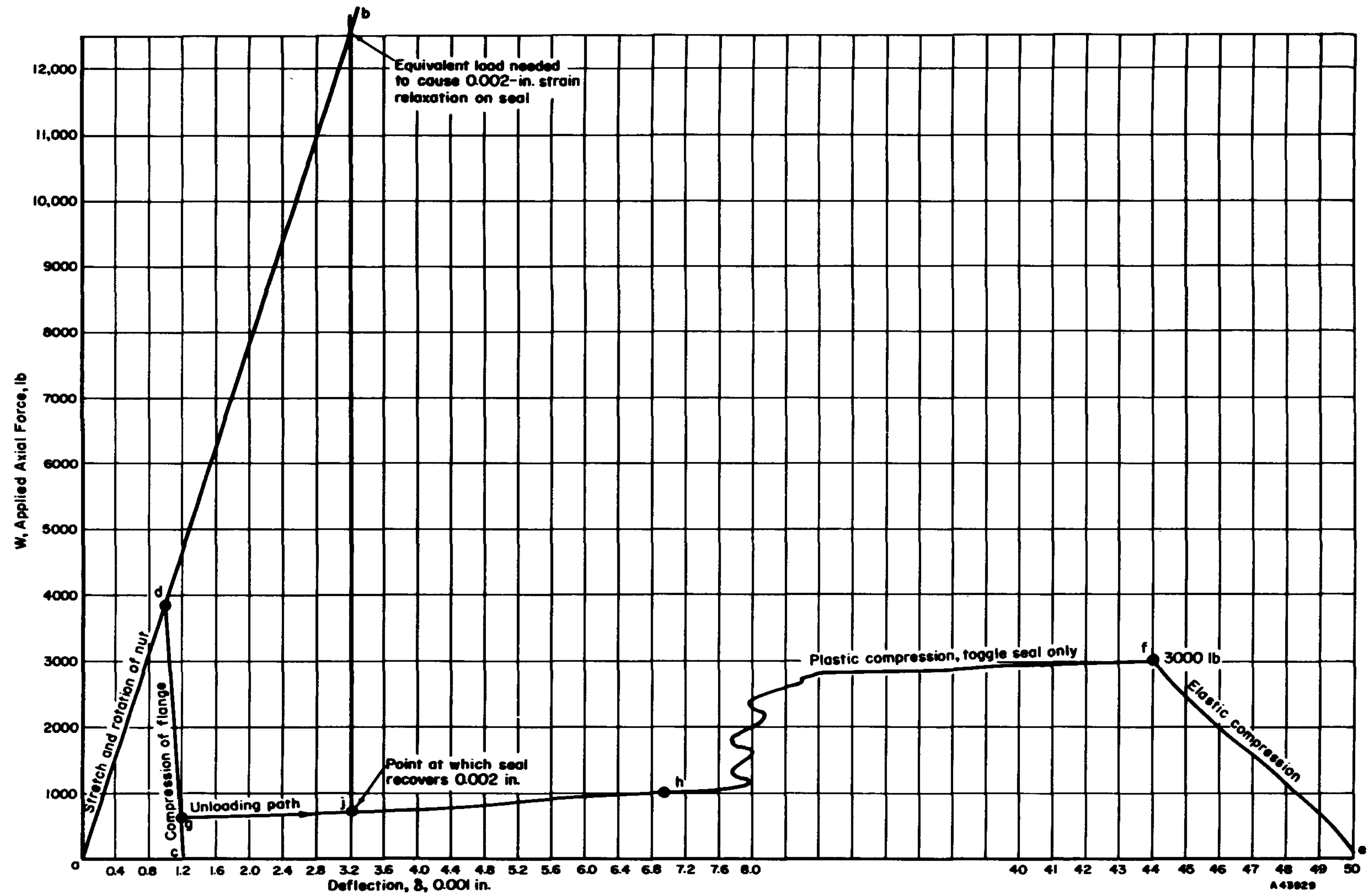

FIGURE 56. FORCE-DEFLECTION CURVE FOR TOGGLE SEAL

The stretch and rotation of the nut (Line adb) and the flange compression (Line cgd) are based on the analysis of the 1-in. threaded connection shown in Figure 19, with a flat metal gasket. However, if a toggle seal were used, the compression force-deflection plot would follow the discontinuous Line efgd. At Point g the seal would be completely seated, and additional torque would be translated to preload in the retaining members, Line c d. The negative slope of Line ef represents the elastic deflection of the seal alone. At Point f plastic yielding throughout the seal member commences, and the force, W, decreases at a low rate until Point g, at which time the axial load is nearly zero because all the force is transmitted in a radial direction.

The total elastic recovery is 0.0057 in. and is represented by Point h. However, not all of this recovery is available because the seal would be unsupported and would fail because of fluid pressure, vibration, or structural collapse. If an elastic recovery of only 0.002 inch, which is less than half of the total recovery possible, is considered, the equivalent load needed to cause this amount of backoff is 12,500 lb. This is far in excess of any expected operational load. A recovery of 0.002 inch is considered greater than that expected in actual practice.

Conclusions

Although not apparently an ideal seal, the toggle seal does represent a mechanical device which approaches the ideal more nearly than other types of mechanical seals. The Belleville disk washer was used as an illustration because it represents the simplest form of toggle seal. The exact nature of the seating action is unknown, especially on a microscopic level at the seal-contact area. Knowledge of this action is essential for proper analysis and development of an optimum toggle seal.

On the basis of the preliminary analysis the Belleville disk appears to be the logical starting point in any future development. It is simple, and easily manufactured. When properly supported the seal is essentially insensitive to temperature changes. Because of the rotation mechanism, large axial movements and tolerances can be tolerated. Most important, the axial seating force is translated into a radial direction, and when the seal is finally seated the sealing stress is much less dependent on axial backoff or strain relaxation than an axial seal.

On the other hand, because the sealing surfaces are exposed, they can easily be damaged. Special care must be exercised in handling or assembling the fittings. Use of a radial seal also tends to enlarge the fitting radially. The seal is subject to pressure blowout if not properly supported and is not pressure energized. The detrimental effects of these disadvantages on the performance of the seal and methods of minimizing them can best be determined by means of experimental investigations planned for Phase II.

References

(34) Loeb, L. B., The Kinetic Theory of Gases, Chapter 7, Dover Publications, Inc., New York (1961).

(35) "Design Criteria for Zero-Leakage Connectors for Launch Vehicles", General Electric Laboratories, Quarterly Progress Report No. 2, Contract NAS 8-4012 (October 11, 1962).

(36) Rossheim, D.B., and Markl, A.R.C., "Gasket Loading Constants", Mechanical Engineering, Vol. 65, 1943, Page 647.

(37) Richards, C. M., "Positive Gas Sealing With Flared Fittings", SAE Journal (October, 1960).

(38) Andrews, J. N., "Hollow Metallic O-Rings", United Aircraft Products, Inc., Dayton, Ohio (1962).

SUMMARY OF RECOMMENDATIONS

Five primary recommendations have been formulated on the basis of the Phase I efforts:

- **Fitting-to-Fitting Connection**

  The reconnectable union should be either threaded or flanged. Threaded fittings should be limited to those sizes and classes which can be assembled with 2000 in-lb of torque or less. In no case should a threaded connection be used for fittings on tubing greater than 1 in. in diameter.

- **Tube-to-Fitting Connection**

  The connection between the tube and the fitting should be a permanent joint made independent of the seal mechanism or the reconnectable union. Furthermore, the brazed or welded joining method developed by North American Aviation should be adapted to expedite speedy qualification of a mechanical fitting. However, further research should be devoted to development of a cold-welded joint achieved by application of high-energy-rate techniques such as explosive forming or capacitor discharge.

- **Seal**

  Three seals are recommended for further experimental and analytical evaluation before one is selected for inclusion in the final fitting design:

  (1) Toggle

  (2) High-energy-rate formed

  (3) Internal-pressurized O-ring

- **Fitting Classes**

  For threaded fittings, four classes should be specified on the basis of temperature range and maximum pressure. Flanged fittings in general should be designed to satisfy specific service conditions by application of the design procedure illustrated in this report. This procedure in its more complete form should be specified as standard.

- **Phase II Research Program**

  Phase II research should be divided into two periods. A period of 10 weeks should be devoted to the selection of the most promising seal.

A period of 3 months should then be devoted to tests of a few assemblies of a total fitting.

INFORMATION REVIEW AND BIBLIOGRAPHY

Considerable effort was expended to determine the extent of available knowledge in the open literature and the experience of manufacturers, users, and designers relative to fittings and similar components. This effort is described briefly. A selected bibliography is given of the references which have been of assistance in Phase I.

Information Review

Technical information was obtained through personal interviews with engineers and designers and from written reports of test and development programs on fittings. Additional related data basic to fitting design were collected and reviewed.

Technical Interviews

During the first month of the project the Battelle staff visited various organizations with experience in the design, manufacture, and use of aircraft and missile fittings. The organizations visited were:

(1) Aerojet-General
(2) Aerospace Corp.
(3) Armour Research Foundation
(4) Astronautics Division, General Dynamics
(5) Douglas Aircraft
(6) Flexonics Division, Calumet and Hecla Co.
(7) General Electric Co.
(8) Jet Propulsion Laboratory
(9) Lockheed Aircraft Co., Burbank
(10) Lockheed Missile and Space Division
(11) Marman Division, Aeroquip Corp.
(12) Parker-Hanifin Corp.
(13) Resistoflex Corp.
(14) Rocketdyne Division, North American Aviation
(15) Space Technology Laboratory
(16) Stanford Research Institute
(17) Weatherhead Corp.

The data sought during these visits related primarily to specific past experience with and knowledge of fitting failures. The types of failure, possible causes, and the location in the piping system were items of major interest. Design philosophy was discussed only in general terms. Unfortunately, little failure-analysis work had been done in this area. Moreover, results of the work which had been done had not been published. When failure data were available, they were very general.

Most of the information received consisted of technical reports of laboratory tests and analytical studies of present and new designs. The most frequent comments of the engineers interviewed were:

(1) The basic seal design of flared type fittings is inadequate, and the seal is subject to deterioration with increased pressure and temperature.

(2) Human error during assembly is the major source of difficulties with "zero-leak" fittings.

(3) Stricter quality control should be imposed on the manufacturers of fittings.

(4) Future specifications should classify the fitting according to the application.

Technical Literature

During the first two months a literature survey was conducted. Documents were collected, analyzed, and catalogued. Thereafter, additional pertinent documents were added to the file as they were noted. The file presently consists of more than 500 documents and is divided into eight major categories:

(1) Bolts
(2) Design
(3) Fittings
(4) Flanges
(5) Materials
(6) Seals
(7) Testing
(8) Threads.

The major sources of data are Armed Services Technical Information Agency, Interservice Data Exchange Program, Machine Design, Mechanical Engineering, Defense Metals Information Center, Transactions of American Society of Mechanical Engineers, Society of Automotive Engineers, and internal reports and memos from individual companies.

A comprehensive literature search, even if restricted to just one or two of the major categories, would have been beyond the scope of the Phase I program. New and typical information only was gathered. When it appeared that a document contained redundant information, it was usually omitted.

Reports dealing with the state of the art of flared and flareless fittings were conducted on a restricted basis also. Only major reports known to contain original test data were collected. The state-of-the-art study was intended to provide only sufficient data for failure analysis or analytical evaluation.

Bibliography

The references listed below are those which proved to be of greatest value in conducting the Phase I work.

Bolts

Appleberry, W. T., "How Fastener Tension Varies with External Joint Loads, Part I", Assembly and Fastener Engineering, 26-30, (April, 1961).

Appleberry, W. T., "How Fastener Tension Varies with External Joint Loads, Part II", Assembly and Fastener Engineering, 32-36 (May, 1961).

Appleberry, W. T., "How Fastener Tension Varies with External Joint Loads, Part III", Assembly and Fastener Engineering, 32-36 (June, 1961).

Dolan, T. J., and McClow, J. H., "The Influence of Bolt Tension and Eccentric Tensile Loads on the Behavior of a Bolted Joint", Procedures of Society of Experimental Stress Analysis, 29-43 (1959).

Harker, T. W., "Manufacture and Characteristics of High-Temperature Bolts", Metal Progress, 125-128 (October, 1953).

Lenzen, K. H., "Strength and Clamping Force of Bolts", Product Engineering, 130-133 (December, 1947).

Mordfin, L., "Some Problems of Fatigue of Bolts and Bolted Joints in Aircraft Applications", National Bureau of Standards, OTS PB 161637 (January, 1962).

Paslay, P. R., "On the Determination of the Influence of an Axial Preload Owing to Bolting on a Cylindrical Pressure Vessel", Journal of Engineering for Industry, 215-218 (May, 1961).

Pringle, O. A., "Loosening of Bolted Joints", Machine Design, 135-136 (February 2, 1961).

Silwones, S. S., Degen, Robert, A., "Test Results Guide - High Temperature Design of Bolted Assemblies", Product Engineering, 79-83 (September 30, 1957).

Smoley, E. M., and Kessler, F. J., "Retaining Tension in Gasketed Joints, Part II", Assembly and Fastener Engineering, 33-36 (October, 1961).

Spiotta, R. H., "Thread Rolling May be for You", Machinery, 182-194 (November, 1957).

Sproat, R. L., "A Checklist on Fasteners Reliability", Missile Design & Development, 58 (June, 1960).

Design

Flieder, W. G., Loria J. C., Smith, W. J., "Bowing of Cryogenic Pipelines", Journal of Applied Mechanics, 409-416 (September, 1961).

Jacobs, Robert B., "Cryogenic Piping System Design Considerations", Heating, Piping & Air Conditioning, 130-140 (February, 1960).

Fittings

Allin, F. R., and Courtot, L. B., "Evaluation of Flareless Fittings for Low Density Gas Applications", Weatherhead Company, Test Report No. 69,460-F (September 8, 1958).

Beachley, N. H., "Survey of Hydraulic Fittings in Air Force Ballistic Missile Programs", Space Tech. Lab., Report 7431.2-289, 1-9 (August 25, 1960).

Cornish, H. E., and Bloom, J. C., "Development of High Pressure Seals For AN Straight Thread Fittings", Applied Hydraulics, (18-24) (November, 1949).

Courtot, L. B., "Refinement of Precision Flareless Fittings", Weatherhead Company, Engineering Progress Report (September, 1958).

Cowdrey, F. W., "Flareless Hydraulic Fittings Keep F-104 'Dry'", Aviation Age (July, 1957).

Davenport, C. R., "The Why and How of Weatherhead Ermeto Flareless Fittings", Weatherhead Company by special permission of Lockheed Aircraft Corporation.

Hallesy, H. W., "Development of a Permanent and a Reconnectable Tube Fitting for High Pressures and/or High Temperatures", Boeing Aircraft, Report D6-5327 (March, 1960).

"Buttress-Threaded Tube Ends Raise Coupler-Joint Efficiency", Iron Age, 90-91 (November 24, 1960).

Lewis, S., "Leakage Problems with Conventional Fittings", Space Tech. Lab. Report 9733.5-460, 1-7 (May 24, 1961).

Lewis, S., "MS & AN Fittings", Space Tech. Lab., Report GM60-7640.5-507, 1-4 (August 22, 1960).

Mayhew, W. E., "Design and Development of a 1000 F Hydraulic System", Republic Aviation Report, AD 231 731 (July, 1959).

Mayhew, W. E., "Design and Development at a 1000 F Hydraulic System", Republic Aviation Report, AD 257 940 (June, 1960).

Richards, C. M., "Precision Sleeves Improve Flareless Fittings", Hydraulic & Pneumatics, 120-122 (April, 1962).

Seibel, L. L., and McGillen, V. W., "Hydraulic and Pneumatic Fitting and Tubing Test Program", North American Aviation Report, AD 235 024 (November, 1959).

Flanges

Dittoe, T. A., "Structural Test Requirements, Bolted Flanged Joints for Ducts", Convair Astronautics, General Dynamics Corp., Report AZS-27-250 (March 25, 1956) Contract AF 04(645)-4.

Donald, M. B., and Salomon, J. M., "The Behavior of Narrow-Faced, Bolted, Flanged Joints Under the Influence of Internal Pressure", Proc. Inst. Mech. Eng. (London), 173 (17), 461-468 (1959).

George, H. H., Rodabaugh, E. C., and Holt, Marshall, "Performance of 6061-T6 Aluminum Flanged-Pipe Assemblies Under Hydrostatic Pressure", ASME Paper #56 - PET-19 (1956).

George, H. H., Rodabaugh, E. C., and Holt, M. "Aluminum Alloy Welding Neck Flanges Performance Equal to Carbon Steel", Heating, Piping and Air Conditioning, 95-97 (October, 1957).

Hillmer, W., "The Wedge-Ring Joint", Michelson Lab. Report, AD 260 021, 1-7 (June, 1961).

Halford, D. E., "Structural Procedure Report, Bolted Flanged Joints for Ducts", Convair Astronautics, General Dynamics Corp., Report No. 7B 2326-1 (July 30, 1959) Contract AF04(645)-104.

Labrow, J., "Design of Flanged Joints", Proc. Inst. Mech. Eng. (London), 156 (1), 66-73 (1947).

Markl, A. R. C., and George, H. H., "Fatigue Tests on Flanged Assemblies", Transactions of ASME 77-87 (January, 1950).

Sperry, A. M., Jr., "Structural Test Results of Bolted Flanged Joints for Ducts", Convair Astronautics, General Dynamics Corp., Report No. 7B2326-2 (June 27, 1960).

Materials

Arcand, Lionel, "Materials Selection for the Hydrogen Rocket", Aircraft & Missiles, 32-35 (January, 1960).

Boyd, W. K., and White, E. L., "Compatibility of Rocket Propellants with Materials of Construction", DMIC Memorandum 65, OTS PB 161215 (September 15, 1960).

Corruccini, R. J., "Properties of Materials at Low Temperatures, Part I", Chemical Engineering Progress, 53 (6), 262-267 (June, 1957).

Corruccini, R. J., "Properties of Materials at Low Temperatures, Part II", Chemical Engineering Progress, 53 (7), 342-346 (July, 1957).

Corruccini, R. J., "Properties of Materials at Low Temperatures, Part III", Chemical Engineering Progress, 53 (8), 397-402 (August, 1957).

Croucher, T. R., and Nickols, R. C., "The Use of Alloys at Cryogenic Temperatures", HD. 6593D Test Group, Edwards AFB, California, Memo I (August, 1961).

Favor, R. U., Deel, O. L., and Achbach, W. P., "Design Information on 17-7 PH Stainless Steel for Aircraft and Missiles", DMIC Report 137, OTS PB 151096 (September 23, 1960).

Favor, R. J., Deel, O. L., and Achbach, W. P., "Design Information on AM-350 Stainless Steel for Aircraft and Missiles", DMIC Report 156, AD 262407 (July 28, 1961).

Grigger, J. C., and Miller, H. C., "The Compatibility of Materials with Chlorine Trifluoride, Perchloryl Fluoride & Mixtures of These", Pennsalt Chem. Corp. Report, AD 266 391, 1-100 (April, 1961).

Jaffe, Leonard D., and Rittenhouse, John B., "Behavior of Materials in Space Environments", ARS Journal 320-346 (March, 1962).

Campbell, J. E., "Compilation of Tensile Properties of High-Strength Alloys", DMIC Memorandum 150, AD 275 263 (April 23, 1962).

Marin, J., "Design for Fatigue Loading, Part I", Machine Design, 88-94 (January 24, 1957).

Marin, J., "Design for Fatigue Loading, Part II", Machine Design, 95-99 (February 7, 1957).

Marin, J., "Design for Fatigue Loading, Part III", Machine Design, 124-134 (February 21, 1957).

Marin, J., "Design for Fatigue Loading, Part IV", Machine Design, 95-99 (March 7, 1957).

Marin, J., "Design for Fatigue Loading, Part V", Machine Design, 154-157 (March 21, 1957).

Rinehard, John S., "The Behavior of Metal Under High and Rapidly Applied Stresses of Short Duration", Navord Report 1183 (September 27, 1949).

Stewart, W. C., and Shreitz, W. G., "Thermal Shock & Other Comparison Tests of Austenitic and Ferritic Steels for Main Steam Piping - A Summary Report", Trans. of ASME, 1051-1072 (August, 1953).

Stamdler, I., "Hypersonic Fasteners Use Exotic Forms and Materials", Space/ Aeronautics, 56-62 (September, 1961).

Sterner, C. J., and Singleton, Alan H., "The Compatibility of Various Metals With Liquid Fluorine", Air Products, Inc., WADD TR 60-819, AD 260 087 (March, 1961).

"The Manufacture of Rene 41 Components", Symposium on Processing Materials for Re-Entry Structures, WADD TR 60-58 (May, 1960).

Wetheimer, E. G., "Selecting Fastener Materials", Machine Design, 150 (February 4, 1960).

York, H. J., "Compatibility of Various Materials of Construction With Nitrogen Tetroxide N_2O_4", Aerojet-General Corp. Liquid Rocket Plant, Eng. Divn., Research & Materials Dept. Report RM-13 (October 22, 1958).

Manufacturing

Carlson, R. J., Hanes, Hugh D., Hodge, E. S., Peterson, J. H., Simons, C. C., and Smith E. G., Jr., "Joining Zircaloy-Stainless Steel and SAP Alloys By Friction Rolling and Explosive Techniques", Report to the AEC, BMI-1594 (September 4, 1962).

Douglass, John J., "Forming Practices with High Explosives", Du Pont Technical Information Bulletin (May 26, 1960).

Johnson, P. C., Stein, B. A., and Davis, R. S., "Basic Parameters of Metal Behavior Under High Rate Forming", report to Watertown Arsenal Laboratories AD 271 401 (November, 1961).

Pipher, F. C., Rardin, G. N., and Richter, W. L., "High Energy Rate Metal Forming", Lockheed Aircraft Corporation, California Division, Technical Report, AD 254 776 (October 18, 1957, to August 1, 1960).

Reason, R. E., "Surface Finish", Product Engineering (September 16, 1957).

Roth, Julius, "The Forming of Metals by Explosives", The Explosives Engineer (March-April, 1959).

Roth, Julius, "Metal Deformation by Explosives", Hercules Powder Co., Research Center (July, 1961).

"Tubular Joining by Induction Brazing and Fusion Welding Methods", SAE Aerospace Mfg. Forum (October 8, 1962).

Simons, Charles C., "Explosive Metalworking", DMIC Memorandum 71, OTS PB 161221 (November 3, 1960).

"Metal Forming and Its Application in Today's Industries", Winchester-Western Division, Olin Mathieson Chemical Co., New Haven, Connecticut.

Seals

Ashmead, R. R., "Static Seals for Missile Applications", Jet Propulsion, 331-340 (July, 1955).

Beacham, T. S., and Towler, F. H., "Hydraulic Seals", Proc Inst. Mech. Eng. (London), 532-569 (November, 1948).

Cass, E., McCuistion, T. J., "O-Ring Compression Force", Applied Hydraulics, 132-133 (October, 1959).

Dymkowski, J. V., "Pneumatic System Design", Aeronautical Engineering Review, 50-66 (March, 1958).

Eddy, R. W., "Low-Temperature Seals", Chrysler Corporation Missile Division Memorandum EDR 825, 1-31 (April, 1958).

Gilder, G., "Modular Hydraulic System Development", Chance Vought, AD 273 209 (August, 1961).

Hull, J. W., "Ring-Spring Design for High Performance Metal Static Seals", Hydraulics & Pneumatics, 122-126 (September 1960).

Jordan, J., "Extreme Temperature Sealing", Missile Design & Development (January, 1959).

Kupiec, H. P., "Testing of Metal Boss Seals", Aircraft Equip. Testing Co., AD 74 322, 1-61 (April, 1955).

Logan, S. E., "Static Seal for Low-Temperature Fluids", Jet Propulsion, 334-340 (July, 1955).

Liberto, R. R., "Research and Development on the Basic Design of Storable High-Energy Propellant Systems and Components", Bell Aerosystems Company, AFFTC TR-60-61 (May 19, 1961).

Liberto, R. R., "Titan II Storable Propellant Handbook", Bell Aerosystems Company, AFFTC TR61-32 (June, 1961).

Newell, G. C., "Preliminary Results of All Metal Boss Evaluation & Development", presented to SAE Committee A6, Montreal, Canada, April, 1962, by Boeing Aircraft, Transport Division, 1-11 (September, 1961).

Richards, C. M., "Missile Piping Methods", Convair Astronautics, General Dynamics Corp., ERR-AN-120, 1-17.

Skinner Seal Co., "Metal Seals Solve Missile Leakage Problems", Aviation Age, 49-51 (May, 1957).

Shaw, C. J., "Laboratory Test and Evaluation of Seals Used in the Propellant Line Systems", Douglas Aircraft, Report DEV-3227 (March 30, 1960).

Willis, W. W., "An All-Metal Sealing Joint", Missile Design & Development, 18-19 (August, 1958).

Testing

Currie, W. E., "Industrial Hydraulic Tube Fittings Meet New Fields and Problems", SAE Paper S317 (September, 1961).

Currie, W. E., "Pressure & Pull Tests on Size 24 "Ferulok" 17-4 PH Ferrules", Parker Appliance Co. Report 4320 D-5214, 1-11 (April 17, 1959).

Cerbin, W. G., "Performance Characteristics of Flareless and Flared Fittings", Weatherhead Company Report 1060, 1-9 (August, 1959).

Carlson, A. F., "Interim Report of Conical Seals for Flared Tubing", Convair Astronautics, General Dynamics Corp., AN 59MD3008-1.

Dubrow, A., "Investigation of the Effect of Pre-Stress on Fatigue-Vibration Life of High Pressure Hydraulic System Tubing", Aeronautical Materials Laboratory, Philadelphia, Pennsylvania, AML NAM AE 6272, 1-13 (April 5, 1955).

"Avica Ferrule Type Tube Fittings", Douglas Aircraft, Technical Memorandum DM 18-P & M-L0567 (February 28, 1958).

"Freon Leakage Test of Avica Tube Coupling", DC8 P & M-L0094 (March 28, 1957).

"Avica 2" Ferrule-Type Tube Assemblies", Douglas Aircraft, Technical Memorandum DM 18-P & M-L0940, (September 24, 1958).

Floreen, E. D., "Double Seal Conoseal Joints for High Temperature Gas Cooled Reactor", Marman Division, Aeroquip Corporation (July, 1962).

"Summary of Test Results of Various Configurations of Couplings with Gamah Metal Seals", Gamah Corp., 1-12 (December 17, 1960).

Lundback, A. V., "Evaluation of Annealed Stainless Steel Tubing and "AN" Fitting Joints", Aerojet-General SCR 56 (June 21, 1961).

Lenhart, H. G., and Gartside, W., "Flared Tubing Fatigue Test", Boeing Aircraft, T 2-1432, 1-33 (November 11, 1957).

Le Fevre, William Jr., "Torsional Strength of Steel Tubing as Affected by Length", Product Engineering, 133-136 (March, 1949).

Oliva, J., "Report on Test on Dynatube", Resistoflex Corp., TRA-1490, 1-31 (July 15, 1960).

Oliva, J., "Report of Test on Dynatube Assemblies – High Temperature", Resistoflex Corp., TRA-1491, 1-4 (August 17, 1960).

Oliva, J., "Report of Test on Dynatube Assemblies – Air & Helium Test", Resistoflex Corp., TRA-1525, 1-4 (May 25, 1961).

Oliva, J., "Report of Test on Dynatube Assemblies – Helium Testing", Resistoflex Corp., TRA-1562, 1-7 (April 9, 1962).

Perkins, C. C., "Testing of Seal Designs and Materials", Arnold Engr. Dev. Center, AD 72503, 1-39 (February, 1955).

Pittiglio, C. L., "Hydrostatic Tests of High-Pressure Steel Valves and Fittings", Navy Department, AD 215 727 (May, 1949).

White, H. F., "Missile Leak Report", Convair Astronautics, General Dynamics Corp., AR 141-1-3 (March, 1962).

Whelan, J. S., "Test of 6,000 psi Socket Weld Fittings", U. S. N. Engineering Experiment Station, AD 206 396 (January, 1958).

Threads

Almen, J. O., "Fatigue Durability of Prestressed Screw Threads", Product Engineering", 153-156 (April, 1951).

Bronson, K. R., and Faroni, C. C., "Vibration Resistance of Thread Locking Devices", Product Engineering, 58-61 (October 10, 1960).

Gerstung, H., "Friction as a Factor in Bolt Tension, Galling, Seizing, Part I", Assembly & Fastener Engineering, 32 (January, 1961).

Gerstung, H., "Friction as a Factor in Bolt Tension, Galling, Seizing, Part II", Assembly & Fastener Engineering, 38 (February, 1961).

Goodier, J. M., "The Distribution of Load on the Threads of Screws", Journal of Applied Mechanics, A10-A16 (March, 1940).

Hanneman, W. M., "How Much Torque Tightens A Screw", Machine Design, 179-182 (October 13, 1960).

Inglesby, J. V., "Strength of Screw Threads of Whitworth Form", Journal of the Royal Aeronautical Society, 710-717 (April, 1945).

Kalevitch, R., "Pneumatic High Pressure Fitting Operational Test", Douglas Aircraft Report 2364, 1-11 (January 10, 1956).

Modes, E. E., "Selection of Screw Thread for Maximum Axial Force", Product Engineering, 244-245 (March, 1946).

Schwartz, A., "New Thread Form Reduces Bolt Breakage", Steel, 86 (September 4, 1950).

Smith, C. W., and Low, A. C., "The Effect of Fit and Truncation on the Strength of Whitworth Threads under Static Tension", Machinery, 817-823 (June 16, 1949).

Waltermire, W. G., "Coarse or Fine Threads", Machine Design 134-140 (March 17, 1960).

Walker, P. B., "Fatigue of a Nut and Bolt", Journal of the Royal Aeronautical Society, 62 (570), 395-407 (June, 1958).

APPENDIX I

CALCULATION METHODS FOR STRESSES AND DISPLACEMENTS

Introduction

Most of the calculation methods described herein have been used for many years in the design of flanged connections for pipelines and pressure vessels. In particular, the stress calculation method for outwardly projecting flanges were developed by Waters, et al. (39)*, in 1937 and for several years has been a mandatory appendix to the American Society of Mechanical Engineers Boiler and Pressure Vessel Code, Section VIII, "Unfired Pressure Vessels"(40). Displacement calculations, in commercial flange design, are used only for unusual designs or critical conditions since, in general, the incentive for minimum-weight design does not exist in piping and pressure-vessel applications to the same degree as in missile components. The calculation methods described herein have not been generally applied to the design of small (2 in. tube diameter and under) fittings, insofar as the authors are aware.

The calculation methods are based on the usual assumptions in engineering elastic theory, viz., the material is homogeneous and isotropic, stresses are proportional to strains, and displacements are small. In addition, in some of the calculation methods, it is assumed that the shells are thin walled and that radial dimensions of circular plates are large compared with the plate thickness and, in flange design, the flange radial width is small compared with the inside diameter**.

In addition to the general assumptions of elastic plate and shell theory, several additional assumptions are made in flange-calculation methods, e.g., the effect of bolt holes in the flange ring can be neglected, the localized bolt loads are uniformly distributed along the bolt circle, and the effect of the external moment on the flange depends only on the product of the bolt load and the lever arm.

As in many engineering elastic-stress-analysis methods, local stress concentrations are not calculated. For example, the design method computes the stress in a bolt as W/A_B, where W is the total load*** and A_B is the total root area of the bolts. Actually, as is well known, there may be higher stresses at the thread roots, depending on the root radius, and high local contact stresses will generally exist. Similarly, in the case of nuts on threaded fittings or flanges on bolted fittings, there may be "notches" (e.g., re-entrant corners) where high stresses may exist and, in general, there will be areas in which high local contact stresses occur.

Another approximation involved in the calculation method is the estimate of the lever arm in the calculation of moments. The lever arm is generally assumed to extend between midpoints of loaded surfaces; in the actual fitting the lever arms may be

*References for Appendix I are listed on page 140.

**In small-size standard pipe flanges this theoretical assumption is not justified, since the radial flange width may be several times the flange inside diameter. In the minimum-weight designs considered, however, the assumption is justified even for small-size flanges.

***W is used for load in this Appendix, rather than F as used in the text, to avoid conflict with the calculation parameter F used in this Appendix.

significantly changed by small construction tolerances. In addition, lever arms may be significantly altered by small elastic deformations; fortunately, these lever arm changes are such as to reduce the lever arm and hence make the calculation methods conservative.

It should be apparent from the above discussion that the calculation methods presented here are intended as a guide to the engineering design of fittings rather than methods of accurately calculating the stresses in a fitting. The use of the methods is justified, in part, by successful application to similar designs over a period of many years. It must be recognized, however, that the proposed application to minimum-weight design involving high-strength, low-ductility materials includes conditions where little experience is available. Accordingly, test verification of some of the fittings is recommended.

Outwardly Projecting Flanged Cylinders

Stress Calculations

Figure 57 applies to the flanged stub end of threaded fittings and to flanges of bolted-flanged fittings. The moment applied to the flange is $M_o = Wh_G$, where W is the total load. The stress calculation method used for this shape was developed by Waters, et al.[39], and forms a part of the ASME Boiler and Pressure Vessel Code[40], Section VIII, Appendix II, "Rules for Bolted-Flanged Connections". The calculation method gives maximum stresses in the flange per unit moment applied by the loading. The method is applicable to either loose or integral flanges; integral flanges may have either a tapered hub or uniform-wall hub. The calculation method gives three values of S/M_o: the longitudinal bending stress in the hub, the radial bending stress at the inside of the ring, and the tangential stress at the inside of the ring. The maximum stress is taken as the largest of these three stresses. The maximum stress per unit moment is then multiplied by the applied moment to find the maximum stress. The stress equations for the integral flanges are:

Longitudinal Hub Stress

$$\frac{S_H}{M} = \frac{f}{Lg_1^2B'} \tag{41}$$

Radial Ring Stress

$$\frac{S_R}{M_o} = \frac{(4/3\ te + 1)}{Lt^2B'} \tag{42}$$

Tangential Ring Stress

$$\frac{S_T}{M_o} = \frac{Y}{t^2B} - Z\,\frac{S_R}{M_o}\ . \tag{43}$$

APPENDIX I

CALCULATION METHODS FOR STRESSES AND DISPLACEMENTS

Introduction

Most of the calculation methods described herein have been used for many years in the design of flanged connections for pipelines and pressure vessels. In particular, the stress calculation method for outwardly projecting flanges were developed by Waters, et al.(39)*, in 1937 and for several years has been a mandatory appendix to the American Society of Mechanical Engineers Boiler and Pressure Vessel Code, Section VIII, "Unfired Pressure Vessels"(40). Displacement calculations, in commercial flange design, are used only for unusual designs or critical conditions since, in general, the incentive for minimum-weight design does not exist in piping and pressure-vessel applications to the same degree as in missile components. The calculation methods described herein have not been generally applied to the design of small (2 in. tube diameter and under) fittings, insofar as the authors are aware.

The calculation methods are based on the usual assumptions in engineering elastic theory, viz., the material is homogeneous and isotropic, stresses are proportional to strains, and displacements are small. In addition, in some of the calculation methods, it is assumed that the shells are thin walled and that radial dimensions of circular plates are large compared with the plate thickness and, in flange design, the flange radial width is small compared with the inside diameter**.

In addition to the general assumptions of elastic plate and shell theory, several additional assumptions are made in flange-calculation methods, e.g., the effect of bolt holes in the flange ring can be neglected, the localized bolt loads are uniformly distributed along the bolt circle, and the effect of the external moment on the flange depends only on the product of the bolt load and the lever arm.

As in many engineering elastic-stress-analysis methods, local stress concentrations are not calculated. For example, the design method computes the stress in a bolt as W/A_B, where W is the total load*** and A_B is the total root area of the bolts. Actually, as is well known, there may be higher stresses at the thread roots, depending on the root radius, and high local contact stresses will generally exist. Similarly, in the case of nuts on threaded fittings or flanges on bolted fittings, there may be "notches" (e.g., re-entrant corners) where high stresses may exist and, in general, there will be areas in which high local contact stresses occur.

Another approximation involved in the calculation method is the estimate of the lever arm in the calculation of moments. The lever arm is generally assumed to extend between midpoints of loaded surfaces; in the actual fitting the lever arms may be

*References for Appendix I are listed on page 140.

**In small-size standard pipe flanges this theoretical assumption is not justified, since the radial flange width may be several times the flange inside diameter. In the minimum-weight designs considered, however, the assumption is justified even for small-size flanges.

***W is used for load in this Appendix, rather than F as used in the text, to avoid conflict with the calculation parameter F used in this Appendix.

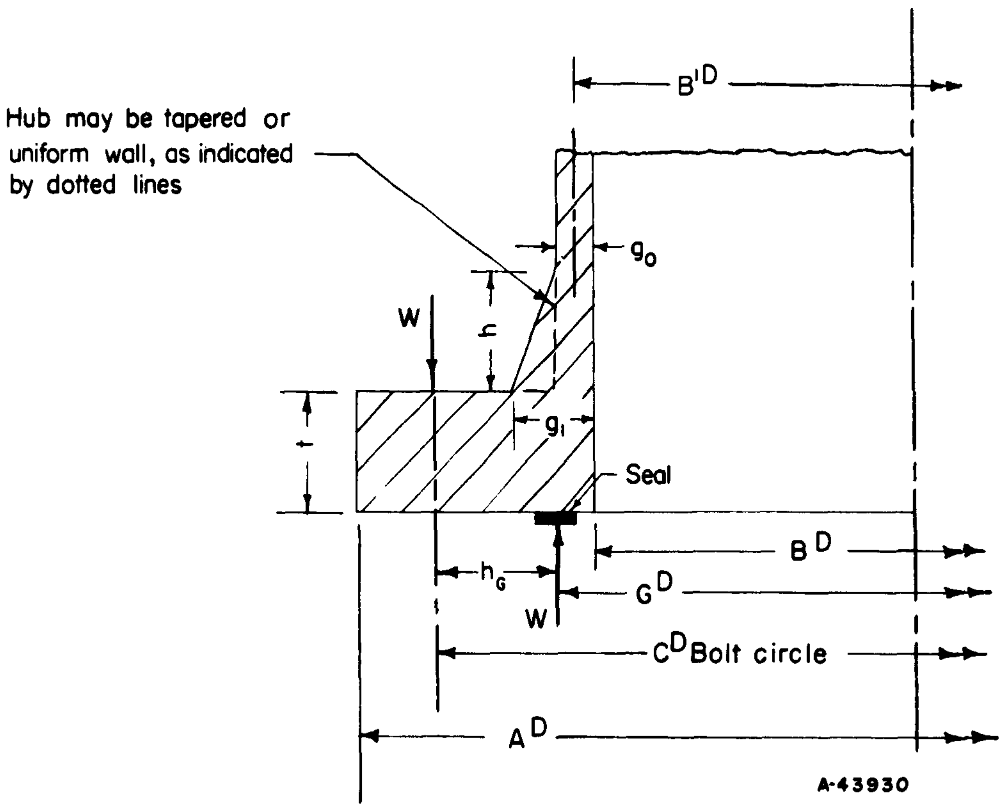

FIGURE 57. DIMENSIONS OF AN OUTWARDLY PROJECTING FLANGE ATTACHED TO A CYLINDRICAL SHELL

For a loose ring flange, only one stress is calculated:

Tangential Ring Stress

$$\frac{S_T}{M_o} = \frac{Y}{t^2 B} . \tag{44}$$

The dimensional parameters A, B, B$'$, t, g_1, g_o and h are shown in Figure 57. Other parameters are: U, Y, Z, and T as functions of K = A/B as shown in Figure 58. F, V, and f are functions of g_1/g_o and $h/\sqrt{B' g_o}$, as shown in Figure 59 and Figure 60. Values of e, d, and L are obtained by the equations

$$e = \frac{F}{h_o} \tag{45}$$

$$d = \frac{U}{V} h_o g_o{}^2 \tag{46}$$

$$L = \left[\frac{te + 1}{T} + \frac{t^3}{d} \right] , \tag{47}$$

where $h_o = \sqrt{B' g_o}$.

Displacement Calculations

The rotation of the flange ring due to an applied moment, M_o, is given by Wesstrom and Bergh[41] as

$$\theta_m = \frac{0.91\ V}{L h_o g_o{}^2 E} M_o , \tag{48}$$

where V, L, h_o, g_o, and M_o are as defined in the preceding section on stress calculations and E is the modulus of elasticity of the flange material.

The axial displacement is $\theta_m h_G$, where h_G is the lever arm of the applied load as shown by Figure 57. The axial displacement of a bolted fitting with two identical flanges is $2\theta_m h_G$. Where the two flanges making up the joint are not identical, the total axial displacement is $(\theta_m + \theta_m')h_G$ where θ_m and θ_m' are calculated by Equation (48) for the two flanges.

The rotation of the flange ring due to the radial component of the internal pressure is given by Rodabaugh[42] as

$$\theta_P = \frac{2.57 \times 10^{-8} B^2 \gamma}{t(t^2 + 1.82\ g_e \gamma)} P , \tag{49}$$

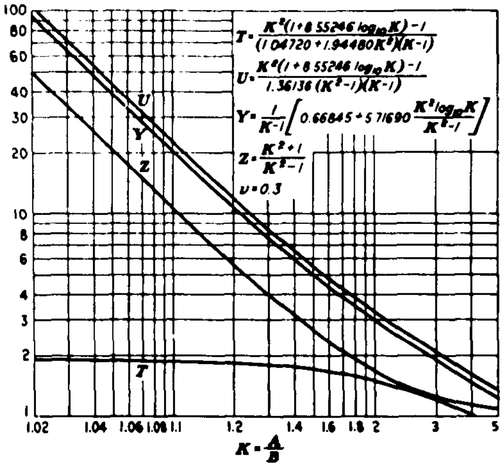

FIGURE 58. VALUES OF T, U, Y, AND Z WHEN $\nu = 0.3$

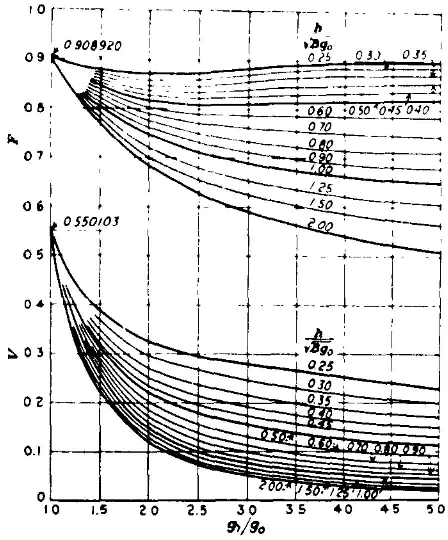

FIGURE 59. VALUES OF F AND V FOR AN INTEGRAL FLANGE

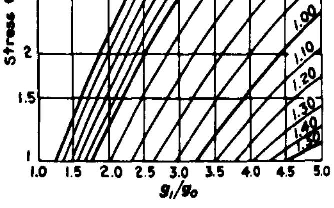

FIGURE 60. VALUES OF STRESS-CORRECTION FACTOR

Figures 58, 59, and 60 are taken from Reference 39.

where

$$P = \text{internal pressure, psi}$$

$$\gamma = \frac{g_e(Z + 0.3)\left(1 + \dfrac{1.82\,t}{h_o'}\right)}{1 + \dfrac{Bg_e^3\,(Z + 0.3)}{h_o' t^3}\left(2 + \dfrac{1.82\,t}{h_o'}\right)}$$

(for $E = 3 \times 10^7$, μ = Poisson's ratio = 0.3)

$$h'_o = \sqrt{Bg_e}$$

g_e = average hub thickness through a distance from the back of the flange ring of $\sqrt{\dfrac{B(g_o + g_1)}{2}}$.

Z, B, t, g_o and g_1 are defined in the preceding section on stress calculations.

The axial displacement in a bolted fitting with two identical flanges is $2\theta_p h_G$, where h_G is shown in Figure 57.

Under Equation (19) in the text of the report, in the definition of α, the term q_r is equal to θ_p/P. [Equation (19) is discussed in the last section of this Appendix.]

Inwardly Projecting Flanges

Figure 61 illustrates an idealized shape, consisting of a cylindrical shell with an inwardly projecting flange, which can be used in designing the nut on threaded fittings.

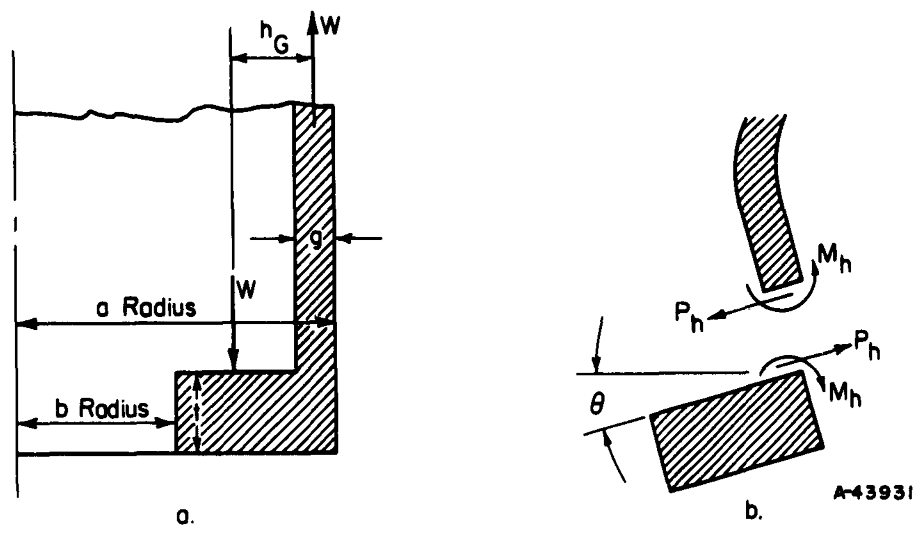

FIGURE 61. INWARDLY PROJECTING FLANGED CYLINDER NOMENCLATURE

where

$$P = \text{internal pressure, psi}$$

$$\gamma = \frac{g_e(Z + 0.3)\left(1 + \frac{1.82\,t}{h_o'}\right)}{1 + \frac{Bg_e^3\,(Z + 0.3)}{h_o' t^3}\left(2 + \frac{1.82\,t}{h_o'}\right)}$$

(for $E = 3 \times 10^7$, μ = Poisson's ratio = 0.3)

$$h'_o = \sqrt{Bg_e}$$

g_e = average hub thickness through a distance from the back of the flange ring of $\sqrt{\frac{B(g_o + g_1)}{2}}$.

Z, B, t, g_o and g_1 are defined in the preceding section on stress calculations.

The axial displacement in a bolted fitting with two identical flanges is $2\theta_p h_G$, where h_G is shown in Figure 57.

Under Equation (19) in the text of the report, in the definition of α, the term q_r is equal to θ_p/P. [Equation (19) is discussed in the last section of this Appendix.]

Inwardly Projecting Flanges

Figure 61 illustrates an idealized shape, consisting of a cylindrical shell with an inwardly projecting flange, which can be used in designing the nut on threaded fittings.

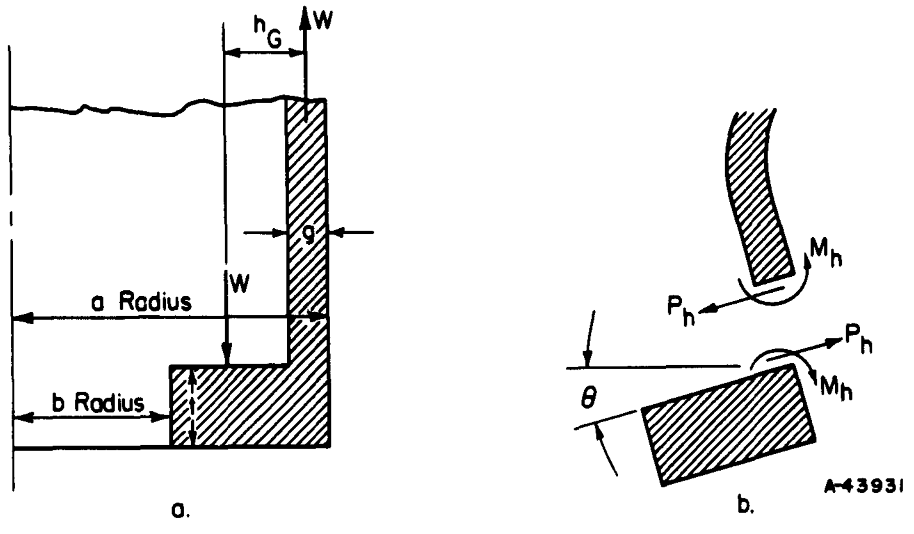

FIGURE 61. INWARDLY PROJECTING FLANGED CYLINDER NOMENCLATURE

Stress Calculations

The moment applied to the flange ring in Figure 61a is $M_o = W \times h_G$ where W is the total load. Under the applied moment M_o, the flange will rotate as indicated in Figure 61b. There will be a moment M_h and a shear P_h acting at the juncture of the flange and the cylindrical shell; these are moments and forces per unit length.

The radial (outward) displacement w of the end of the cylindrical shell, loaded with end moment M_h and shear P_h, is given by Timoshenko(43) as

$$w = \frac{1}{2\beta^3 D} (P_h - \beta M_h) , \tag{50}$$

where

$$\beta = \sqrt[4]{\frac{3(1-\mu^2)}{a^2 g^2}}$$

$$D = \frac{Eg^3}{12(1-\mu^2)}$$

E = modulus of elasticity

μ = Poisson's ratio.

It is assumed that the relatively rigid flange does not undergo any radial displacement, hence

$$\frac{1}{2\beta^3 D} (P_h - \beta M_h) = 0 \tag{51}$$

and

$$P_h = \beta M_h . \tag{52}$$

The rotation of the end of a cylinder, loaded with an end moment M_h and shear P_h, is given by Timoshenko(43) as

$$\theta = - \frac{1}{2\beta^2 D} (P_h - 2\beta M_h) . \tag{53}$$

The rotation of the flange ring is also given by Timoshenko(43) as

$$\theta = \frac{6M_f (a + b)}{Et^3 \ln \frac{a}{b}} , \tag{54}$$

where M_f, the moment applied to the ring per unit length of the ring center line, is

$$M_f = \frac{M_o}{\pi(a + b)} - M_h \frac{2a}{a + b} - P_h \frac{t}{2} \frac{2a}{a + b} . \tag{55}$$

Since the rotation of the flange ring must be equal to the rotation of the end of the cylindrical shell, Equations (53) and (54) give

$$-\frac{1}{2\beta^2 D}(P_h - 2\beta M_h) = \frac{6M_f(a+b)}{Et^3 \ell n \frac{a}{b}} . \tag{56}$$

Substituting $P_h = \beta M_h$ from Equation (52) and M_f from Equation (55) in Equation (56):

$$\frac{M_h}{2\beta D} = \frac{6(a+b)}{Et^3 \ell n \frac{a}{b}}\left[\frac{M_o}{\pi(a+b)} - M_h\left(\frac{2a}{a+b}\right)\left(1+\frac{\beta t}{2}\right)\right] . \tag{57}$$

Solving Equation (57) for M_h:

$$M_h = \frac{M_o}{\pi\left[\frac{Et^3 \ell n\, a/b}{12\beta D} + 2a\left(1+\frac{\beta t}{2}\right)\right]} . \tag{58}$$

Replacing D by its magnitude $Eg^3/12(1-\mu^2)$,

$$M_h = \frac{M_o}{2\pi a\left[\frac{(1-\mu^2)}{2\beta a}\left(\frac{t}{g}\right)^3 \ell n\frac{a}{b} + 1 + \frac{\beta t}{2}\right]} . \tag{59}$$

Equation (59) gives M_h in terms of the loading ($M_o = Wh_G$), the dimensions, and the material constant, μ. The maximum stress per unit applied moment are given by:

Longitudinal Hub Stress

$$\frac{S_H}{M_o} = \frac{3}{\pi a g^2\left[\frac{(1-\mu^2)}{2\beta a}\left(\frac{t}{g}\right)^3 \ell n\frac{a}{b} + 1 + \frac{\beta t}{2}\right]} \tag{60}$$

Radial Ring Stress

$$\frac{S_R}{M_o} = \frac{3\left(1+\frac{\beta t}{2}\right)}{\pi a t^2\left[\frac{(1-\mu^2)}{2\beta a}\left(\frac{t}{g}\right)^3 \ell n\frac{a}{b} + 1 + \frac{\beta t}{2}\right]} \tag{61}$$

Tangential Ring Stress

$$\frac{S_T}{M_o} = \frac{3(1-\mu^2)t}{2\pi a b g^3 \beta\left[\frac{(1-\mu^2)}{2\beta a}\left(\frac{t}{g}\right)^3 \ell n\frac{a}{b} + 1 + \frac{\beta t}{2}\right]} . \tag{62}$$

Displacement Calculations

The rotation of the flange ring due to an applied moment, M_o, is given by Equation (53) and using $P_h = \beta M_h$ from Equation (52):

$$\theta = \frac{M_h}{2\beta D} \quad . \tag{63}$$

The magnitude of M_h is given in terms of M_o by Equation (59). θ in terms of M_o is then

$$\theta_m = \frac{3(1 - \mu^2)\, M_o}{\pi a \beta g^3 E \left[\frac{(1 - \mu^2)}{2\beta a} \left(\frac{t}{g} \right)^3 \ell n \frac{a}{b} + 1 + \frac{\beta t}{2} \right]} \quad . \tag{64}$$

The axial displacement is $\theta_m h_G$.

Parts in Tension or Compression

Parts which are considered to be loaded in tension or compression are:

Bolts of bolted fittings (tension)

Cylindrical shell portion of nut in threaded fittings (tension)

Flanges of bolted fittings (compression)

Threaded stub end of threaded fittings (compression)

Flange of flanged stub end of threaded fittings (compression)

Seals (compression).

Stress Calculations

The general expression for stress in parts subjected to tension or compression is

$$S = \frac{W}{A} \quad , \tag{65}$$

where

W = total load, lb

A = cross-sectional area perpendicular to load, in.^{2}

For bolts:

$$A = A_b = A_{b1} \times n$$

where

A_{b1} = cross-sectional area at root of threads for one bolt, in.^{2}

n = number of bolts

A_b = total bolt area.

Displacement Calculations

The general expression for displacement in parts subjected to tension or compression is

$$\delta = \frac{W\ell}{AE} , \tag{66}$$

where

W = total load, lb

ℓ = axial length, in.

E = modulus of elasticity of material, psi

A = cross-sectional area perpendicular to load, in.^{2}

Threads in Threaded Fittings

The nominal shear stress on the threads, S_T, is

$$S_T = \frac{W}{A_T} , \tag{67}$$

where

A_T = 0.80 $\ell\pi D$, in., where the 0.80 is an approximate factor to account for thread clearances of the buttress or NF threads used in the threaded fittings.

ℓ = thread length, in.

D_p = thread pitch diameter, in.

Bending stresses and local contact stresses in the threads will, of course, be substantially higher than the nominal shear stress. The thread length should be ample to keep these local stresses at a tolerable level.

General Displacement Equation for Bolted Fittings, Equation (19) of Text

Equation (19) of the text (with F changed to W for nomenclature of this Appendix) is

$$W_2 = W_1 + \alpha P ,$$

where

P = internal pressure, psi

$$\alpha = \frac{\pi h_G}{4Q}\left\{\left[\frac{q_G}{h_G} - 2q_F\,(h_T - h_G)\right]G^2 - 2q_F B^2(h_D - h_T) - \frac{8}{\pi}\,q_r\right\}$$

$$Q = q_B + q_G + 2q_F h_G{}^2$$

$$q_B = \frac{\ell_o}{A_B E_B}$$

$$q_G = \frac{V_o}{A_G E_G}$$

$$q_F = \frac{0.91\ V}{Lh_o g_o^2 E_F}\ \text{(integral flanges) or}\ \frac{0.829}{t^3 E_F \log \frac{A}{B}}\ \text{(loose ring flanges)}$$

$$q_r = \frac{\theta_P}{P}\ \text{where}\ \theta_P\ \text{is defined by Equation (49)}$$

ℓ_o = bolt length, in.

V_o = seal thickness (in axial direction), in.

A_B = total bolt area, sq in.

A_G = total gasket area, sq in.

E_B, E_G, E_F = modulus of elasticity of bolt, seal, and flange material, respectively.

h_G = 1/2 (C-G)

h_D = 1/2 (C-B)

h_T = 1/2 (h_D + h_G)

Dimensions A, B, C, G, t, and g_o are shown in Figure 57. L, V, and h_o are defined in the first section of the Appendix under "Outwardly Projecting Flanged Cylinders".

References

(39) Waters, E. O., Wesstrom, D. B., Rossheim, D. B., and Williams, F.S.G., "Formulas for Stresses in Bolted Flanged Connections", ASME Transactions (1937).

(40) American Society of Mechanical Engineers Boiler and Pressure Vessel Code, Section VIII, "Unfired Pressure Vessels", American Society of Mechanical Engineers, 345 East 47th Street, New York 17, N. Y. (1959).

(41) Wesstrom, D. B., and Bergh, S. E., "Effects of Internal Pressure on Stresses and Strains in Bolted-Flanged Connections", ASME Transactions (1951).

(42) Rodabaugh, E. C., discussion of Reference (41).

(43) Timoshenko, S., Strength of Materials, Part II, D. Van Nostrand Co., 250 Fourth Avenue, New York 3, N. Y.

APPENDIX II

DISCUSSION OF DESIGN FOR CREEP OR RELAXATION

Since mechanical tube connections of the types discussed are highly strain sensitive at higher temperatures, plastic flow as a function of time, i.e., creep or relaxation, becomes a dominant factor in design. The basic problem of the relaxation of a bolt in a rigid flange has been considered by several investigators(44-47)*. The method proposed here has been selected because of its simplicity in design application and because of the limited available data on the newer alloys, such data being confined to tensile creep tests with no available relaxation-test data.

The elastic displacement of any part of the structure is proportional to the elastic strain at that time, i.e.,

$$\delta = K\epsilon. \tag{68}$$

In a member with uniform stress, such as the bolts in tension, K is independent of plastic deformations. In the flanges, however, K is a function of plastic deformations since such deformation redistributes the stress. A conservative(48) assumption is that K is a constant for all parts of the fitting and ϵ is the maximum strain corresponding to the maximum calculated elastic stress. Use of K as a constant for all parts of the fitting implies that:

(1) All parts of the fitting operate at the same maximum stress level. (This may be accomplished by appropriate design of the fitting; however, if this is not the case, an alternative method is indicated later in this Appendix.)

(2) All parts are made of the same material.

(3) All parts operate at the same temperature.

(4) In parts subjected to bending stress, relaxation does not alter the stress distribution.

With the assumption of constant K:

$$\text{at } t = 0: \quad \delta_o = K\epsilon_o \tag{69}$$

$$\text{at } t = t: \quad \delta_t = K\epsilon_t \quad , \tag{70}$$

where t = time, hr. The difference between δ_o and δ_t is the plastic displacement occurring in time t, giving

$$\delta_o - \delta_t = \delta_p \tag{71}$$

$$K\epsilon_o - K\epsilon_t = K\epsilon_p \quad . \tag{72}$$

*References for Appendix II are listed on page 145.

The elastic strains ϵ_o and ϵ_t are proportional to the stresses S_o and S_t, giving

$$\epsilon_t = \epsilon_o \frac{S_t}{S_o} \tag{73}$$

Substitute ϵ_t from Equation (73) in Equation (72):

$$\epsilon_p - \epsilon_o \left(1 - \frac{S_t}{S_o}\right) = 0 \quad . \tag{74}$$

Differentiating Equation (74) with respect to time:

$$\frac{d\epsilon_p}{dt} + \frac{\epsilon_o}{S_o}\frac{dS_t}{dt} = 0 \quad . \tag{75}$$

The values of $d\epsilon_p/dt$ in Equation (75) are best obtained from relaxation tests of the material at the required temperature. However, in the absence of relaxation-test data, $d\epsilon_p/dt$ may be obtained from creep-test data, particularly when the effect of first-stage creep is handled separately. While Equation (75) could be integrated graphically from creep-test data, in order to expedite design work it is desirable to express $d\epsilon_p/dt$ analytically. A widely used expression is

$$\frac{d\epsilon_p}{dt} = C_1 S_t^n \quad , \tag{76}$$

where

ϵ_p = plastic strain, in in.

t = time, hr

S_t = stress, psi.

C_1 and n are material constants and are functions of the temperature. These constants can be obtained empirically from a series of creep tests of the material at the required temperature and at various stress levels.

The expression for $d\epsilon_p/dt$ in Equation (76) is independent of time; this is approximately true for second-stage creep but is not valid for first- or third-stage creep. The design method covers the effect of first-stage creep by means of a pseudo modulus of elasticity, E^1, obtained directly from experimental creep data by extrapolating the second-stage creep back to zero time as indicated by Figure 62.

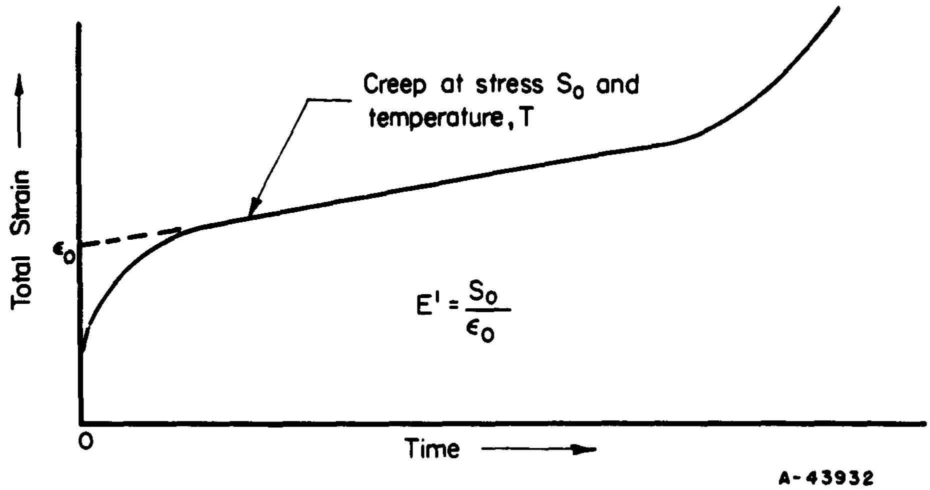

FIGURE 62. METHOD OF ESTABLISHING VALUE OF E^1

The initial preload F_1 is considered to be reduced (in zero time) to a new value $(F_1)_T$ as given by the equation

$$(F_1)_T = F_1 \times \frac{E^1}{E_r} \quad , \tag{77}$$

where E_r is the modulus of elasticity at room temperature, i.e., the temperature at which the preload F_1 was applied to the fitting.

Since the fitting structure by its nature is limited to very small strains, it is unlikely that third-stage creep will be encountered; hence, Equation (76) is adequate for the particular design problem.

Since $\epsilon_o / S_o = 1/E_T$, where E_T is the modulus of elasticity at the design temperature, inserting this relationship along with $d\epsilon_p/dt = C_1 S^n$ in Equation (75) we obtain

$$C_1 S_t^n + \frac{1}{E_T}\frac{dS}{dt} = 0 \quad , \tag{78}$$

which may be written

$$dt = -\frac{dS}{C_1 E_T S_t^n} \tag{79}$$

By integrating Equation 79:

$$t = \int_0^t dt = -\frac{1}{C_1 E_T}\int_{S_o}^{S_t}\frac{dS}{S_t^n} \quad . \tag{80}$$

$$t = \frac{1 - \left(\frac{S_t}{S_o}\right)^{n-1}}{C_1 E_T (n-1) S_t^{n-1}} \quad (81)$$

Equation (81) is the well-known equation for relaxation of a bolt under constant total strain. However, it was derived here to be applicable to a connection consisting of several parts, made of the same material, each of which is subjected to the same stress and temperature and where it is assumed that the stress-displacement relations do not change as a result of loadings* or creep. The restriction to the theory that all parts are operating at the same stress can be removed by a relatively simple extension of the theory. If the connection is considered as three parts (flanges, bolts, seal of a bolted-flanged connection), the equation for calculating service life becomes

$$t = \frac{\left[1 + \frac{K_2}{K_1} + \frac{K_3}{K_1}\right]\left[1 - \left(\frac{S_t}{S_o}\right)^{n-1}\right]}{\left[1 + \left(\frac{K_2}{K_1}\right)^n + \left(\frac{K_3}{K_1}\right)^n\right] C_1 E_T (n-1) S_t^{n-1}} , \quad (82)$$

where the K's are defined by the elastic displacement-stress relations: $\delta_1 = K_1 S$, $\delta_2 = K_2 S^1$, $\delta_3 = K_3 S^1$ for flanges, bolts, and seal**, respectively, and S^1 is the stress in the flanges.

Removal of the restriction that all parts of the connections be made of the same material and operate at the same temperature required considerable additional design effort since the resulting equation,

$$dt = \frac{-\left(1 + \frac{K_2}{K_1} + \frac{K_3}{K_1}\right) dS'}{C_{11} S_t^{n_1} + C_{12}\left(\frac{K_2}{K_1} S_t'\right)^{n_2} + C_{13}\left(\frac{K_3}{K_1} S_t'\right)^{n_3}} , \quad (83)$$

with the n's all different and noninteger, must be numerically or graphically integrated.

The removal of the restriction that the stress-displacement relations, for parts in bending, do not change with creep presents formidable difficulties. Some progress on this problem[48,49] has been made for the case of a ring in torsion. However, even for this comparatively simple structure numerical integration methods are required. The case of the ring with attached cylindrical shell is much more complex.

*Actually, the stresses in a fitting structure do vary with loads. The stress variation in the parts that contribute most to relaxation (bolts and flanges in bolted fittings, nuts and stub ends in threaded fittings), however, is relatively small. The stress in the seal decreases with increasing internal pressure so that the assumption that stress in the seal does not vary with loads is generally conservative from the standpoint of relaxation.

**It should be recognized that the K's may be functions of the internal pressure and external loads.

The theoretical refinements discussed above, along with other desirable refinements to the theory, are not within the scope of this project. Accordingly, the preliminary design work has been based on the simplified concept described above with the expectation that, due to a number of conservative assumptions, the resulting designs will be adequate.

References

(44) Marin, Joseph, Engineering Materials, Prentice-Hall, Inc., New York (1952).

(45) Finnie, Iain, and Heller, W. R., Creep of Engineering Materials, McGraw-Hill Book Company, New York (1959)

(46) Popov, E. P., "Correlation of Tension Creep Tests with Relaxation Tests", ASME Journal of Applied Mechanics (June, 1947).

(47) Robinson, E. L., "Steam-Piping Designs to Minimize Creep Concentrations", ASME Transactions (1955).

(48) Waters, E. O., "Analysis of Bolted Joints at High Temperature", ASME Transactions (1938).

(49) Marin, Joseph, discussion of paper, "Formulas for Stresses in Bolted-Flanged Connections", ASME Transactions (1937).

APPENDIX III

SELECTION OF THREAD PROFILES FOR FITTINGS

The selection of threads is a function of the over-all design of a specific fitting, and therefore the discussions and evaluations presented are qualitative rather than quantitative. These discussions are limited to a few basic factors without taking into consideration all of the factors that influence thread behavior and the behavior of the threaded connections. For example, materials properties and various means of improving thread behavior are not considered. The discussions are limited to the most common case, in which one of the threaded members is subjected to a tension load and the other to a compression load.

Bolted Fittings

When a bolted fitting is loaded or preloaded, the bolt elongates and the nut compresses axially. This is the primary cause for nonuniform load distribution along the threads, as shown in Figure 63, and it is the reason that the first thread next to the

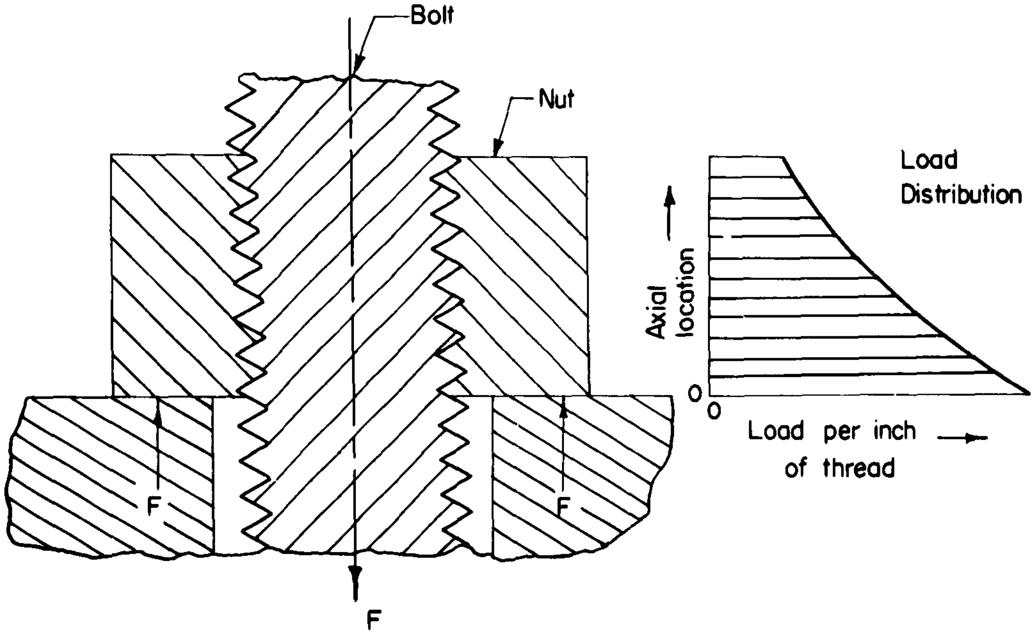

FIGURE 63. ILLUSTRATION OF NONUNIFORM LOAD DISTRIBUTION IN A NUT TIGHTENED ON A BOLT

loaded nut surface carries more load than the other threads. The nonuniformity in load distribution is mitigated somewhat by cantilever-type bending of threads, by radial contraction of the bolt, and by radial expansion of the nut. The radial contraction and expansion are caused by two factors: (1) Poisson's effect from tension and compression and (2) the radial component on thread flank surfaces resulting from the axial bolt load. These radial movements or thread recessions occur mainly in the first threads and are beneficial from the standpoint of load distribution among the threads. However, they cause circumferential hoop stresses and a decrease in thread-engagement depth of the highest loaded critical threads. Thread bending increases the critical stresses at the roots of the threads.

The expansion of the nut may be restrained somewhat by the friction between the loaded-nut face and the flange surface. The thread recession could be decreased essentially to only that resulting from Poisson's effect if buttress threads were used instead of a basically triangular thread form. This would create, however, a trade-off condition because the elimination of circumferential hoop stresses and the decrease in nominal contact pressure (because of less thread recession) would be gained at the expense of less favorable load distribution along the threads and lower fatigue strength of the bolt.

Since the bolt accounts for most of the weight in a bolt-nut combination, it is advantageous, from the standpoint of the strength-weight ratio, to select a thread profile that permits use of the strongest bolts, particularly for fatigue loading. This leads to the conclusion that bolts with triangular threads with a 60-degree included angle and with full-radius roots should be used in flanged fittings, even if they do require higher tightening torques than buttress threads for the same axial load. Since almost all threaded fasteners are made with such threads, a practical advantage results in that commercial high-strength fasteners can be employed. At first it may appear that an Acme thread would constitute an acceptable compromise between the 60-degree triangular thread and a buttress thread. However, this is not the case. For the same thread pitch and, thus, roughly for the same major and minor diameters, the Acme thread is weaker than either the triangular or buttress threads.

Among the 60-degree thread profiles, the following were considered:

(1) Standard threads with basically flat roots (MIL-S-7742), having a nominal thread-engagement depth equal to 83.33 per cent of the theoretical depth (defined as $h = 3/4\ P \cos 30°$, where P is thread pitch)

(2) Threads with a full-radius root (MIL-B-7838), having a nominal thread-engagement depth equal to 83.33 per cent of the theoretical depth

(3) Reduced-depth threads with an increased full-radius root (MIL-S-8879), having a nominal thread-engagement depth equal to 75 per cent of the theoretical depth

(4) Reduced-depth threads proposed by Standard Pressed Steel Co., with a still greater full-radius root, having a nominal thread-engagement depth equal to 55 per cent of the theoretical depth.

For external bolt threads of the same size and pitch, the major diameter is nominally the same for all four profiles. The nominal minor diameter is essentially the same for the first two profiles. It becomes larger for the 75 per cent thread and still larger for the 55 per cent thread as a consequence of the increase in root radius and the decrease in thread depth. The major diameter of the internal threads is also essentially the same for all four profiles. The minor diameter of the internal threads is increased with the corresponding increase in the minor diameter of the external threads to avoid interference of the internal-thread crests with the root radius of the external threads.

The most common failures that occur with such preloaded bolted connections are:

(1) A transverse fracture of the bolt from overstress, creep, or fatigue, usually starting at the root of the first engaged thread

(2) Longitudinal failure of the nut due to excessive circumferential hoop stresses

(3) Stripping of the mating threads because of overload

(4) Seizure of the mating threads, caused by excessive contact pressure.

Considering only the strength of the bolt for all failure modes — overstress, creep, and fatigue — the reduced-depth thread is clearly superior to the full-depth thread. The larger minor diameter provides a larger load-carrying cross section, and the larger root radius has a lower stress concentration, which is important for fatigue strength. The published data support the above statement and show higher ultimate tensile strength, stress-rupture strength, and higher fatigue strength for the reduced-depth threads. It appears that the biggest gain for the reduced-depth thread lies in its improved fatigue characteristics, mainly due to the enlarged root radius. Because of the latter, the standard threads with a full-radius root (MIL-B-7838) are to be preferred in all cases over the standard threads with flat roots (MIL-S-7742). Whenever fatigue is the primary consideration, the 75 per cent threads (MIL-S-8879) or even the SPS-proposed 55 per cent threads may be the best unless considerations other than fatigue limit their use.

In the case of nut failures from excessive circumferential hoop stresses, there should be no essential differences between reduced-depth and full-depth threads, provided all other conditions are equal. The stripping strength of reduced-depth threads on the bolts should theoretically decrease with the thread depth but not necessarily in proportion, because of decrease in "shear" area. It is being claimed, however, that the stripping strength of reduced-depth threads on the bolts remains equal to that of full-depth threads until the engagement depth decreases to about 50 per cent of the theoretical depth, and then it drops off rather rapidly. Actually, there are not enough data available to make a valid conclusion. At any rate, it appears that the stripping strength of the 55 per cent thread on the bolt may be lower than that of full-depth or the 75 per cent thread if the thread recession is considered.

Because of lack of sufficient experience data, an uncertainty exists concerning the behavior of reduced-depth threads with respect to thread seizure. From an elementary point of view, the nominal contact pressures, defined as the axial force divided by the projected area of threads, are higher in the reduced-depth threads, and therefore such threads should be more susceptible to seizure and galling. Because of thread bending under load, the actual contact between threads is concentrated in a limited area rather than being distributed uniformly over the entire thread flank. Galling and seizing of threads is thus governed mainly by the peak contact stresses. Because of the complexities involved, it is virtually impossible to predict analytically the quantitative peak contact stresses and subsequent amount of thread galling or seizing. Judging from the geometries involved, higher peak contact pressures can be expected in the 55 per cent thread than in the 75 per cent or full-depth threads, and therefore thread galling or seizing may become a problem in reduced-depth threads.

It becomes apparent that, from the viewpoint of bolt strength, the reduced-depth threads should be used unless galling, seizing, or stripping occurs. One of the requirements for all mechanical fittings is that they should be capable of sustaining several assemblies and disassemblies. If only thread galling or mild seizing would occur in some fasteners of the flanged connections, the damaged fasteners could probably be easily replaced during reassembly when needed. Since the 75 per cent thread (MIL-S-8879) is widely accepted by the aircraft industry, it can be reasonably assumed that its stripping strength is sufficient, and therefore it appears to be advantageous to use it for fasteners in flanged fittings.

Use of the 55 per cent thread in fasteners for flanges fittings is not recommended at this time because of the uncertainties concerning its stripping strength and thread seizure. Such a thread form, however, may be considered for future use, provided that these uncertainties are eventually resolved favorably.

Threaded Fittings

Here, the threaded members are "sleeves" with or without wrench flats. The internal member has the external threads and the external member has the internal threads. In most cases, the internal threads are loaded in tension and the external threads in compression, which is opposite to a normal bolt- and-nut combination. Regardless of the load directions, the primary function of the threads is to provide or sustain high axial forces. At the same time, the sleeves should be of a minimum weight design. Buttress threads fulfill both of these requirements because they develop the highest axial force for a given torque value and because they do not develop hoop stresses in the sleeves, therefore, they permit minimum wall thickness. The lower fatigue strength as compared with the 60-degree threads is of little consequence for this application because the critical location, as far as the fatigue strength of the fitting is concerned, is the tube-to-fitting connection. Since there is practically no disengagement of threads due to radial forces in buttress threads, they are also expected to be better from the standpoint of preload relaxation.

In view of these considerations, buttress threads are recommended for larger size threaded fittings. In smaller size threaded fittings, the increased cost of buttress threads as compared with that of NF threads may not be justified since, based on preliminary designs of a 1/8 in. threaded fitting, it appears that excess material will be present in the nut because of manufacturing requirements. If this occurs, the reduction of radial thrust by use of buttress threads would be only a minor advantage. Also, in small sizes, the advantage of high axial force for a given torque, which may be obtained with buttress threads, is of less importance since in small sizes the required axial force is relatively small. The size division between threaded fittings with NF threads and those with buttress threads will depend upon required design details in intermediate sizes.

APPENDIX IV

TORQUE RELAXATION TESTS ON FLARED AND FLARELESS FITTINGS

Definition of Torque Relaxation and Sources of Test Data

Threaded flared fittings, when used for critical applications, are tightened with a torque wrench to a specified torque magnitude and the flareless fittings are tightened according to some specified procedures. Upon checking the torque on these fittings at some later time, it is often found that the torque is less than that originally applied to the fitting. This phenomenon has been termed "torque relaxation". Test data on torque relaxation are available from the following three sources:

(A) Seibel, L. L., and McGillen, V. W., "Hydraulic and Pneumatic Fitting and Tubing Test Program", WADC Technical Report 59-267 (November, 1959).

(B) Richards, C. M., "Torque Relaxation in Flared Tube Fittings", Convair/Astronautics, Division of General Dynamics Corporation (July 18, 1960).

(C) Guthmann, P., "Tube Connections, A State-of-the-Art Study", Report No. 1058, Chrysler Corporation, Missile Division, Huntsville Operations (October, 1961).

Test Data From Source (A)

The data available are from Phase III tests of Source (A), pages 24-73, plus Appendix I, "Procedures for Phases III and IV".

Test Specimens

Fittings were either (1) precision flared*, (2) MS- flareless, or (3) super-flareless** types. Material for fittings and tube was 300 series stainless steel, except the sleeves of MS- flareless fittings were of 1112 or 1113 case-hardened steel plated with nickel or cadmium.

Sizes tested were 4, 6, 8, 12, and 16 (nominal tube OD in sixteenths inch).

* AN- fittings with close tolerances and inspection controls.

** MS- fittings with minor dimensional changes, closer tolerances, and closer controls on hardness and surface finish.

Assembly of Fittings on Tubes

Fittings were assembled by standard procedures. The measured torque used in assembly is shown in Table 13.

TABLE 13. TORQUE USED IN ASSEMBLY OF TEST FITTINGS ON TUBING

Nominal Size	Assembly Torque[a], in-lb			
	Flared Fittings		Flareless Fittings	
	Min	Max	Min	Max
4	140	200	120	360
6	280	345	384	600
8	450	525	400	1080
12	900	1100	900	1300
16	1200	1400	1150	2400

(a) From page 89 of Source (A).

Specimens for Tests 1 or 4 were not lubricated (see below for test number significance). Dixon's Graphite Grease No. 3 was used as a lubricant on the shoulder of the sleeve where it mates with the nut on specimens for Tests 2 and 3.

Test Procedures

All fittings were initially subjected to the following two tests: (1) water hydrostatic-proof test at 6,600 psi for 5 minutes, and (2) helium leakage test at 3,300 psi for 5 minutes. Thereafter, all fittings were subjected to vibrations under the conditions shown in the following tabulation:

Test	Ambient Temperature, F	Fluid Temperature, F	Fluid Pressure, psi	Fluid
1	Room	Room	Cycled 0 to 4,500	OS45-1[a]
2	1200	500	3000	OS45-1[a]
3	800	800	3000	Nitrogen
4	Room	-320	750	Liquid nitrogen

(a) Hydraulic fluid.

In all four test series the fittings were subjected to vibration from the attached tubing severe enough to cause fatigue failure of the tube in about 50 per cent of the test specimens in a period of 5 hours and 10 minutes, or less.

Finally, all fittings were again helium leak tested at 3000 psi for 5 minutes (on Tests 2, 3, and 4 after the assembly had returned to room temperature).

Torque-Relaxation Measurements

The breakaway torque in the uncoupling direction was measured after completion of the four above tests.

A "reference" for the breakaway torques of the MS- flareless and the precision flared fittings was established on additional specimens. This was done by conducting torque measurements on six specimens of each type in each size. (These were presumably not pressure tested and were not vibrated. The time lapse between assembly and checking of the breakaway torque is not stated.)

Results

Averages of test results are shown in Table 14.

TABLE 14. AVERAGE UNCOUPLING TORQUE AS PER CENT OF INSTALLED TORQUE[(a)]

Type of Fitting	Condition	Average Per Cent of Installed Torque				
		4 Size	6 Size	8 Size	12 Size	16 Size
Precision flared	Reference	78	78	86	82	76
	After Test 1	54	55	50	75	68
	After Test 2	145	98	--	137	131
	After Test 3	--	--	--	124	138
	After Test 4	52	37	58	73	60
MS flareless	Reference	78	77	78	72	--
	After Test 1	41	49	57	64	70
	After Test 2	138	46	--	--	--
	After Test 3	58	--	27	--	--
	After Test 4	50	70	62	75	59
Super flareless	Reference	--	--	--	--	--
	After Test 1	51	64	57	72	78
	After Test 2	108	98	110	112	71
	After Test 3	108	98	125	106	142
	After Test 4	40	60	60	69	70

(a) "Reference" and "After Test 1" data from Source (A), Table 5.
"After Test 2" data from Source (A), Table 7.
"After Test 3" data from Source (A), Table 9.
"After Test 4" data from Source (A), Table 10.

Test Data From Source (B)

Test Specimens

Fittings were standard AN- flared type taken at random from Convair stock (presumably made of 300 series stainless steel). The tubing was 0.500-in. OD x 0.028-in. wall, per MIL-T-6845. Tubing was flared in accordance with MS 33584, using regular production equipment, and inspected to Convair production standards. All tests were on the 1/2-in. nominal size.

Purpose of the tests was to compare torque relaxation of standard AN- fittings with torque relaxation when using standard AN- fittings plus conical copper seals. The coppe seals used were from three sources:

Designation	Description
CV-A	Convair manufacture typical of those used by Convair in production
VS	Made by Voi-Shan Manufacturing Company, Culver City, California
GM	Made by Gasket Manufacturing Company, Los Angeles, California

Test Production

The specimens were lubricated on the male threads and the back of the sleeve shoulder with Kel-F-90 fluorocarbon grease.

Each specimen was assembled to 475 in-lb torque, using a Richmont snap-indicating torque wrench.

Specimens selected at random were re-torqued without disassembly, using the original torque wrench at the time periods noted in Table 15. The angular movement of the nut required to restore the original torque was recorded.

Results

Results are shown in Table 15.

Test Data From Source (C)

Test Specimens

Fittings were AN- flared type. Material for fitting and tubes was 300 series stainless steel. Tests were run with conical gaskets made of copper or tin-plated copper. Size was 3/4-in.

Test Procedure

Thirty-two fittings were assembled, using an assembly torque of 900 to 1000 in-lb. These were divided into four sets of eight fittings each. Residual torque was measured on one set at 20, on the second set at 48, on the third at 168, and on the fourth at 336 hours after assembly. (Other details of the procedure are not known.)

TABLE 15. TORQUE RELAXATION AS INDICATED BY DEGREES OF NUT ROTATION REQUIRED TO RESTORE ORIGINAL TORQUE, SOURCE (B)

	Nut Rotation, degrees																	
	No Copper Seal						CV-A Seal						VS or GM Seal					
	Time[(a)], days						Time[(a)], days						Time[(a)], days					
Sample	1/4	1	2	7	15	Total	1/4	1	2	7	15	Total	1/4	1	2	7	15	Total
1	5	3	1/2	0	2	10-1/2	7	5	3	5	5	25	4	1	0	4	1/2	9-1/2
2	6	1/2	0	0	0	6-1/2	7	1	0	0	0	8	1	4	2	0	0	7
3	5	3	1/2	2	1	11-1/2	4	0	0	2	1/2	6-1/2	5	0	0	0	0	5
4	6	1	1	4	2	14	3	0	0	0	0	3	2	0	0	0	0	2
5	2	2	1/2	2	0	6-1/2	7	2	1	3	1/2	13-1/2	--	3	2	0	1	6
6	1	1	1/2	1/2	0	3	2	2	0	3	2	7	--	--	5	0	0	5
7	3	3	1	3	2	12	3	1/2	0	1	0	4-1/2	--	--	--	0	0	0
8	3	0	1	1	0	5	3	1	2	1	0	7	3	3	4	0	0	10
9	--	3	1	4	1	9	--	1-1/2	1	1	2	5-1/2	3	3	1/2	4	4	14-1/2
10	--	4	2	3	3	12	--	2	1/2	3	2	7-1/2	5	2	0	1/2	4	11-1/2
11	--	--	0	1	2	3	--	--	1-1/2	5	2	8-1/2	3	0	0	4	4	7
12	--	--	3	4	4	11	--	--	0	0	0	0	--	3	2	2	2	9
13	--	--	--	4	2	6	--	--	--	2	2	4	--	--	1-1/2	0	3	4-1/2
14	--	--	--	3	4	7	--	--	--	4	2	6	--	--	4	0	0	4
15	--	--	--	--	8	8	--	--	--	--	10	10	--	--	--	3	2	5
16	--	--	--	--	4	4	--	--	--	--	9	9	--	--	--	--	4	4

(a) Elapsed time since initial assembly.

Results

Results of these tests are shown in Table 16.

TABLE 16. RESULTS OF TESTS FROM SOURCE (C)

Elapsed Time, hr	"Readout" Torque, per cent of initial torque		
	Max	Min	Avg
20	100	84	97
48	100	72	88
168	100	79	91
336	92	65	80

Discussion of Test Data

General Observations on Test Data

The test data generally shows good correlation between the three data sources. Since torque relaxation is probably an indication of axial-load reduction, and axial-load reduction implies a reduced resistance to leakage, the data are useful in assessing the performance of flared and flareless fittings. It should be noted, however, that the test data do not provide correlation between torque relaxation and axial load, nor is there any readily apparent correlation between torque relaxation and leakage.

The test data indicate that torque relaxation is not significantly affected by the use of conical copper seals, which implies that the source of torque relaxation is not at the sealing surfaces. There is no experimental evidence that torque relaxation is necessarily related to the threads. The mechanism of torque relaxation (i.e., what specifically causes torque relaxation) is not discussed in the available sources. Some aspects of the mechanism of torque relaxation are briefly analyzed in the following discussion.

Torque Relaxation Under "No-Load"

The three sources of test data all indicate that some torque relaxation occurs under "no-load" conditions; i. e. , in fittings that have not been subjected to internal pressure, bending, vibration, or temperature variation between assembly and re-check of the torque. Sources (A) and (C) indicate that torque relaxation under "no-load" conditions reduces the torque to about 80 per cent of initial value. Several hypotheses may be suggested to explain or partially explain the observed torque relaxation:

(1) Creep of stainless steel. While austenitic stainless steel is ordinarily considered to have negligible creep at room temperature, in the case of fittings local contact stresses may be very high; extremely small creep may be sufficient to explain the observed torque relaxation. Displacement calculations on a 1/2-in. flared fitting, tightened with 475 in-lb

assembly torque, indicate an axial displacement of 0.00017-inch will reduce the axial load (and presumably torque) to 80 per cent of its initial value.

(2) Flow of lubricant film. As a rough estimate, the lubricant film in a tightened flared fitting might be about 10^{-4} in. thick. If this film exists on both the thread surface and nut-to-sleeve interface, a decrease in the lubricant film thickness to 2/3 of its original thickness would provide sufficient axial displacement to explain a decrease in axial load to 80 per cent of initial load in the 1/2-inch size.

(3) Locked-up stresses. In tightening the nut on a flared fitting, the frictional resistance of the nut produces torsional stress in the hub of the nut. These locked-up torsional stresses result in a torque in the uncoupling direction, which could explain why uncoupling torques are less than coupling torques.

Unfortunately, none of the hypotheses seem adequate to explain or fully agree with the test data; thus, the mechanism for torque relaxation at "no-load" is not known.

Torque Relaxation Under Loads or Temperature Increase

When loads are applied or temperature increase occurs, torque relaxation in AN- or MS- fittings* can readily be explained, if it is postulated that in a torqued-up AN- or MS- fitting there are highly stressed areas. As discussed in the text of the report, internal pressure or bending will add to the loads on the nut, and if the material was already stressed near its yield strength, plastic flow will occur. With the same postulate, an elevated temperature, even as low as 300 or 400 F, would be expected to produce torque relaxation, since increasing temperature lowers the short-time yield strength of austenitic stainless steel as indicated by Table 17.

TABLE 17. YIELD STRENGTH AS FUNCTION OF TEMPERATURE FOR TYPE 304 STAINLESS STEEL

Temperature, F	Yield Strength, psi
70	34,000
300	23,000
500	19,000
700	16,500
900	15,000
1100	13,000
1300	11,000
1500	10,000

* Designs of threaded fittings shown in the text of this report include a spring action follow-up on the nut which will partially compensate for small amounts of yielding and thereby reduce torque relaxation.

The data from Source (A) indicates substantially greater torque relaxation after loading than at "no-loads" (after Tests 1 and 4, Table 14). With regard to the elevated-temperature test results (after Tests 2 and 3, Table 14), it is possible that the increased torque values (over 100 per cent) may have resulted from hardening of the lubricant or partial seizing or galling of the contact surfaces under high contact stresses at elevated temperatures.

Relaxation of Torque Relaxation to Thread Form

The test data does not provide any information about the effect of thread form on torque relaxation since all tests were run on fittings with National Fine threads. Theories[50,51] on local stresses in threads are based on the assumption of elasticity, which is only indirectly applicable to torque relaxation in which plastic flow presumably occurs. Further, such theories are based on "perfect" thread geometry; thread tolerances, particularly on lead and flank angle, may be more significant in torque relaxation than the detailed thread form.

References

(50) Heywood, R. B., "Tensile Fillet Stresses in Loaded Projections", Proc. I. Mech. Engr., 160, 124 (1949).

(51) Sopwith, D. G., "The Distributions of Load in Screw Threads", Proc. Inst. Mech. Eng. (London), 373-383 (October, 1947).

APPENDIX V

LEAKAGE FLOW ANALYSIS

The flow through a seal can be analyzed as a laminar flow of a viscous fluid if the mean free path of the gas molecules is less than the smallest passage dimension. If the mean free path is the same order of magnitude as the passage dimension, the flow becomes molecular rather than laminar, and a correction for slip flow at the wall must be applied to the laminar-flow analysis. In general the flow is laminar if

$$\frac{\lambda}{h} < 1 = \text{Knudsen's number}$$

λ = Mean free path of molecule, in.

h = Passage height, in.

It is possible to analyze the flow through a seal on the basis of laminar flow, applying a correction which is a function of Knudson's number if Knudsen's number approaches 1.0.

The Laminar-Flow Analysis

In the following the complete derivation is given since the case of flow through slots is not given in the literature, which discusses flow through capillary tubes.[52]

Consider a narrow slot of height h, width w, and length ℓ, as shown in Figure 64. Flow is in the direction of ℓ, and the width w would correspond to the periphery of a circular seal.

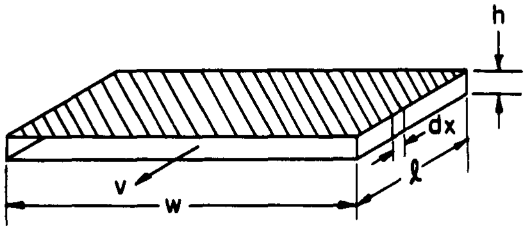

FIGURE 64. SLOT ASSUMED FOR LAMINAR-FLOW ANALYSIS

Consider now a section dx in length and of unit width through Figure 64 in the plane of ℓ, as shown in Figure 65. Since the flow is laminar, the velocity must be zero at the walls, and the velocity profile will be symmetrical about the center line of the passage. A pressure difference, dp, acts across the length dx. If we now consider a section δh in height, we can write the pressure force on the segment,

$$F_1 = -\delta h dp.$$

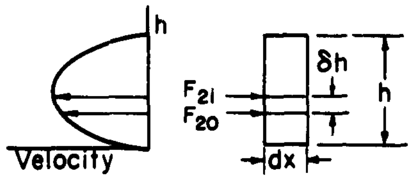

FIGURE 65. FLOW AT SECTION dx OF SLOT

The pressure force must be equal and opposite to the viscous shearing forces on the segment if the flow is to be steady. The viscosity is defined as the ratio of shear stress to velocity gradient. Thus the shearing forces must have the form

$$F_2 = \eta dx \frac{dv}{dy},$$

where

η = viscosity
v = velocity
y = ordinant in h direction.

At the outer surface of the element δh, the shearing force will be

$$F_{2o} = \eta dx \frac{dv}{dy}.$$

Since the velocity increases as the center line is approached, the force on the inner surface of the element will be

$$F_{2i} = \eta dx \frac{d}{dy}\left(v + \frac{dv}{dy}\delta h\right).$$

Also, the velocity gradient, dv/dh, is greater at the outer surface of the element, and the net shearing force on the element will be

$$F_2 = F_{2o} - F_{2i} = \eta dx \left[\frac{dv}{dy} - \frac{d}{dy}\left(v + \frac{dv}{dy}\delta h\right) \right].$$

If the element is not accelerating, the pressure force must equal the shearing force:

$$F_1 = F_2$$

$$-\delta h dp = \eta dx \left[\frac{dv}{dy} - \frac{d}{dy}\left(v + \frac{dv}{dy}\delta h\right) \right]$$

$$= \eta dx \left[\frac{dv}{dy} - \frac{dv}{dy} - \delta h \frac{d^2 v}{dy^2} - \frac{dv}{dy}\frac{d\delta h}{dy} \right].$$

Leaving out the second-order term results in

$$-\delta h dp = \eta dx \delta h \frac{d^2 v}{dy^2}$$

$$\frac{1}{\eta}\frac{dp}{dx} = \frac{d^2 v}{dy^2}.$$

Considering first the right side of this equation, assume a solution of the form

$$v = A + By + Cy^2$$

$$\frac{dv}{dy} = B + 2Cy \ , \ \frac{d^2v}{dy^2} = 2C$$

and

$$2C = \frac{1}{\eta}\frac{dp}{dx} \ .$$

From the laminar flow requirement, v = 0 when y = 0; therefore, A = 0.

The flow must also be symmetrical about the center line. Therefore,

$$\frac{dv}{dy} = 0 \text{ when } y = \frac{h}{2}$$

$$0 = B + 2Cy = B + \frac{1}{\eta}\frac{dp}{dx}\frac{h}{2}$$

and

$$B = -\frac{h}{2\eta}\frac{dp}{dx} \ .$$

The equation for the velocity profile is therefore

$$v = -\frac{h}{2\eta}\frac{dp}{dx}\, y + \frac{1}{2\eta}\frac{dp}{dx}\, y^2$$

$$= -\frac{1}{2\eta}\frac{dp}{dx}\,(hy - y^2).$$

The volume flow rate through the slit will be

$$Q = 2w\int_0^{h/2} v\,dy = -\frac{w}{\eta}\frac{dp}{dx}\int_0^{h/2} (hy - y^2)\,dy$$

$$= -\frac{w}{\eta}\frac{dp}{dx}\left[\frac{hy^2}{2} - \frac{y^3}{3}\right]_0^{h/2}$$

$$= -\frac{w}{12\eta}\frac{dp}{dx}\,h^3.$$

The mass flow rate through the slit is

$$M = \rho Q = -\frac{p}{12RT}\frac{wh^3}{\eta}\frac{dp}{dx} \ .$$

Since, from continuity, the mass flow must be constant

$$\frac{dM}{dx} = 0 = \frac{wh^3}{12RT\eta}\left[p\frac{d^2p}{dx^2} + \left(\frac{dp}{dx}\right)^2\right] \ , \tag{84}$$

an isothermal process being assumed.

Let

$$Z = -\frac{dp}{dx} \ ;$$

then,

$$\frac{dZ}{dx} = -\frac{d^2p}{dx^2} = \frac{dZ}{dp}\frac{dp}{dx} = -Z\frac{dZ}{dp} \ .$$

The bracketed term in Equation (84) then becomes

$$p\,Z\,\frac{dZ}{dp} + Z^2 = 0$$

or

$$\frac{dZ}{Z} + \frac{dp}{p} = 0\ ,$$

which can be integrated to

$$\log Z + \log p = \log C_1$$

or

$$Zp = C_1\ .$$

Since

$$Z = -\frac{dp}{dx}$$

$$p\frac{dp}{dx} = -C_1,$$

which can be integrated to

$$\frac{p^2}{2} = -C_1x + C_2\ .$$

From the boundary conditions

$$p = p_1 \text{ when } x = 0$$

and

$$p = p_2 \text{ when } x = \ell\ .$$

Therefore,

$$C_2 = \frac{p_1^{\ 2}}{2}\ ,$$

and

$$C_1 = \frac{1}{2\ell}\left(p_1^{\ 2} - p_2^{\ 2}\right).$$

The equation for the pressure variation lengthwise in the slit is therefore

$$p^2 = p_1^{\ 2} - \frac{x}{\ell}\left(p_1^{\ 2} - p_2^{\ 2}\right).$$

Referring again to the mass-flow equation

$$M = \rho Q = -\frac{pwh^3}{12RT\eta}\frac{dp}{dx}\ ,$$

we can write

$$-p\frac{dp}{dx} = \frac{1}{2\ell}(p_1^{\,2} - p_2^{\,2})$$

$$M_L = \frac{wh^3\,(p_1^{\,2} - p_2^{\,2})}{24RT\eta\ell} .$$

Since $p_1^{\,2} - p_2^{\,2} = (p_1 - p_2)(p_1 + p_2)$, this can be written in terms of the average pressure or density;

$$M_L = \frac{wh^3\,(p_1 - p_2)\,p_{avg}}{12\,RT\eta\ell}$$

$$M_L = \frac{wh^3\,(p_1 - p_2)\,\rho_{avg}}{12\eta\ell}$$

Since leakage rates are usually measured at the discharge pressure, p_2, it is also useful to write the mass-flow equation in terms of the discharge pressure

$$M_L = \frac{wh^3\left[\left(\frac{p_1}{p_2}\right)^2 - 1\right] p_2\rho_2}{24\eta\ell} . \qquad (85)$$

Molecular Flow

The flow is molecular if the mean free path of the gas molecules is large compared with the passage height. In this case the laminar-flow boundary condition of zero velocity at the wall is no longer true. There is some slip along the wall.

Knudson develops an equation (52) for the flow in this regime as

$$M = -\frac{8}{3}\sqrt{\frac{2}{\pi}}\sqrt{\frac{\rho}{p}}\,\frac{A^2}{O}\,\frac{dp}{dx} .$$

where

A = flow area of passage
O = parameter of passage.

If the passage is in the form of a slot, of height h and width w,

$$\frac{A^2}{O} = \frac{w^2h^2}{2(w + h)} .$$

If h<<w

$$\frac{A^2}{O} \cong \frac{wh^2}{2}$$

from which

$$M = -\frac{4}{3}\sqrt{\frac{2}{\pi}}\sqrt{\frac{\rho}{p}}\,wh^2\,\frac{dp}{dx} .$$

Since the mass flow is constant,

$$\frac{dM}{dx} = 0 = -\frac{4}{3}\sqrt{\frac{2}{\pi}}\sqrt{\frac{\rho}{p}}\ wh^2 \frac{d^2p}{dk^2}$$

or

$$\frac{d^2p}{dx^2} = 0 .$$

This differential equation has a solution of the form

$$p = a + bx$$

$$\frac{dp}{dx} = b .$$

But,

$$\frac{dp}{dx} = -\frac{3}{4}\sqrt{\frac{\pi}{2}}\frac{M}{wh^2}\sqrt{\frac{p}{\rho}} = b .$$

Therefore,

$$p = a - \frac{3}{4}\sqrt{\frac{\pi}{2}}\sqrt{\frac{p}{\rho}}\ \frac{Mx}{wh^2}$$

Using the boundary conditions

$$p = p_1 \quad \text{at } x = 0$$

and

$$p = p_2 \quad \text{at } x = \ell ,$$

it follows that

$$a = p_1$$

$$M_M = \frac{4\ \sqrt{2}\ wh^2}{3\ \sqrt{\pi}\ \ell}\sqrt{\frac{\rho}{p}}(p_1 - p_2)$$

$$p = p_1 - \frac{3}{4}\sqrt{\frac{2}{\pi}}\sqrt{\frac{p}{\rho}}\ \frac{Mx}{wh^2} .$$

Note that the pressure distribution along the length of the passage is linear for the molecular-flow case, rather than parabolic as in the laminar-flow case. The mass flow rate is proportional to the square of the passage height, rather than the cube.

Comparison of Laminar and Molecular Flows

The flow equation for the laminar-flow case is

$$M_L = \frac{wh^3\ (p_1 - p_2)\ p_{avg}}{12RT\eta\ell}$$

and for the molecular flow case

$$M_M = \frac{4}{3}\sqrt{\frac{2}{\pi}}\ \frac{wh^2}{\ell}\sqrt{\frac{\rho}{p}}\,(p_1 - p_2) .$$

From kinetic theory of gases, an approximate relationship between viscosity and mean free path is found:

$$\eta = \frac{1}{3}\rho\ \bar{C}\ \lambda\ ,$$

where

$\bar{C}$ = mean velocity of the gas molecules

$= \sqrt{\frac{8}{\pi} RT}$

ρ = density = $\frac{p}{RT}$.

The equation for mass flow rate in the molecular case can therefore be written

$$M_M = \frac{4}{3}\sqrt{\frac{2}{\pi}} \times \frac{1}{3}\sqrt{\frac{8}{\pi}}\ \frac{wh^2\ (p_1 - p_2)\ p_{avg}\ \lambda}{\eta RT}$$

$$= \frac{16\ wh^2\ (p_1 - p_2)\ p_{avg}\ \lambda}{9\pi\ \eta RT}\ .$$

The ratio of molecular to laminar flow can then be written

$$\frac{M_M}{M_L} = \frac{16 \times 12\ \lambda}{9\pi \quad h} = 6.8\,\frac{\lambda}{h}\ .$$

Transition Flows

For the transition region of flow between laminar and molecular flow, a relationship of the form

$$M = M_L + E\ M_M$$

is used, where E is a constant found experimentally to be approximately 0.9 for single gases and 0.66 for mixtures of gases.(52)

Using the ratio of molecular to laminar flow and E = 0.9, the total flow is

$$M = M_L\ (1 + 0.9 \times 6.8\,\frac{\lambda}{h}) = M_L\ (1 + 6.1\,\frac{\lambda}{h}).$$

The mean free path should be evaluated at the average pressure in the passage.

References

(52) Loeb, L. B., The Kinetic Theory of Gases, 3d Edition, Dover Publications, Inc., New York (1961).

Air Force Flight Test Center, Edwards Air Force Base, California.
Report RTD-TDR-63-14. . DEVELOPMENT OF MECHANICAL FITTINGS, PHASE I. Phase Report, February 1963, 167 p incl. illus., tables, 52 refs. plus bibliography.

Unclassified Report

This program's purpose is to develop a family of lightweight mechanical fittings for service with rockets' fluid systems. Phase I was to define and investigate the design parameters and to initiate preliminary designs. The work consisted of a review of the design and use of present fittings, a review of candidate materials, the establishment of recommended fitting, classes, and the development of preliminary design concepts. Three

(over)

I. Projects 6753, Task 30549
II. Contract AF 04(611) -8176
III. Battelle Memorial Institute,
IV. E. C. Rodabaugh, J. W. Adam, B. Goobich

major conclusions were: (1) the reconnectable union should be either threaded or flanged, (2) the tube-to-fitting connection should be a permanent joint independent of the seal, and (3) three sealing methods show promise. Recommendations for future work are: (1) the brazed or welded joining method developed by North American Aviation should be adapted for the tube-to-fitting joint, (2) high-energy-rate joining methods should be investigated, (3) the best of the three promising seals should be developed, and (4) the preliminary fitting-to-fitting designs should be detailed and evaluated.

Air Force Flight Test Center, Edwards Air Force Base, California.
Report RTD-TDR-63-14. . DEVELOPMENT OF MECHANICAL FITTINGS, PHASE I. Phase Report, February 1963, 167 p incl. illus., tables, 52 refs. plus bibliography.

Unclassified Report

This program's purpose is to develop a family of lightweight mechanical fittings for service with rockets' fluid systems. Phase I was to define and investigate the design parameters and to initiate preliminary designs. The work consisted of a review of the design and use of present fittings, a review of candidate materials, the establishment of recommended fitting, classes, and the development of preliminary design concepts. Three

(over)

I. Projects 6753, Task 30549
II. Contract AF 04(611) -8176
III. Battelle Memorial Institute,
IV. E. C. Rodabaugh, J. W. Adam, B. Goobich

major conclusions were: (1) the reconnectable union should be either threaded or flanged, (2) the tube-to-fitting connection should be a permanent joint independent of the seal, and (3) three sealing methods show promise. Recommendations for future work are: (1) the brazed or welded joining method developed by North American Aviation should be adapted for the tube-to-fitting joint, (2) high-energy-rate joining methods should be investigated, (3) the best of the three promising seals should be developed, and (4) the preliminary fitting-to-fitting designs should be detailed and evaluated.